8-27-2009

Characterization of dissolved organic matter by separation and fluorescence spectroscopy

Yurong Deng

Yurong Deng

Candidate

Chemistry and Chemical Biology

Department

This dissertation is approved, and it is acceptable in quality and form for publication on microfilm:

Approved by the Dissertation Committee:

, Chairperson

Accepted:

Dean, Graduate School

Date

CHARACTERIZATION OF

DISSOLVED ORGANIC MATTER BY

SEPARATION AND FLUORESCENCE SPECTROSCOPY

BY

YURONG DENG

B.S., Chemistry, Sichuan University, P.R.China 1995
M.S., Chemistry, Sichuan University, P.R.China 1998

DISSERTATION

Submitted in Partial Fulfillment of the
Requirements for the Degree of

Doctor of Philosophy
Chemistry

The University of New Mexico
Albuquerque, New Mexico

July, 2009

DEDICATION

To

My parents, Yuanrong Zhou and Chengwen Deng

ACKNOWLEDGMENTS

I heartily acknowledge Dr. Stephen Cabaniss, my advisor and dissertation chair, for providing such a good place to work. He gave me both freedom and direction, and set an example that I will aspire to for the rest of my career. Without his advice and encouragement, I couldn't finish my work.

I have had an excellent committee of professors to offer me guidance and advice as I progressed through this Ph.D. program, and I am grateful to all of them: Dr. Kerry Howe, Dr. David Keller, and Dr. Wei Wang.

My fellow UNM graduate students have made my time here a pleasure, and I would not have made it without their friendship and support. Special thanks are given to Aliyar Mousavi and Dr. Zhimin Li, who gave me support in both. I thank Elizabeth Field and Maceo Martinet for providing samples and test.

CHARACTERIZATION OF

DISSOLVED ORGANIC MATTER BY

SEPARATION AND FLUORESCENCE SPECTROSCOPY

BY

YURONG DENG

ABSTRACT OF DISSERTATION

Submitted in Partial Fulfillment of the
Requirements for the Degree of

Doctor of Philosophy
Chemistry

The University of New Mexico
Albuquerque, New Mexico

JULY, 2009

CHARACTERIZATION OF DISSOLVED ORGANIC MATTER BY SEPARATION AND FLUORESCENCE SPECTROSCOPY

by

Yurong Deng

B.S., Chemistry, Sichuan University, P.R.China 1995

M.S., Chemistry, Sichuan University, P.R.China 1998

Ph.D., Chemistry, University of New Mexico, New Mexico 2009

ABSTRACT

The goal of this work is to evaluate new methods of extracting and fractionating dissolved organic matter (DOM) using liquid-liquid and solid-phase extraction (SPE), monitored by optical spectroscopy.

DOM in aquatic systems from different sources was characterized by three-dimension excitation-emission matrix fluorescence spectroscopy (3DEEMS) and UV absorbance spectroscopy. UV and visible humic-like fluorescence were observed in all water samples -- humic acids (HA), fulvic acids (FA), river water, wastewater, and their fractionations. Their fluorescence centers varied with environment in the range of $\lambda_{ex}/\lambda_{em}$ = 220-250 nm/390-460 nm for UV humic-like fluorescence (peak A) and $\lambda_{ex}/\lambda_{em}$ = 300-340 nm/390-460 nm for visible humic-like fluorescence (peak C). pH change didn’t shift

maximum excitation and emission wavelengths but did change the emission intensities of peaks A and C. Peaks A and C always occur together, although relative intensities may change. Protein-like fluorescence peaks were observed in pairs with higher emission intensity at shorter wavelengths than at longer wavelengths. Tryptophan-like fluorescence (peaks T_1 and T_2) was observed at $\lambda_{ex}/\lambda_{em}$ = 230 nm/356 nm and $\lambda_{ex}/\lambda_{em}$ = 280 nm/356 nm in river water and wastewater. Tyrosine-like fluorescence (peaks S_1 and S_2) was observed at $\lambda_{ex}/\lambda_{em}$ = 220 nm/309 nm and $\lambda_{ex}/\lambda_{em}$ = 280 nm/309 nm only in a wastewater sample without extensive biological pretreatment. A new peak was observed at $\lambda_{ex}/\lambda_{em}$ = 250-260 nm/460 nm (peak B), and overlapped with peaks A and C in all water samples and their isolates. Another peak specific to one river water sample was observed at $\lambda_{ex}/\lambda_{em}$ =260 nm/340 (peak D) which could be mis-identified as peak T_2.

Partitioning of NOM into organic solvents was investigated with and without ion-pairing reagent. No extraction of either peak A or C occurred without ion-pairing reagent. Alteration of the partitioning of these two fluorophores by ion-pairing reagent and non-polar solvents enriched peak A in the aqueous phase and peak C in the organic phase. Maximum excitation and emission wavelengths shifted with the addition of ion-pairing reagent due to enhanced peak overlapping and solvent effects. Peak A is the sum of several superposed peaks rather than a simple one. Liquid-liquid extraction could separate different fluorophores but it’s not easy to use.

Rio Grande river water was isolated and fractionated using Solid-phase Extraction (SPE). Humic-like fluorophores (peaks A and C) could be retained by and eluted from the apolar Sep-pak C18 cartridge, Empore C18 Disk, polymeric Oasis HLB and MAX cartridges. Both humic-like fluorophores are negatively charged and visible humic-like

fluorophores (peak C) are more hydrophobic than UV humic-like fluorophores (peak A). Tryptophan-like fluorophores were excluded from those sorbents and occur as neutral or positively charged hydrophilic molecules. Based on the extraction recovery, Empore C18 Disk has the highest recovery (90%) for humic-like fluorophores and Oasis HLB is good for isolating protein-like fluorophores. Oasis MAX discriminates most strongly against protein-like fluorophores, producing only humic-like fluorophores.

Although protein-like fluorescence was expected to correlate with protein content of wastewater samples, protein concentration correlates strongly with SUVA and less strongly with fluorescence intensity of peak T_1 and peak T_2 in sewage-derived wastewater.

RO membranes concentrate both humic-like and protein-like fluorophores, but protein-like fluorophores go through RO membrane more easily than humic-like fluorophores.

TABLE OF CONTENTS

LIST OF FIGURES

LIST OF TABLES

CHAPTER 1

Introduction

1.1 Overview

1.1.1 NOM and its roles in the environment

Naturally-occurring organic matter (NOM) is ubiquitous in surface and ground waters and it is derived from both external and internal sources of organic materials as a result of various biotic and abiotic reactions [Kitis et al., 2001]. NOM is a heterogeneous mixture of aromatic and aliphatic structures with attached functional groups and molecular weights ranging from several hundreds to hundred of thousands of Daltons. These organic materials include humic substances and identifiable classes of biochemicals such as hydrophilic acids, proteins, lipids, polysaccharides, amino acids, and hydrocarbons [Simpson et al. 2002; Piccolo et al., 2002; Leenheer et al., 1989; Leenheer et al., 2001]. Humic substances (HSs), biogenic, heterogeneous organic substances that can generally be characterized as being yellow to black in color, of high molecular weight and refractory [Aiken et al, 1985], typically comprise the majority (up to 80%) of the organic carbon in the freshwater [Steinberg et al., 2008]. NOM is supposed to have a highly polyelectrolytic and aromatic nature, and the possibility of intra- and inter-molecular aggregation by hydrogen-bonding, nonpolar interactions and polyvalent cation interactions [Kononva, 1961].

NOM takes an active role in the ecology of freshwaters (global carbon cycle,

photochemical processes) [Garrels et al., 1975; Leenheer, 2003], biogeochemistry (immobilize, react and transport organic contaminants and metals) [Perdue and Ritchie, 2003], and environmental chemistry (react with halogen to produce disinfection by-product) [Liang and Singer, 2003; Stevens et al, 1976; Christman et al., 1983; Pomes et al., 1999].

Dissolved organic matter (DOM), the soluble portion of NOM, is an important energy source for microbes and a source of carbon in aquatic environment, hence it is a significant component of the carbon cycle. DOM also controls the chemical speciation and toxicity and transportation of trace metals through complexation reactions in aquatic environments [Stevenson, 1994; Thurman, 1985; Breault et al., 1996]. CDOM (chromophoric dissolved organic matter) is used to remotely sense ocean color in estuaries and coastal regions, has important effects on the penetration of solar UV radiation, and plays a central role in the photoreactions of organic substances and certain biologically important metals such as ion and copper [Miller et al., 2002; Zepp et al., 2004]. DOM is known to cause problems in drinking water and wastewater treatment processes, for example, it can (1) compete with low molecular weight organic pollutants for adsorption sites on activated carbon; (2) contribute to membrane fouling; and (3) produce disinfection byproducts (DBPs) upon reaction with oxidants during potable water disinfection [Jaffe et al., 2004]. DOM is considered to be the principal organic precursor to DBP formation and is present in nearly all water supplies. DOM contains both humic and non-humic substances. The former is considered more hydrophobic by XAD separation, while the latter is more hydrophilic. Accounting for about half of the DOM, aquatic humic substances, which comprised of fulvic acids and humic acids

(Figure 1.1 and Figure 1.2), have been the most common precursors of THMs (Trihalomethanes) [Pomes et al., 1999].

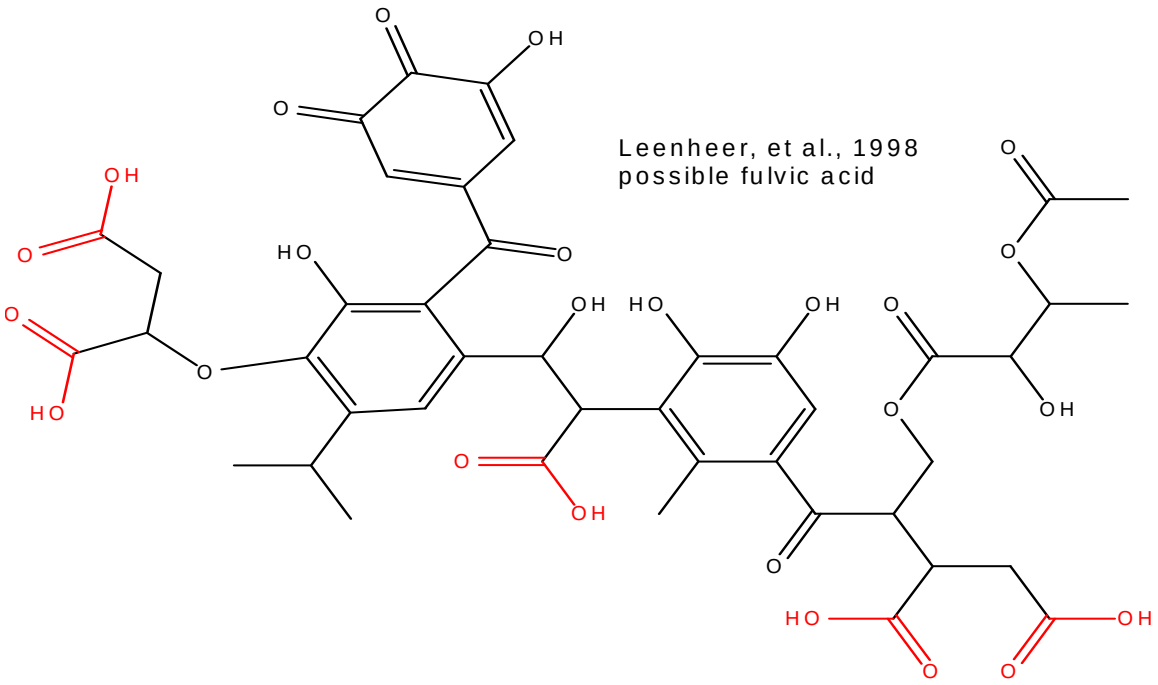

Figure1.1 Molecular structure model of fulvic acid proposed by J.A.Leenheer [Leenheer, 1998]

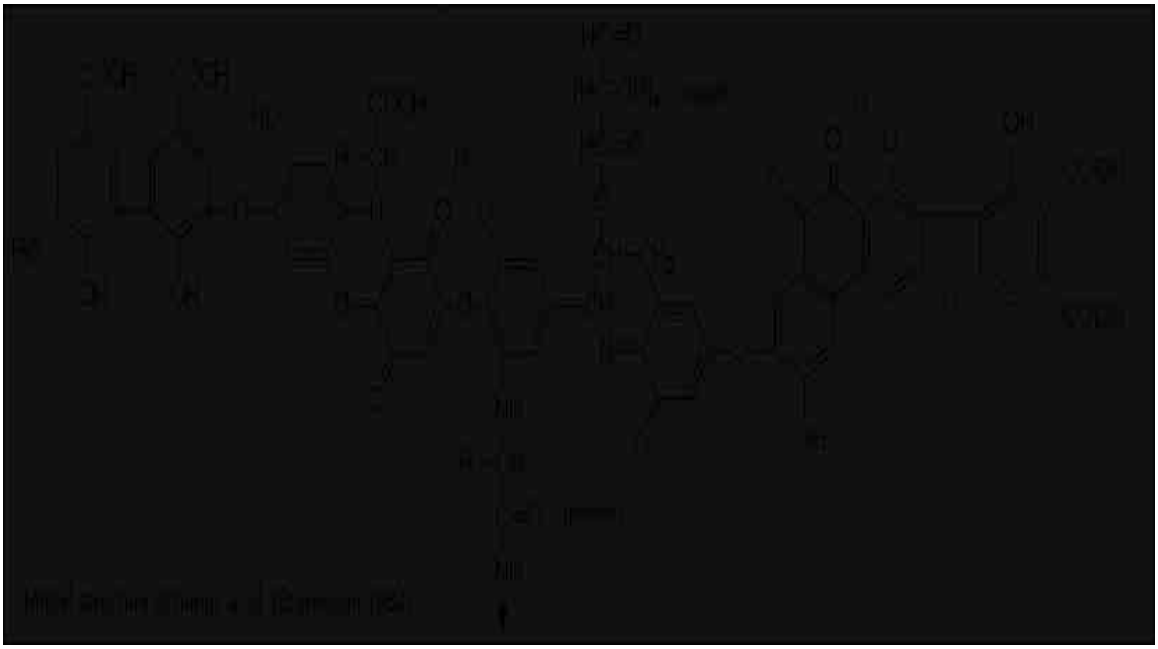

Figure1.2 Molecular structure model of humic acid proposed by F.J.Stevenson [Piccolo and Stevenson, 1982]

Most of the difficulties encountered in defining the structures and reactivities of NOM come from its chemical heterogeneity and geographical variety. Therefore, no single structure model can be used to describe NOM from different sources. The main obstacles to improved understanding of DOM chemistry composition and structure are (1) difficulties in extracting unbiased (i.e., not altered by the extraction) and sufficiently large amounts of DOM from source waters needed for detailed analysis and constrained by the ability to obtain a representative fraction of the DOM pool [Thurman, 1985; Edges, 1992; Benner, 2002]; (2) the low resolution of most previously applied instrumental approaches; (3) data analysis of heterogeneous samples is another problem. Analytical limitations have restricted researchers to either describing broad, bulk properties or characterizing in detail small fractions of the total DOM pool [Mopper, 2007]. Any characteristic to be used as a surrogate should be conservative and the technique employed should be able to detect small differences among the various sources of materials.

1.1.2 Isolation and fractionation of DOM

DOM undergoes a variety of reactions in natural and engineered environmental systems. In order to disclose the nature and reactivity of DOM in water treatment processes, it has been useful to fractionate the complex DOM into more homogeneous fractions. In this regard, DOM is an operational definition based on isolation procedures rather than on specific molecular features. Due to the essential roles in the environmental process, a variety of separation and concentration techniques have been tried to provide

samples for detailed structural analysis of DOM. An ideal isolation and concentration method should (1) recover all DOM; (2) produce a conserved (unbiased and uncontaminated) distribution of all solutes and chemical properties that existed in the original sample (i.e., minimize chemical or physical alteration of the sample); (3) be able to process very large volumes of water in minimal time; and (4) minimize the retention of inorganic salts [Mopper, 2007].

The most commonly used techniques for the concentration and isolation of DOM fractions are Solid-Phase Extraction (SPE), High-performance Liquid Chromatography (HPLC) and membrane filtration [Amy et al., 1987; Aiken et al.,1992]. Each technique fractionates the DOM by a different process and presumably a component unique with respect to its reactivity, structure and bioavailability.

Solid phase extraction is the very popular technique currently available for rapid and selective sample preparation. It separates DOM based upon its polarity and ionogenic properties including normal phase, reversed phase and ion exchange sorbents. Retention of an analyte by normal phase SPE is primarily due to interactions such as hydrogen bonding, polar interaction between polar functional groups of the analyte and polar groups on the sorbent surface. The primary retention mechanism of ion-exchange SPE is the electrostatic attraction of the charged functional group in the compound to the charged group that is bonded to the sorbent surface. The retention mechanism of reversed phase extraction is based on partitioning distribution of analyte between the polar solvent and the sorbent. Polymer-based media such as XAD resin and polymer-bonded silica media are two types of reversed phase sorbents: the former is used for retaining hydrophobic compounds which contain some hydrophilic functionality, especially

aromatics; while the latter allows small, hydrophobic organic compound of interest to reach the bonded silica surface and flushes the large interfering compounds.

Solid phase extraction is achieved through the interaction of three components: the sorbent, the analyte and the solvent. Isolations and fractions of DOM components are operationally defined depending on their affinities to different resins and their back-elution efficiencies. Commercial humic acids and fulvic acids from IHSS are obtained by fractionation of DOM by the Amberlite XAD (non-ionic macroporous resin) with a polystyrene resin as stationary phase. They impose a chemical-based separation instead of physical basis. The procedure of resin separation depends upon controlling the electrical charge of the humic matter. The processes could remove or destroy some functional groups with implications on the behavior and character of the original samples by condition of high pH and highly charged. There is a question on how representative isolated portions are of the materials in their natural states. Moreover, the isolations have low recovery (<80%) and the operation is labor and time consuming. The mechanism of isolation by the most commonly used C18 SPE is based on non-polar intermolecular interactions between the organic compounds in solution and the stationary C18 hydrocarbon sorbent bonded onto a silica surface. It favors the sorption of most of the chromophoric DOM. However, silica sorbents are not stable at extremely acidic pH values and hence recoveries are small (20% ~ 70%) [Simjouw et al, 2005] and non-reproducible. Preparation and purification of functionalized solid phases for DOM extraction are time consuming, and their use in DOM extraction necessitates that the DOM experiences major shifts in matrix pH, salinity and polarity.

HPLC can be used for analytical separations. Fractionation of DOM should not change the environment of the sample much, because the ratio and the distribution of hydrophobic and hydrophilic components will be influenced by many factors, such as pH etc. HPLC can not only identify the different fractions, but also provide quantitative information on the hydrophobicity (RP-HPLC) or molecular weight of DOM (HPSEC) [Zhou et al., 2000; Chin et al., 1997]. More importantly, an advantage of this technology is the absence of any extreme chemical conditions or changes in chemical composition, in contrast to the traditional XAD resin adsorption technique. Moreover, HPLC is an easily operated and labor saving technology without extensive pretreatment and could be utilized as an on-line monitor. Woelki [Woelki et al., 1997] investigated the effect of pore size on separation DOM by reverse phase HPLC and found different pore size from 100A to 4000A resulting in different shapes and resolution of chromatogram. They demonstrated that RP-HPLC is based on both adsorption processes and size exclusion phenomena. This exclusion phenomenon combined with irreversible adsorption by hydrophobic interaction results in poor recovery, and this can be avoided by using non-porous packing column [Dejanovic and Cabaniss, 2004]. In this case, the results obtained by size-exclusion chromatography of HSs should be accepted carefully. The reason is given by natural tendency of HSs to undergone conformational changes and/or aggregation as a response to changed conditions mainly in their aqueous solutions [Hutta, 2003].

Membrane filtration such as UF (ultrafiltration) and NF (nanofiltration) are physical separation processes that segregate according to molecular weight (MW) or molecular sizes of DOM. Membranes are typically characterized by molecular weight

cut-off (MWCO) values which are calibrated by measuring membrane rejection of macromolecules with known molecular weights. The best that can be achieved with a single type of membrane is good removal of inorganic solutes and good recovery of DOM. For example, the median recoveries for UF, NF and RO are 70%, 90% and 90% respectively [Perdue and Ritchie, 2003]. The fundamental problem that arises if membranes are used to concentrate DOM is the co-concentration of inorganic solutes. Even though the mean percent rejection of DOM by RO could be up to ~99%, the co-concentration of sulfate anions and dissolved silica could not be easily separated from the concentrated DOM. Membrane is an isolating method to concentrate a broad spectrum of organic matter whereas resin and SPE are isolating and fractionating methods.

Given the polydispersity of the chemical structures involved and the complexity of the physical and chemical properties which these compounds exhibit, it is doubtful that a single, universally satisfactory method could ever be developed [Bouvier et al., 1998]. The fractions of humic substances responsible for hydrophobic-hydrophobic interactions may differ from the fractions responsible for electrostatic interactions as well as biological interactions. Which technique is more appropriate for the isolation of DOM depends on the focus of the research.

1.1.3 Water treatment & DOM

Water has become one of the hottest topics of the decade and water usage has increased tenfold in the last ten years. A recent report by United Nations noted that one third of the world's population lives in areas suffering from water shortages. Furthermore, increasing industrial demands for water are putting additional stress on water supplies

[Mcllvaine, 2008]. In many parts of the world, water resources are not meeting water demand. Worldwide, there is concern that freshwater sources are at risk, both in terms of replenishment and water quality.

Water has become a precious commodity. The increasing demand for fresh water has focused attention on alternative sources of water, for example, river water from the Rio Grande to supplement groundwater shortage for Albuquerque of New Mexico, seawater desalination for Florida, reuse of the effluents from wastewater treatment plant in small communities in arid areas. Whether water is for human consumption, pharmaceutical manufacturing, semiconductor fabrication or steam generation, adequate purity is essential. Both suppliers and customers are finding new ways to purify water [Mcllvaine, 2008].

Membrane filtration has become an accepted process to purify water. Many full-scale water treatment facilities are operating with different types of membrane. Membrane technology applications have grown steadily, coincident with public demand for high water quality and strict regulations. Membrane processes are compact, stable and provide a very high quality of effluent that is increasingly desirable where discharges go to recreational water, or to be reused for green belt watering, toilet flushing, recharging underground water, etc, or where upgrading of an existing installation is required. Because of lower membrane costs and simplicity of operation (by eliminating coagulation, flocculation and sedimentation processes), membrane applications have been considered a cost-effective substitute for conventional drinking water treatment and are receiving increased attention associated with water quality and cost reduction [Lee et al., 2004].

Membrane separation is an advanced technology available for removal of micron, sub-micron and ionic species. Semi-permeable membranes of different materials, pore sizes and configurations are typically utilized to filter out undesirable impurities. Reverse Osmosis (RO) rejects most ions, Nanofiltration (NF) and Ultrafiltration (UF) reject some ions, and Microfiltration (MF) is only for suspended solids removal. During membrane treatment processes, particle/colloid removals are based on size (Table 1.1). MF and UF differ from NF and RO based on the size of the permeating species, mechanism of rejection, relative magnitudes of the permeate flux (flux is the rate of water volume flow across a unit area of membrane) and the pressure differential across the membrane.

The categories of membrane are operationally defined.

Table 1.1 Membrane glossary.

	Definition	Pore size	Molecular weight cut off	Level
MF	MicroFiltration	0.1~ 0.2 µm	0.1 ~ 1 µm	Suspended solid
UF	UltraFiltration	0.001~ 0.1 µm	0.01~ 0.1 µm	Macro molecular
NF	NanoFiltration	0.001~0.01 µm	0.001 ~ 0.01 µm	Molecular
RO	Reverse Osmosis	< 0.001µm	< 0.001µm	Ionic

RO, once known as "Hyperfiltration", passes a solution across a semi-permeable membrane to separate water from dissolved solids. It is unlike filtration to separate solids from water and hold onto them on a medium or surface. RO employs the tightest skin membranes with smallest pore size around 0.0001 micrometers, where 90-99% of all ions are rejected, more than 99.9% of viruses, bacteria and pyrogens are removed, and virtually all organics are eliminated. Pressure of 200 to 1,200 psig (pound-force per

square inch gauge) is normally required for applications ranging from brackish water purification to seawater desalination. Clogged membrane and higher salinity require higher pressure. The pH tolerance of RO membrane ranges from 3 to 12.

Nanofiltration(NF), also known as "Membrane Softening" process, employs less tight skin membranes with larger pore size around 0.001 micrometers, where 60-80 % of all ions are rejected, 90 % - 95 % of divalent ions are removed, and organic compounds in the 300 to 1000 molecular weight range are eliminated. Nanomembrane will reject ions that are divalent and larger (i.e. calcium, magnesium, carbonate), while allowing lighter monovalent ions (i.e. sodium, potassium, chloride) to pass through. In the nanofiltration process more water passes at a lower pressure and pressures of 100 to 200 psig are typically required to economically soften water without the pollution of salt-regeneration experienced with the resin softening process.

Ultrafiltration (UF) is another membrane separation process but with a larger molecular weight cut off than either RO or NF. Like NF, UF membranes operate at much lower pressures with less waste, but reject only large molecules (i.e. NOM, sugars,) and are frequently used in food and beverage processing or as pretreatment to protect RO membranes or other treatment equipment. UF is similar to the RO and NF processes, has no significant rejection of dissolved solids. It employs loose skin membranes with a relatively large pore size around 0.01 micrometers, where virtually no ions are rejected, but contaminants such as organics, bacteria, and pyrogens are rejected. Most ions and small organics such as glucose are allowed to pass the membrane porous structure. Because of the high membrane MWCO (molecular weight cut off) of UF, it may not be effective for removal of DBP (disinfection by-product) precursors, although it

is efficient in reducing turbidity, particles, suspended solids, total coliforms as well as oil and grease.

MF is similar to the RO, NF and UF processes but does not reject dissolved solids or ions. Pore sizes of MF membranes are around 0.1 micrometers (0.1-0.2 μm in water treatment), and only rejects particulates and suspended solids with sizes larger than the membrane pore size. MF process can use extremely low operating pressure (1 to 25 psig) for the separation process to take place. MF is quite different than RO, NF or UF in that it doesn't separate and reject materials to a waste stream, but traps particles onto the surface or within the body of the filter. If properly applied, MF can be very effective in the removal of bacteria and protozoan cysts (i.e. Giardia and Cryptosporidium).

One of the most significant issues affecting the development of membrane filtration is fouling. Accumulation of excess particles in a thin layer adjacent to the membrane surface, increases resistance to solvent flow and thus reduces the permeate flux. All membranes are subject to fouling, but fouling is acceptable as long as it is reversible and manageable. Serious irreversible fouling implies a substantial loss of capacity for membrane facility, and frequent replacement of membrane modules increases operating cost. Fouling represents a serious constraint for employing low-pressure membrane systems as a substitute for conventional treatment [Lee et al., 2004].

Membrane fouling is determined by the coupled influence of physical and chemical interactions. These interactions and the resulting properties of the fouling layer are controlled by the foulant characteristics, feedwater solution chemistry (pH, ionic strength, divalent cation concentration), membrane properties (surface charge, hydrophobicity, pore size and morphology), hydrodynamic conditions (permeate flux, cross-flow

velocity) and solute-solute and solute-membrane interactions (steric, hydrophobic, and electrostatic interactions). Shape and size of molecules and roughness of membranes may be more important or influential than hydrophobicity of membrane. The physicochemical characteristics of the foulant, such as charge and molecular conformation, directly control the fate of foulant accumulation and the properties of the fouling layer and, therefore, have significant impact on membrane permeate flux. Laboratory-scale crossflow studies have demonstrated that high ionic strength, high Ca concentration, low pH, high initial permeation rate and low crossflow velocity all favor membrane fouling.

Since fouling results in deterioration of membrane performance (i.e. permeate water flux and quality) and ultimately shortens membrane life, effective preventive strategies can only be devised if the mechanism of fouling is understood.

Tansel et al [Tansel et al., 2000] elucidated four fouling mechanisms: gel layer formation (cake resistance), pore blockage, concentration polarization and adsorption. Generally, more than one type of mechanism contributes to the fouling for any specific system. Concentration polarization and gel layer formation take place primarily on the membrane surface where the pressurized source water is in contact with the membrane. Low MW molecules enter pores, causing pore blockage and adsorption type of fouling, while high MW molecules form a layer of gel or concentration polarization on top of the membrane surface, preventing small MW organics from entering the membrane pores [Tansel et al., 2000; Li and Chen, 2004]. Therefore, UF membranes seem like to be more affected by cake/gel layer formation (surface coverage). MF membranes are susceptible to pore blockage.

Fouling mitigation techniques can be classified into three categories: fouling control, pretreatment technologies, and anti-fouling membranes and modules [Sheikholeslami, 1999].

Fouling control strategies include interval operation, sub-critical flux operation and periodic physical or chemical cleaning etc. Reversible fouling could be controlled by changing process parameters or by hydraulic cleaning such as water/air backwash, air scouring and water flushing (only concentration polarization). However, gel layer formation, pore blockage and adsorption are most often irreversible, and require chemical cleaning such as acid or base solutions. Despite efforts to reduce membrane fouling by improving membrane properties, optimizing operation conditions and pretreatment of feedwater, fouling is inevitable. As a result, one long term solution to ensure sustainable operation of membrane systems is to remove the foulant deposited via chemical cleaning when there is a significant drop in permeate flux or salt rejection, or when there is a need to increase the transmembrane pressure significantly to maintain the desired water flux [Li and Elimelech, 2004]. Fouling problems are a major challenge in membrane technology. Pretreatment by integrating a larger pore membrane (MF) into the RO systems resulted in longer membrane lifespan. Modification in membrane properties, modules and also feed water physical properties are intended to reduce fouling problems. Future development in membrane technologies should include more environmental friendliness and cost effectiveness.

In the area of freshwater colloidal and organic matter characterization, good protocols were developed for bench scale testing of different types of membranes followed by analytical techniques for studying the fouling layer. These studies have

provided insight into the fouling mechanisms for fresh surface waters and have led to great strides in the acceptance and rapid growth of the use of membrane in the drinking water industry. However, these mostly came from lab results only, little pilot plant or "real world" work was reported. Furthermore, feed water recovery, one of the most important parameters in membrane plants, usually approaches zero in such laboratory-scale setups because of the very small area of the membrane used, which result in negligible recovery or change in concentration factor.

1.1.4 Analytical methods for DOM

The characterization of both physical and chemical properties of NOM is important because of its role in the fate, reactivity and transport of inorganic and organic pollutants, and its impacts on potable water treatment unit operations.

A wide range of routine measurements have been developed to characterize DOM. These include TOC (total organic carbon), DOC (dissolved organic carbon), BOD (biological oxygen demand), COD (chemical oxygen demand). TOC is commonly synonymous of DOM in the aquatic environment [Henderson et al, 2009]; DOC, the soluble potion of TOC, is a more general parameter in water supply (0.1 mg/L~50mg/L) and detects all dissolved organic carbon without selection. BOD and COD are accepted as surrogates for monitoring organic contaminants and wastewater treatment processes [Lee and Ahn, 2004]. However, the procedures to obtain these parameters are tedious and time consuming. The isolation procedures to obtain a sufficient sample for structural characterization require processing large volumes of water and are labor intensive by these conventional methods. These methods are not practical in studies involving many

sampling sites or many time points. Therefore, simple characterizations of DOM that could be carried out rapid with small volumes of water samples would be convenient. Of particular importance is the ability to analyze bulk water samples rather than samples subjected to isolation, fractionation, and/or concentration. Optical sensing technologies based on UV absorption and fluorescence spectroscopy have been proposed to resolve these problems.

DOM contains chromophores and fluorophores through which DOM interacts with UV and visible radiation. Chromophores attenuate incident UV and visible light. UV-vis spectra of DOM are typically broad and nearly featureless because the number of possible types of chromophores is large and none possess an easily distinguishable spectrum. The absorbance of DOM decreases with increasing wavelength in nearly exponential fashion. Also, a variety of fluorophores in DOM absorb light over a wavelength of ~300-500 nm and emit fluorescent light at wavelengths somewhat longer than that of the incident light [Perdue and Ritchie, 2003; Senesi et al., 1989]. Fluorescence spectra of DOM are much more highly structured than the absorbance spectra.

For the purpose of describing the characteristics of DOM, different surrogate parameters have been investigated, including TOC, UV absorbance, SUVA (specific ultraviolet absorbance: UV_{254}/DOC), spectral slope (InA~λ). UV-vis absorbance (wavelength= 254-280nm) has often been used to estimate the aromatic content within DOM [Yuan, 2000] and UV absorbance is used to predict DBPs (disinfection by products) formation potential. UV absorbance correlates with THMFP (trihalomethane formation potential) and with molecular size and color [Gray and Bolto, 2003]. SUVA at

a specific wavelength correlates well with aromatic carbon content of DOM and DBP formation potential, because the “activated” aromatic structures constitute the primary sites attacked by chlorine or other oxidants [Fan et al, 2001]. Therefore, it is generally utilized as surrogate parameter to measure the DBPs formation [Lin et al., 2000]. But high nitrate content in low DOC water may interfere with this measurement. It has been demonstrated that SUVA is a sensitive surrogate parameter only for hydrophilic THM (trihalomethane) precursors.

Although UV absorbance spectroscopy has been commercialized for wastewater monitoring [Langergraber et al., 2003; Van Den Broeke et al., 2006], fluorescence has potential advantages over UV-vis absorbance for its higher sensitivity and DOM fingerprinting.

DOM fluorescence spectra are able to illustrate the complexity of its composition and structures. Excitation emission matrix fluorescence spectroscopy (3DEEM) has become a state-of-art technique in aquatic studies due to its non-destructive nature, good sensitivity and simple sample pretreatment. Additionally, a vast array of data is available for interpretation within this approach [Lombardi, 1999]. Rapid data collection (<1s) from small samples (5 mL) with high optical resolution and low detection level (ppb) make this fluorescence technique an attractive method. 3DEEM is widespread in marine and estuarine studies of DOM biological activity and associated protein fluorescence [Determann et al., 1998; Mayer et al, 1999; Parlanti et al., 2000; Yamashita and Tanoue, 2003; Jaffe et al., 2004], characterization of DOM from different sources [Coble, 1996; Jaffe et al., 2004; Clark et al., 2002], and organics held in and released from, sediment and mixing of water bodies [Komada et al., 2002; Sierra et al., 1997]. In the field of

freshwater, EEM has been applied to determine optical properties of DOM [Battin, 1998], the influence of pH on fluorescence of organic matter [Patel et al., 2002], characterization of DOM composition and source [Mounier et al., 1999; Hautala et al, 2000; Katsuyama and Nobuhito, 2002; Her et al., 2003], and comparison of organic matter fluorescence with standard IHSS model compounds [Senesi et al., 1989; Wu et al., 2003; Kalbitz and Geyer, 2001]. Beside these applications in natural waters, researchers have been used 3DEEM to assess water quality and monitor water pollution and optimize water treatment process [Ahmad and Reynolds, 1999].

Fluorescence studies on organic matter in the aquatic environment typically focus on humic substances and amino acids in proteins and peptides. Two main groups of DOM fluorophores are referred to as humic-like (UV humic-like and visible humic-like fluorophores) and protein-like fluorophores (tryptophan-like and tyrosine-like fluorophores). The protein-like fluorophores are so named because their fluorescence occurs in the same regions of optical space as authentic standards of these materials. However, there are still difficulties in identifying individual fluorescent compounds in water.

1.2 Objectives

DOM compositions have been the subject of this investigation. In the absence of a universal extraction method, I evaluated three methods for extractions of DOM. The goal is to achieve an efficient sample preparation method that is amenable for use to characterize DOM.

The use of 3DEEM fluorescence and UV spectroscopy as a diagnostic tool for water and wastewater control was investigated and discussed by linking fluorescence and absorbance analysis and current chemical water quality monitoring techniques.

1.3 References

Ahmad, S.R., and Reynolds D.M. (1999) Monitoring of water quality using fluorescence technique: prospect of on-line process control. *Water Res.* 33(9), 2069-2074.

Aiken, G.R. (1985) Isolation and concentration techniques for aquatic humic substances. *In Humic substances in soil, sediment, and water: Geochemistry, isolation, and characterization* (eds. G.R.Aiken, D.M.McKnight, R.L.Wershaw, and P.MacCarthy). Wiley, New York, pp.363-385.

Aiken, G.R., McKnight, D.M., Thorn, K.A., and Thurman, E.M. (1992) Isolation of hydrophilic organic-acids from water using nonionic macroporous resins. *Organic Geochemistry* 18, 567.

Amy, G.L., Collins, M.R., Kuo, C.J., and King, P.H.(1987) Comparing Gel-permeation chromatography and ultrafiltration for the molecular-weitht characterization of aquatic organic-matter. J. Amer.Water Works Ass. 79, 43.

Battin, T.J. (1998) Dissolved organic matter and its optical properties in a blackwater tributary of the upper Orinoco river, Venezuela. *Organic Geochemistry* 28(9 – 10), 561-569.

Bouvier, E.S.P., Iraneta, P.C., Neue, U.D., McDonald, P.D., Philips, D.J., Capparella, M., and Cheng, Y. F. (1998) Polymeric reversed-phase SPE sorbents - Characterization of a hydrophilic-lipophilic balanced SPE sorbent. *LC GC-Magazine of Separation Science* 16, 53.

Broeke, J., Langergraber, B.G., Weingartner,B.A. (2006) On-line and in situ UV/vis spectroscopy for multi-parameter measurements: a brief review. *Spectroscopy Europe* 18(4), 15-18.

Clark, C.D., Morais J., Jones, G. II, Lamardo, E., Moore, C.A., and Zika, R.G. (2002) A time-resolved fluorescence study of dissolved organic matter in a riverine to marine transition zone. *Marine Chemistry* 78(2 – 3), 121 – 135.

Dejanovic, K. and Cabaniss, S.E. (2004) Reverse-phase HPLC method for measuring polarity distributions of natural organic matter. *Environ. Sci. Technol.* 38, 1108-1114.

Determann, S., Lobbes, J.M., Reuter, R., Rullkotter J. (1998) Ultraviolet fluorescence excitation and emission spectroscopy of marine algae and bacteria. *Marine Chemistry* 62(1 – 2), 137 – 156.

Fan, L., Harris, J., Roddick, F., and Booker N. (2001) Influence of the characteristics of natural organic matter on the fouling of microfiltration membranes. *Water Res.* 35, 4455.

Garrels, R.M., Mackenzie, F.T., and Hunt, C., (1975) Chemical cycles and the global environment. *Assessing human influence*. Los Altos, California, William Kaufman Incp. 340p.

Gray, S.R., Bolto, B.A. (2003) Predicting NOM fouling rates of low pressure membranes, in: *Proceeding of the International Membrane Science and Technology (IMSTEC.* Sydney, Australia.

Hautala, K., Peuravuori, J., and Pihlaja, K. (2000) Measurement of aquatic humus content by spectroscopic analysis. *Water Res.* 34(1), 246-258.

Henderson, R.K., Baker, A., Murphy, K.R. Hambly, A., Stuetz, R.M., and Khan, S.J. (2009) Fluorescence as a potential monitoring tool for recycled water systems: A review. *Water Res.* 43, 863-881.

Her, N., Amy, G., McKnight, D., Sohn, J., and Yoon, Y. (2003) Characterization of DOM as a function of MW by fluorescence EEM and HPLC-SEC using UVA, DOC, and fluorescence detection. *Water Res.* 37(17), 4295-4303.

Jaffe, R., Boyer, J.N., Lu, X., Maie, N., Yang, C., Scully, N.M., and Mock, S. (2004) Source characterization of dissolved organic matter in a subtropical mangrove-dominated estuary by fluorescence analysis. *Marine Chemistry* 84(3-4), 195-210.

Kalbitz, K., and Geyer, W. (2001) Humification indices of water-soluble fulvic acids derived from synchronous fluorescence spectra — effects of spectrometer type and concentration. *Journal of Plant Nutrition and Soil Science-Zeitschrift Fur Pflanzenernahrung Und Bodenkunde* 164(3), 259-265.

Katsuyama, M., and Nobuhito, O. (2002) Determining the sources of storm flow from the fluorescence properties of dissolved organic carbon in a forested headwater catchment. *Journal of Hydrology* 268(1 – 4), 192-202.

Kitis, M., Kilduff, J.E., and Karabfil, T. (2001) Isolation of dissolved organic matter (DOM) from surface waters using reverse osmosis and its impact on the reactivity of DOM to form and speciation of disinfection by-products. *Water Res.* 35(9), 2225-2234.

Komada, T., Schoeld, O.M.E., and Reimers, C.E. (2002) Fluorescence characteristics of organic matter released from coastal sediments during resuspension. *Marine Chemistry* 79(2), 81 – 97

Langergraber, G., Fleischmann, N., and Hofstaedter, F. (2003) A multivariate calibration procedure for UV-vis spectrometric quantification of organic matter and nitrate in wastewater. *Water Science and Technology* 47(2), 63-71.

Lee N., Amy G., Croue J.P., and Busson H. (2004) Identification and understanding of fouling in low-pressure membrane (MF/UF) filtration by natural organic matter (NOM), *Water Res.* 38,4511-4523.

Lee, S., and Ahn, K.H. (2004) Monitoring of COD as an organic indicator in waste water and treated effluent by fluorescence excitation-emission (FEEM) matrix characterization. *Water Science and Technology* 50(8), 57-66.

Leenheer, J. A., Brown, P. A., and Noyes, T. I. In *Aquatic HumicSubstances, Influence on Fate and Treatment of Pollutants.* Suffet, I. H., MacCarthy, P., Eds.; Advances in Chemistry Series 219; American Chemical Society. Washington, DC,1989, pp 25–39.

Leenheer, J.A., Brown, G.K., and MacCarthy, P. (1998) Model of metal binding structures in fulvic acid from Suwannee River, Georgia. *Environ. Sci. Technol.* 32, 2410-2416.

Li, C.W., and Chen,Y.S. (2004) Fouling of UF membrane by humic substance: Effects of molecular weight and powder-activated carbon (PAC) pre-treatment. *Desalination* 170, 59-67.

Li, Q.L., and Elimelech M. (2004) Organic fouling and chemical cleaning of nanofiltration membranes: measurements and mechanism, *Environ. Sci. Technol.* 38, 4683-4693.

Lin,C.F., Lin, T.Y., and Oiver J.H. (2000) Effects of humic substance characteristics on UF performance. *Water Res.* 34(4), 1097-1106.

Mayer, L.M., Schick, L.L., and Loder, T.C. (1999) Dissolved protein fluorescence in two Maine estuaries. *Marine Chemistry* 64(3), 171-179.

Mcllvaine, R. (2008) Reverse Osmosis. *Chemical Engineering* 8, 20-24.

Miller, W.L., Moran, M.A., Sheldon, W.M., Zepp, R.G., and Opsahl, S. (2002) Determination of apparent quantum yield spectra for the formation of biologically labile photoproducts. *Limnology and Oceanography* 47, 343-352.

Mopper, K. (2007) Advanced instrument approaches. *Chemical Review* 107, 419-442.

Mounier, S., Patel, N., Quilici, L., Benaim, J.Y., and Benamou, C. (1999) Three-dimensional fluorescence of the dissolved organic carbon in the Amazon River. *Water Res.* 33(6), 1523-1533.

Parlanti, E., Worz, K., Geoffroy, L., and Lamotte, M. (2000) Dissolved organic matter fluorescence spectroscopy as a tool to estimate biological activity in a coastal zone submitted to anthropogenic inputs. *Organic Geochemistry* 31(12), 1765 – 1781.

Patel, N., Mounier, S., and Benjamin, J.Y. (2002) Excitation-emission fluorescence matrix to study pH influence on organic matter fluorescence in the Amazon basin rivers. *Water Res.* 36(10), 2571 – 2581.

Perdue, E.M., and Ritchie, J.D. (2003) Dissolved organic matter in freshwater. *Surface and groundwater, weathering and soils (*ed. J. I. Drevor). Vol 5. *Treatise on geochemistry* (ed.H.D.Hollard and K.K. Turekian). Elsevier-Pergamon, Oxford. pp 273-318.

Piccolo, A., Conte, P., Trivellone, E., Van Lagen, B., and Burman, P. (2002) Reduced heterogeneity of a lignite humic acid by preparative HPSEC following interaction with an organic acid. Characterization of size-separates by Pyr-GC-MS and H-1-NMR spectroscopy. *Environ. Sci. Technol. 36*, 76–84.

Piccolo, A., Stevenson, F.J. (1982) Infrared-spectra of Cu-2+, Pb-2+, and Ca-2+ complexes of humic-substances. *Geoderma* 27,195-208.

Pomes, M.L., Green, W.R., Thurman, E.M., Orem, W.H., and Lerch, H.E. (1999) DBP formation potential of aquatic humic substances. *J. Am.Water Works Assoc.* 91,103-115

Senesi, N., Miano, T.M., Provenzano, M.R., and Brunetti, G. (1989) Spectroscopic and compositional comparative characterization of I.H.S.S. reference and standard fulvic and humic acids of various origin. *The Science of the Total Environment* 81-82: 143-156.

Sheikholeslami, R. (1999) Fouling mitigation in membrane processes. *Desalination*. 123, 45–53.

Sierra, M.M.D., Donard, O.F.X., and Lamotte, M. (1997) Spectral identification and behaviour of dissolved organic fluorescent materials during estuarine mixing processes. *Marine Chemistry* 58(1 – 2), 51 – 58.

Simjouw,J.P., Minor EC, Mopper K (2005) Isolation and characterization of estuarine dissolved organic matter: Comparison of ultrafiltration and C-18 solid-phase extraction techniques. *Marine Chemistry* 96, 219-235.

Simpson, A. J., Kingery, W.L., Hayes, M.H.B. (2002) Molecular structures and associations of humic substances in the terrestrial environment. *Naturwissenschaften 89,* 84–88.

Stevenson, F. J. (1994) Genesis, composition, reactions. *Humus Chemistry,* 2nd ed.; Wiley & Sons. New York, pp.59-95.

Tansel, B., Bao, W.Y., and Tansel, I.N. (2000) Characterization of fouling kinetics in ultrafiltration systems by resistances in series model, *Desalination* 129, 7-14.

Thurman, E. M. (1985) *Organic Geochemistry of Natural Waters;*M. Nijhoff and W. Junk Publishers: Dordrecht, the Netherlands.

Woelki, G., Friedrich, S., Hanschmann, G., Salzer, R.; Fresenius, J. (1997) HPLC fractionation and structural dynamics of humic acids. *Anal. Chem.* 357, 548-552.

Wu, F.C., Evans, R.D., and Dillon, P.J. (2003) Separation and characterization of NOM by high-performance liquid chromatography and on-line three-dimensional excitation emission matrix fluorescence detection. *Environmental Science & Technology* 37(16), 3687-3693.

Zepp, R.G., Sheldon, W.M., and Moran, M.A. (2004) Dissolved organic fluorophores in southeastern US coastal waters: correction method for eliminating Rayleigh and Raman scattering peaks in excitation-emission matrices. *Marine Chemistry* 89, 15-36.

CHAPTER 2

Fractionating NOM by Ion-pairing Reagent

2.1 INTRODUCTION

Natural organic matter (NOM) plays an important role in pollutant chemistry and geochemistry, including controlling particle stability and transport, metal complexation and production of disinfection by-products (DBP) in water treatment [Christman, 1983]. NOM is a complex mixture of aromatic and aliphatic hydrocarbon structures that have attached functional groups including amides, carboxyls, hydroxyls and ketones [Chen et al., 2002]. Understanding the structural chemistry of hydrophobic and hydrophilic NOM components can be very useful in designing new water treatment processes to remove these disinfection by-product precursors.

DOM (dissolved organic matter), the soluble portion of NOM, is the organic precursor to disinfection by-product (DBP) formation and is present in nearly all water supplies [Stevens et al., 1976; Christman et al.,1983; Liang and Singer, 2003; Pomes et al., 1999]. Two main fractions of DOM, relative hydrophobic (humic substances) and relative hydrophilic (non-humic substances), have been investigated extensively in order to reveal their reactions with disinfectants [Collins et al., 1986; Li and Chen, 2001; Watt et al., 1996]. However, there is still no agreement on what role they play in the DBP formation. Since the hydrophobic/hydrophilic distribution in DOM will influence the relative distribution of different types of DBP, understanding their DBP formation potential and which fractions are the main precursors should help to design procedures

for water treatment. Moreover, knowledge about the partitioning of DOM would improve understanding of the fate and transportation of organic and inorganic pollutants.

Isolation and fractionation procedures of DOM have been discussed fully by Aiken and Stevenson etc, [Thurman and Malcolm, 1981; Aiken, 1984; Stevenson et al., 1994; Aiken, 1988; Perdue and Ritchie, 2003; Mantoura and Riley, 1976]. The most popular methods to isolate and separate DOM are using XAD resin adsorption and membrane separation. The methods which are claimed to fractionate humic substances based on their polarity are XAD resin and RP-HPLC (reverse phase high performance liquid chromatography) [Masami et al., 2006; Shibu et al., 2005; Swietlik et al., 2005; Senesi et al., 1990; Mopper et al., 1993]. XAD resin is generally used for preparation, and HPLC is used analytically.

Most fractionation methods still rely on techniques developed in the 1970's and later on modified in the 1980's [Thurman and Malcolm, 1981; Leenheer and Huffman, 1976; Mantoura et al., 1976]. The most prevalent procedures for fractionating NOM are based on XAD resin, developed initially by Weber and Wilson [Weber, 1975; Perdue and Ritchie, 2003] and currently accepted as a standard by International Humic Substances Society (IHSS). This XAD resin scheme separates NOM into operationally defined polar and non-polar fractions based on the interaction between hydrophobic moieties in NOM and the resins [Leenheer and Huffman, 1976; Thurman, 1982]. XAD resins were used to remove and concentrate humic substances from large volumes of water [Thurman and Malcolm, 1981], and have been used to determine DOM distribution between operational categories based on polarity (relatively hydrophobic or hydrophilic) using pH gradient elution. Combined with ion exchange resins, DOM can also be classified as acid/neutral/

base fractions [Leenheer and Huffman, 1976]. The six fractions are hydrophobic acid, hydrophobic neutral, hydrophobic base, hydrophilic acid, hydrophilic neutral and hydrophilic base [Marhaba et al., 2000]. Imai [Imai et al., 2003] fractionated DOM into 5 classes: aquatic humic substances (AHS), hydrophobic neutrals (HoN), hydrophilic acids (HiA), bases (BaS) and hydrophilic neutrals (HiN).

Resin separations are both operationally and conceptually complicated procedures. First, fractionation of NOM by XAD resin uses extreme conditions such as pH <2 or pH >10, and the strong acidic or basic environment could change the nature of hydrophobic or hydrophilic fractions. Second, hydrophobic and/or hydrophilic portions may be lost in the separation steps either due to irreversible sorption onto the resins or incomplete ability to adsorb [Leenheer and Huffman, 1976; Leenheer, 1981]. Thus, this classical XAD approach is limited to some extent by loss of some compounds, and being time and labor intensive (a multiple-day process).

Use of reverse phase high performance liquid chromatography (RP-HPLC) to discriminate between hydrophobic and hydrophilic fractions of NOM has been complicated by low resolution, low recovery and difficult interpretation [Shibu et al., 2005; Fettig, 1999; Dejanovic and Cabaniss, 2004; Abbt-braun and Frimmel, 1999]. The most important factor in applying RP-HPLC to measure the polarity distribution of DOM is the calibration standards, and the standards should have similar structures with DOM. Since the real structures of DOM are unknown or at least are in debate, the choice of the reference standards and therefore the results of this method are unclear. Moreover, column interaction, suitable data handling of chromatograms etc, limit the development of separation DOM by RP-HPLC [Her et al., 2002].

Hydrophobicity is not an intrinsic parameter of NOM, but depends on the operational method used for its determination [Her et al., 2002]. To a large extent, the procedures depend on controlling the electrical charge and hydrophobic structures of the humic matter. Because the molecular charge of DOM is governed primarily by the degree of ionization of acid groups, pH may be the main factor influencing the hydrophobicity of NOM. At low pH value, NOM is protonated and less ionized, and therefore more hydrophobic. At high pH, NOM is deprotonated and more ionized, thus more hydrophilic.

As chemical and biological products of plant and animal residues [Parlanti et al., 2002; Liang and Singer, 2003], humic substances are similar to the peptides by their polarity and MW distribution. Based on the ideas of peptide purification protocols using anionic ion-pairing reagents for peptide separations [Shibu et al., 2005; Mant and Hodges, 1991; Cunico et al., 1998; Mant et al., 2002], the protocol of peptide separation uses hydrophobic anionic ion-pairing reagent to interact (ion-pair) with positively charged peptide residues. Hydrophobic anions will not only neutralize the positively charged groups, thereby decreasing peptide hydrophilicity, but will increase further the affinity of the peptides for the reversed-phase sorbent, thereby separating the target peptide from the mixtures [Shibu et al., 2005].

This work develops a novel method to fractionate humic matter based on the hydrophobicity following the theory of XAD fractionation and the approach of peptide separation with ion-pairing reagent [Egeberg, 2002; Senesi, 1991; Mcgarry and Baker, 2000; Sutton et al., 2005]. Addition of a hydrophobic cation to DOM will neutralize the negatively charged groups, thereby decreasing the hydrophilicity of humic substances to

allow them to partition into a less polar solvent: this liquid-liquid extraction should be a faster, easier separation method than XAD resin fractionation. The applications of ion-pairing reagent for DOM fractionation have been reported by 3 groups [Smith and Warwick, 1991; Whelan and Kamali, 2003; Masami et al., 2006]. Smith [Smith and Warwick, 1991] applied ion-pair chromatography to separate fulvic acid into a number of organic constituents, and these fractions were just classified by the molecular weight cut-off with no other detail. Whelan [Whelan and Kamali, 2003] tried to separate humic-substances into compound classes by polarity using ion-pair chromatography, but they classed peak clusters with very rough definition such as small or large molecules and polar or least polar etc. Fukushima et al. [Masami et al., 2006] reported that fulvic acid could be separated from soil extracts based on the precipitation of an ion-pair with a cationic surfactant.

Three dimensional excitation and emission matrix fluorescence spectroscopy (3DEEM) has been demonstrated to be a useful, non-destructive analytical method for the characterization of NOM fractions. 3DEEM have been used to characterize and discriminate among humic substances of different origins [Coble, 1990; Coble, 1996; Swietlik et al., 2005]. More recently, this technique has been employed to study the structures of NOM and humic fractions [Sierra et al., 2006; Her et al., 2002; Mopper et al., 1993; Del Castillo et al., 1999; Baker, 2001; Parlanti et al., 2002]. Since the chemical nature of fluorescent material in NOM is still not understood well, successful isolation of specific fluorophores would be significant for NOM chemical characterization [McKnight et al., 2001]. 3DEEM fluorescence spectroscopy is an attractive analytical tool because it is at least an order of magnitude more sensitive to DOM than UV

absorbance [Chen, 2002].

The object of this work is to characterize comparative study of the fluorescence properties of humic acids (HA) and fulvic acids (FA) before and after solvent extraction by using 3DEEM. The specific objectives of this work were: 1) to assess the effects of pH (from pH 2 to pH 14) on NOM, specifically on hydrophobicity; 2) to introduce a new method to separate NOM into different types of fluorophoric groups by addition of a cation ion-pairing reagent; 3) to determine the effect of the ion-pairing reagent and different solvents on separation efficiencies; 4) to investigate the feasibility of this fractionation technology as part of a broader application, future HPLC separation.

2.2 MATERIALS AND METHODS

2.2.1 Materials

Samples. Experiments were carried out with the DOM stock solutions from a Reverse-Osmosis isolate sample from McDonald's Branch (McDonald's RO-sat 5/12/97). International Humic Substances Society (IHSS)-- Suwannee River fulvic acid standard (FA) and Suwannee River humic acid standard (HA) were also used. Solid samples were dissolved in the Milli-Q water to make DOM stock solutions, then the solutions were stored at room temperature (T=25 °C) in the dark until analyzed. The concentrations of DOM samples range from 2.0 mg/L up to 20.0 mg/L as total mass DOM, not DOC. Because molecular charge is the most influential factor governing the hydrophobicity of DOM [20], all of the experiments were maintained at their initial pH during the experiment except the pH dependent experiments.

pH-Dependent experiments. The effects of pH (between 2 and 14) on the fluorescence of humic substances were examined by the dropwise addition of either 1 M NaOH (Merck KGaA, Darmstadt, Germany) or 1 M HCl (Sigma-Aldrich Riedstr, Switzerland). Samples were covered and equilibrated until the pH value was constant. The pH differential between 2.0 mg/L and 20.0 mg/L was less than 0.1, so the effects of the dilution on the pH could be ignored.

Partitioning experiments. A shake-flask method (separation funnel with manual shaking) was employed to determine the organic solvent-water partitioning of dissolved organic matter. Partitioning was performed in the absence and presence of ion-pairing reagent. In the presence of ion-pairing reagent, 0.05 g – 1 g (0.015 M-0.3 M) of tetrabutylammonium hydrogensulfate (>97%, Aldrich, WI, USA) were added to 10.0 mL

20.0 mg/L NOM solution, then extracted by 10 ml acetonitrile (HPLC grade, Burdick & Jackson, MI, USA), diethyl ether (HPLC grade, Burdick & Jackson, MI, USA) or 1-octanol (>98%, Merck KGaA, Darmstadt, Germany) respectively. The contact time for the solutions was 10 minutes. Both the organic and aqueous portions from liquid-liquid separation were analyzed as described below.

2.2.2 Analytical methods

A. Fluorescence spectroscopy

3D EEM Spectroscopy Excitation-emission matrix fluorescence was performed using a Cary Eclipse fluorescence spectrophotometer (Varian Inc). Approximately 3 mL of the sample was placed in the fluorescence quartz cell. To collect a single EEM, excitation wavelength (λ_{ex}) was set to 200 nm and emission wavelength (λ_{em}) was scanned from 300-600 nm; then λ_{ex} was increased by 10 nm and the emission scan repeated until the last scan had λ_{ex} at 400 nm. A λ_{em} step size of 10 nm was chosen for collection of EEM spectra. The slit width was 5 nm for λ_{ex} and 10 nm for λ_{em}. All the EEM spectra were scanned at 600 nm/min with averaging time 0.1 s. And the excitation filter was set auto, the 295-1100 nm emission cutoff filter was used in scanning to eliminate second order Rayleigh light scattering on the DOC response in the emission range of 400-600 nm. PMT gain was set at 750 volts. The baseline noise (RMSE) was 0.3 a.u. (arbitrary unit). Triplicate scans were conducted for the samples and the average standard deviation of maximum intensity is <1%. Fluorescence emission intensities were reported in arbitrary units (a. u.) and always automatically corrected by the measurement system for variations in the excitation lamp spectral profile and any temporal intensity variation. Fluorescence

measurements were made at a regulated temperature, 25°C, because fluorescence is temperature-dependent.

Milli-Q water was used as blank, then Milli-Q blanks were subtracted from each DOM EEM scan. Since the concentration of all samples was less than 20 mg/L and the absorbance is <0.1 a.u., no internal quenching correction was applied. Although no further corrections for fluctuation of instrumental factors and for scattering effects (e.g. primary and secondary inner filter effects) were applied, a comparative discussion on spectra is possible, since all of them were recorded on the same instrument using the same experimental conditions.

It is difficult to make use of all the information collected with EEM spectroscopy. In this paper, characterization of DOM composition will be based on 3-D plots, contour plots, number of fluorescence peaks, position of wavelength-independent fluorescence maximum ($\lambda_{ex}/\lambda_{em}$), fluorescence intensity at $\lambda_{ex}/\lambda_{em}$, and the ratios of different peaks.

B. UV-vis Spectroscopy

UV-vis absorbance spectra were collected on Cary 50Bio UV-Vis spectrophotometer with approximately 3 mL samples. Using baseline correction, absorbance between 200 nm and 600 nm were used to characterize and compare the samples. All absorbance were collected at 24000 nm/min scanning speed, 2 nm data interval. The typical baseline RMSE noise was +0.0055 au (no correction) or +0.0003 au (baseline correction).

All the UV-Vis absorbance measurements were performed using the Milli-Q water as blank.

2.3 RESULTS

All DOM fluorescence peaks are broad and overlapping in the emission spectrum (Figure 2.1). The contour plots of 3DEEM show the number of fluorescence peaks, positions of the fluorescence maxima ($\lambda_{ex}/\lambda_{em}$) and fluorescence intensity at $\lambda_{ex}/\lambda_{em}$ (Figure 2.2). The X-axis represents the emission wavelength λ_{em} from 300 to 600 nm. The Y-axis represents the excitation wavelength λ_{ex} from 200 to 400 nm. The contour lines represent the distribution of fluorescence intensity at different excitation-emission wavelength pairs as the third dimension. The ridge with high fluorescence values at 45° angle in the left upper part of the contour plots represents water Rayleigh scattering, which is not related to the fluorescence characteristics of the sample. Two peaks were easily identified for the DOM fluorescence. The peak at longer excitation wavelength (λ_{ex}= 320-330 nm) has been attributed to visible humic-like fluorophores (peak C) [Coble, 1990; Coble, 1996], with maximum emission intensity at λ_{em}= 450-460 nm. The other peak is responsible for UV humic-like fluorophores (peak A) [Coble 1990,1996]. With fluorescence maximum at λ_{ex}= 210-230 nm and λ_{em}= 430-450 nm, peak A fluorophores had much stronger emission intensity than the peak C fluorophores. The presence of two major types of fluorophores is clearly visible from the topographic views (Figure 2.2).

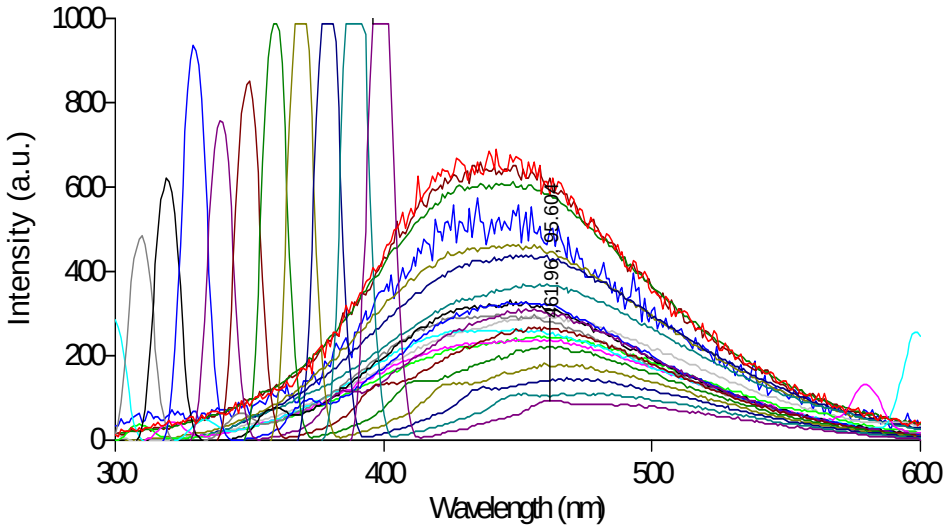

Figure 2.1 2-D Emission spectra of DOM (20 mg/L). X-axis is emission wavelength, Y-axis is fluorescence intensity, and the individual lines are excitation wavelengths.

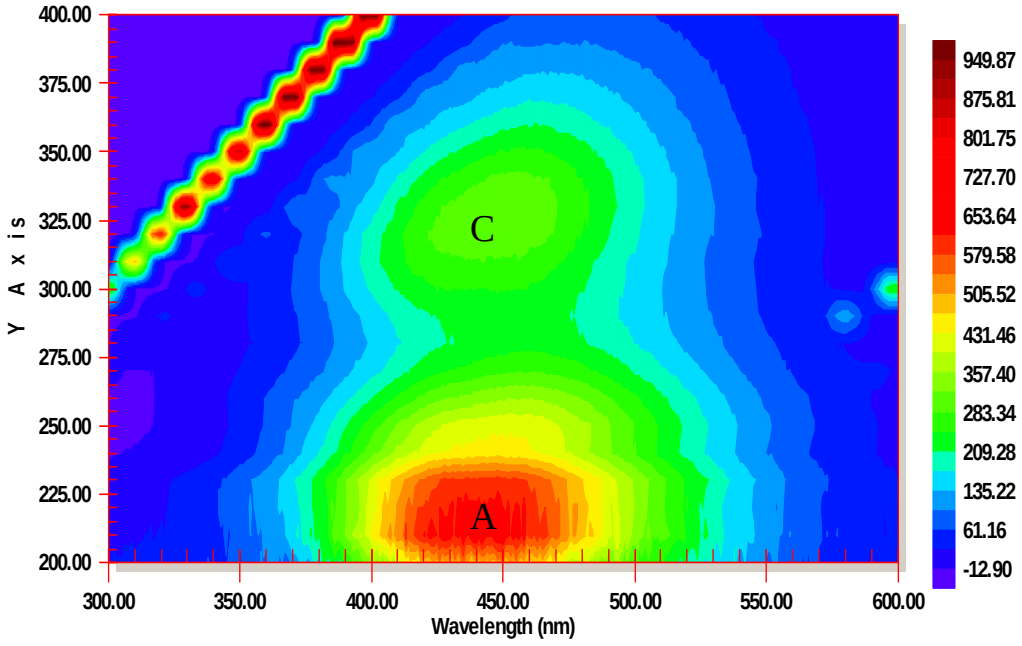

Figure 2.2 The contour map of DOM (20 mg/L) (Peak A is UV humic-like fluorophores, peak C is Visible humic-like fluorophores. The line at the up left corner is first order of Rayleigh scatter). X-axis is emission wavelength, Y-axis is excitation wavelength, and the color is fluorescence intensity.

2.3.1 The relation of DOC with SUVA and FI/DOC

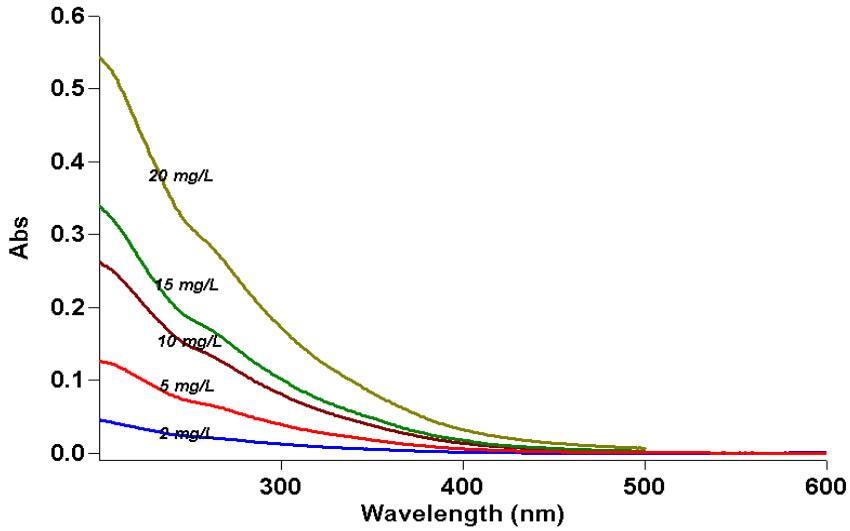

Figure 2.3 UV absorbance spectra of NOM at different concentration (2-20 mg/L).

The linear relationships ($R^2 > 0.98$) between UV absorbance (Figure 2.3) and DOM concentration (Figure 2.4), and between fluorescence intensity and DOM concentration (Figure 2.5) indicate that the inner filter effect did not significantly affect fluorescence analysis for peak As and C at these concentrations (<20 mg/L).

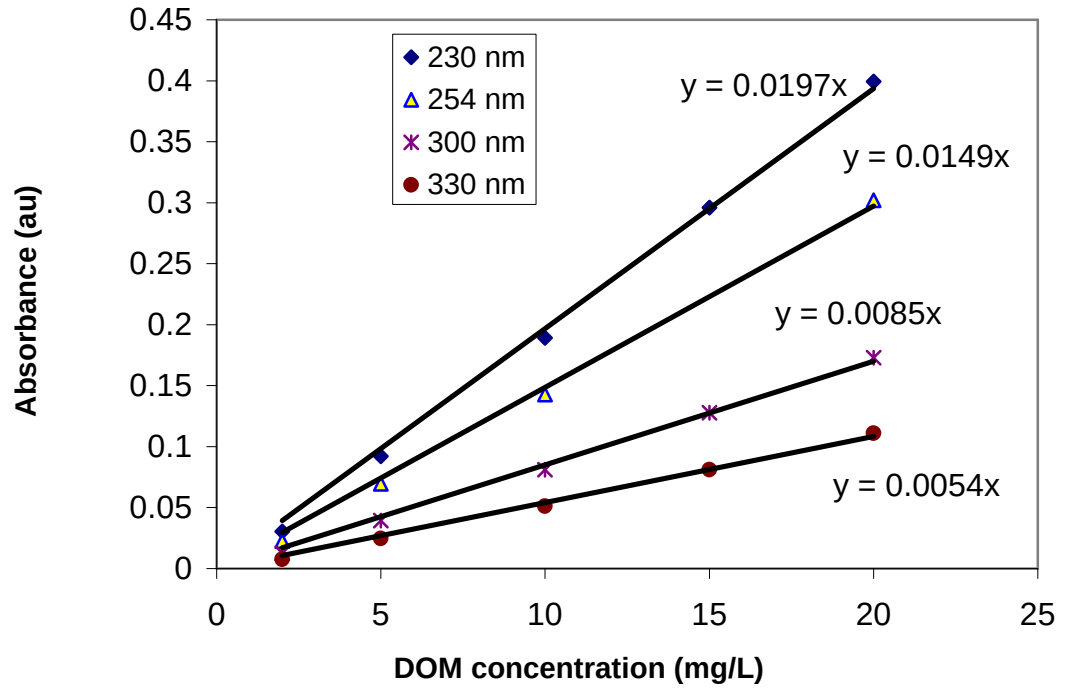

Figure 2.4 The linear relationship between UV absorbance and DOM concentration at four wavelengths of 230 nm, 254 nm, 300 nm and 330 nm.

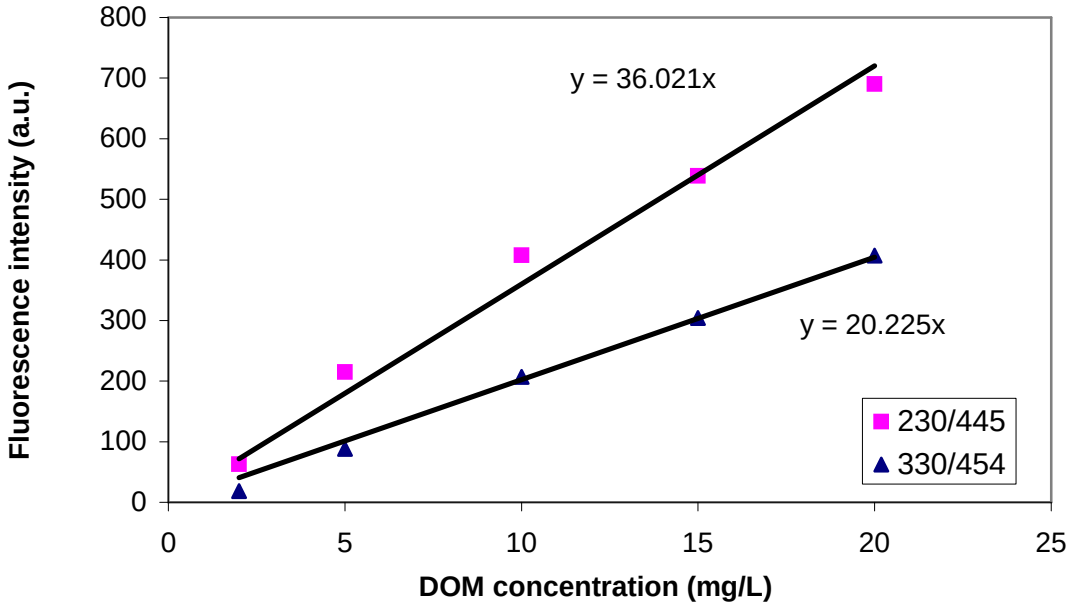

Figure 2.5 The linear relationship between fluorescence intensity and DOM concentration for both peak A ($\lambda_{ex}/\lambda_{em}$= 230/445 nm) and peak C ($\lambda_{ex}/\lambda_{em}$= 330/454 nm).

Specific UV absorbance (SUVA) is the ratio of UV absorbance at a given wavelength (usually 254 nm) to the concentration of DOC in the water solution. SUVA is a practical parameter that provides insight into the nature of NOM and its fractions. It has been correlated to aromatic content [Chin et al., 1994]. SUVA is also believed to indicate the amenability of DOC removal and is a valuable characterization parameter for the assessment of NOM reactivity during water treatment [Croue et al., 1999; Roccaro, 2009; Kitis et al., 2001; Reckhow et al., 1990; Edzwald, 1985].

A similar normalized parameter is maximum emission intensity/DOC (FI/DOC), which should be independent of the concentration of DOC.

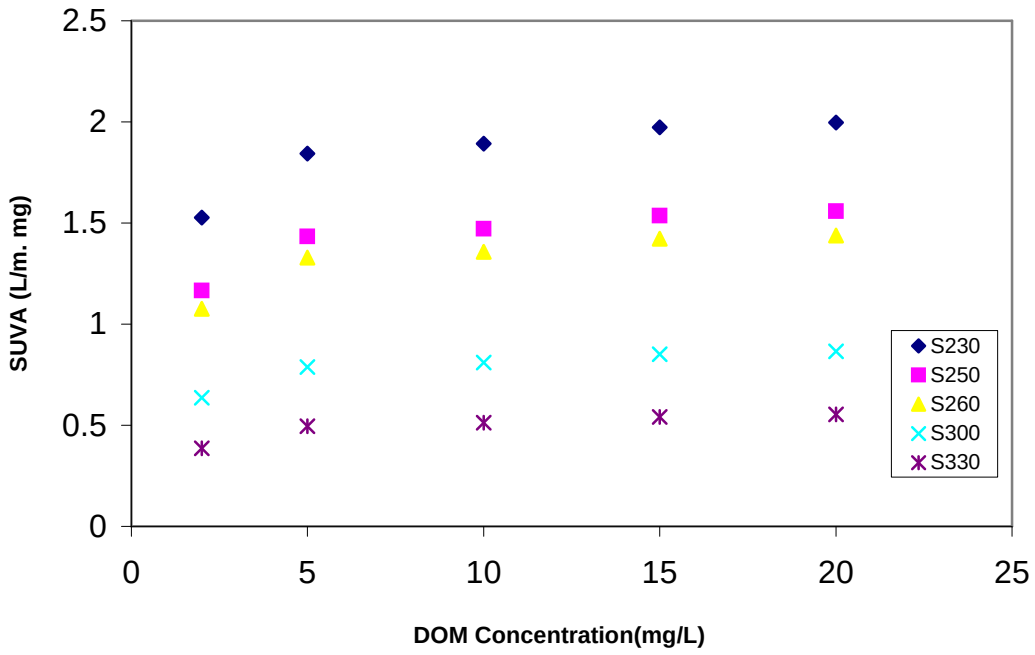

Figure 2.6 SUVA change as function of DOM concentration at different wavelengths.

By investigating the relationship between SUVA and DOC concentration for several excitation wavelengths at maximum intensities (Figure 2.6), SUVA values are close

(standard deviation < 10%) when solution concentration changed from 5 mg/L to 20 mg/L, except the sample with the concentration of 2 mg/L showing a relative lower value. For the Peak A (230, 250, 260), SUVA values were around 1-2 (m^{-1} L mg^{-1}), while for the peak C (300, 330), SUVA values are about 0.3-0.9 (m^{-1} L mg^{-1}).

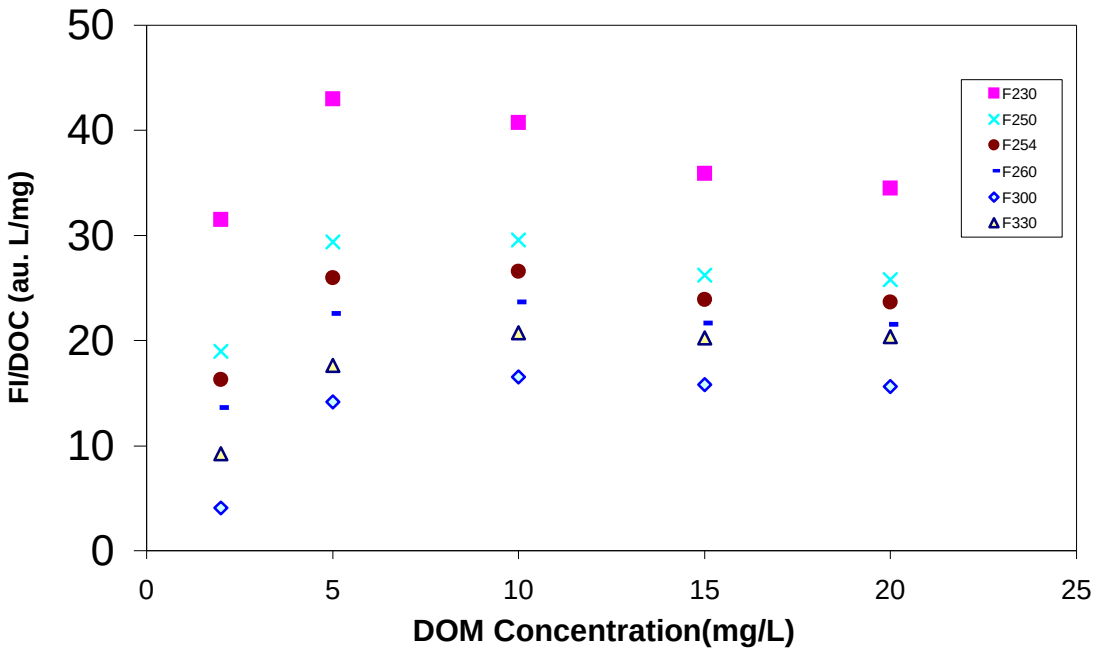

Figure 2.7 Fluorescence intensity/DOC change as function of DOM concentration at different excitation wavelengths at λ_{em}=445 nm (FI=maximum emission intensity).

FI/DOC shows a similar trend from 5 to 20 mg/L except the concentration was 2 mg/L (Figure 2.7).

2.3.2 The effect of pH

A. Change in intensity

Since NOM contains phenolic and carboxyl functional groups (refer to Figures 1.1 and 1.2 in Chapter 1), its charge density is pH sensitive and resulting optical properties

such as absorbance and fluorescence are also pH sensitive (Figure 2.8). The emission and excitation wavelengths of maximum emission intensity are independent of pH from pH= 2 to pH=8 and visually contour maps of peaks A and C do not change. The fluorescence emission intensities of both peaks increase gradually as pH increased from 2 to 8 and reached a maximum at pH 8. After that, emission intensities decrease when pH increased from 8 to 10. This result is different from some previous observations that emission intensity was the highest at most basic pH [Chen, 2002; Mobed et al., 1996; Miano and Sposito, 1988; Pullin and Cabaniss, 1995]. In the same sample solution, if pH was adjusted from 8 to 2, the contour shapes and maximum excitation/emission wavelength do not change, although the maximum emission intensities decrease.

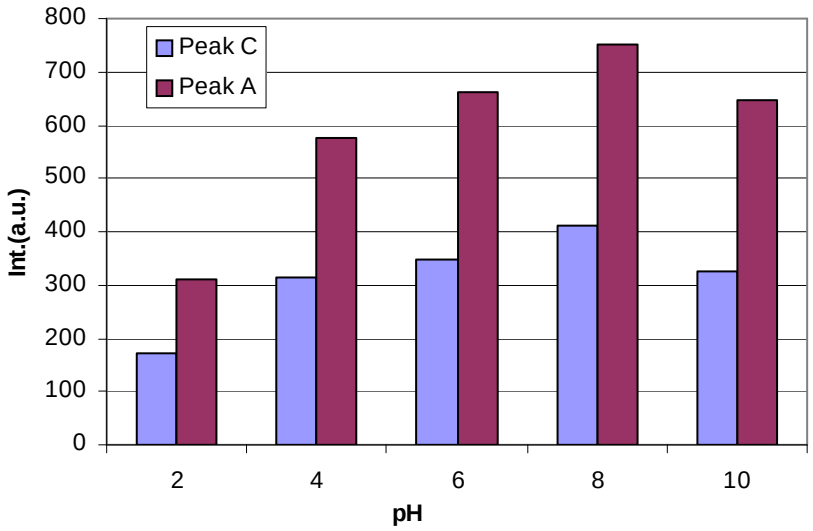

Figure 2.8 The maximum intensities changed with pH varying from 2 to 10 for peaks A and C.

B. Shape change at pH 10

However, for peak C at pH 10, the shape of the contour plots change (Figure not shown) and the excitation spectra are broadened compared to those of the initial sample. The increased sensitivities and its extension of excitation wavelength from 370 nm to 400 nm, make the contour plots show a shape change in this region from circular to oblong as the pH increased from 8 to 10. At pH 10, the shape of peak C altered without the maximum excitation or emission wavelength shift, maximum $\lambda_{ex}/\lambda_{em}$ was still at 330/450 nm. However, the decrease in intensities has small absolute slope as pH increased from 8 to 10, this kind of slow intensity attenuation made the excitation wavelengths (not the maximum λ_{ex}, but the longer excitation wavelengths than λ_{ex}) extend and excitation spectra broaden. But $\lambda_{em\ max}$ don't change and emission spectra keep the same. These extension of excitation spectra resulted in the contour shape of peak C changed from round and wide to elongated and narrow. It looks like the peak C was compressed along the emission wavelengths.

C. Hysteresis after pH 10

The fluorescence of peak C showed hysteresis when pH was raised above 10 and then decreased, even after the pH returned back to its weak acidic environment. In order to investigate the effects of high pH on peak A and C, several different pH values from acidic to basic were explored as pH varied as 5→2→5 (Figure 2.10), 5→10→5 (Figure 2.11). Increased the pH from 5 to 10 and then returned to pH=5 showed a change in the spectra of peak C at pH=5 comparing with the original spectra (pH=5). However, decreasing the pH from 5 to 2 and then retuned to pH=5 did not change the spectra

comparing with the original one. It's very obvious that emission intensities of both peaks A and C are enhanced after increasing pH to a relative high value (pH =10) then back to its original pH. The extent of intensity enhancement of peak C was much less than peak A, the former increased about 40 a.u. and the latter increased almost 130 a.u. comparing the solution at pH=5 before and after basified to pH=10 (Figure 2.9). The difference between peak A and C was, peak C changed both intensity and shapes as a function of pH, while only intensity alteration for peak A. The interesting thing is, intensities and spectra almost don't change at the same pH for both peaks if pH decreased to 2 and then returned back.

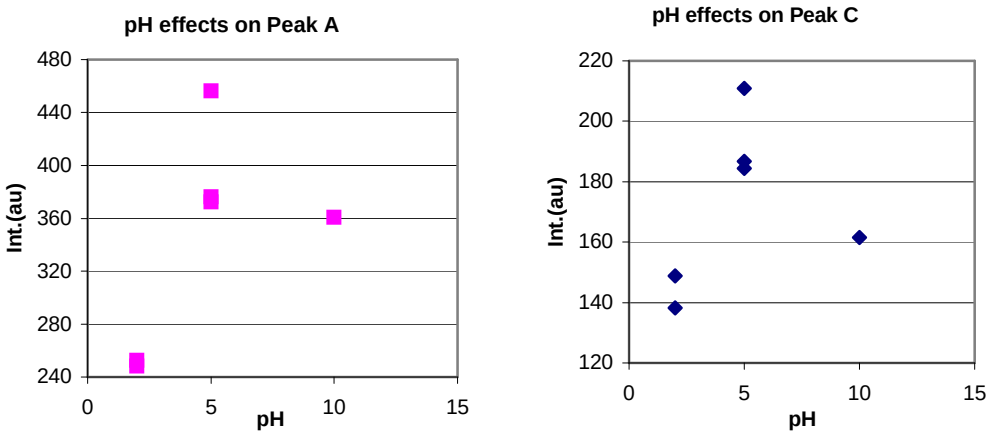

a b

Figure 2.9 The effects of pH on fluorescence intensity of peak A (a) and peak C (b) by the procedures of pH 5→2→5 and pH 5→10→5.

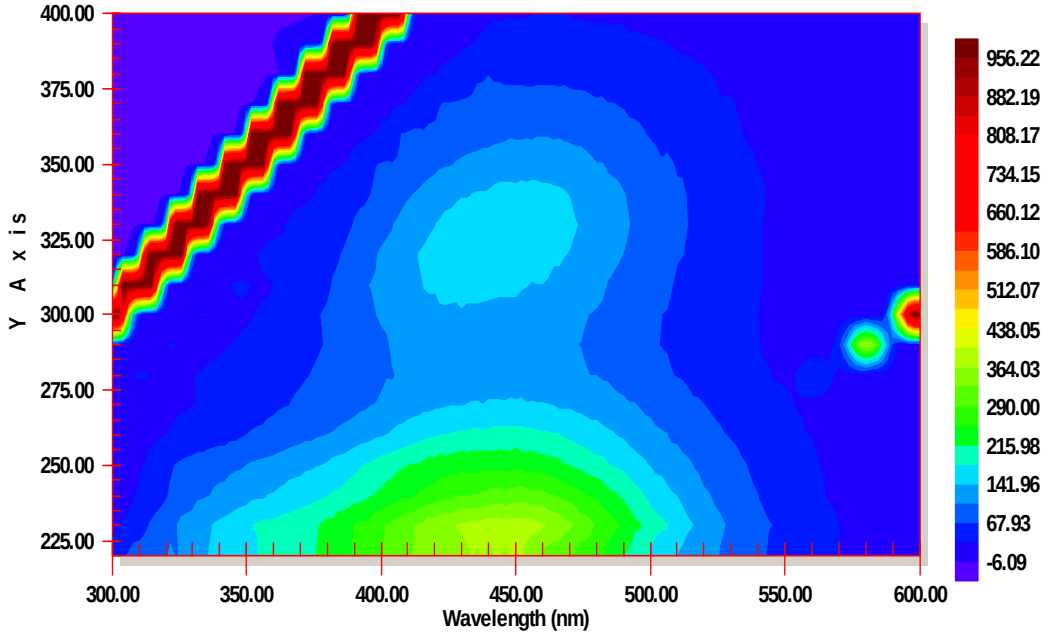

a

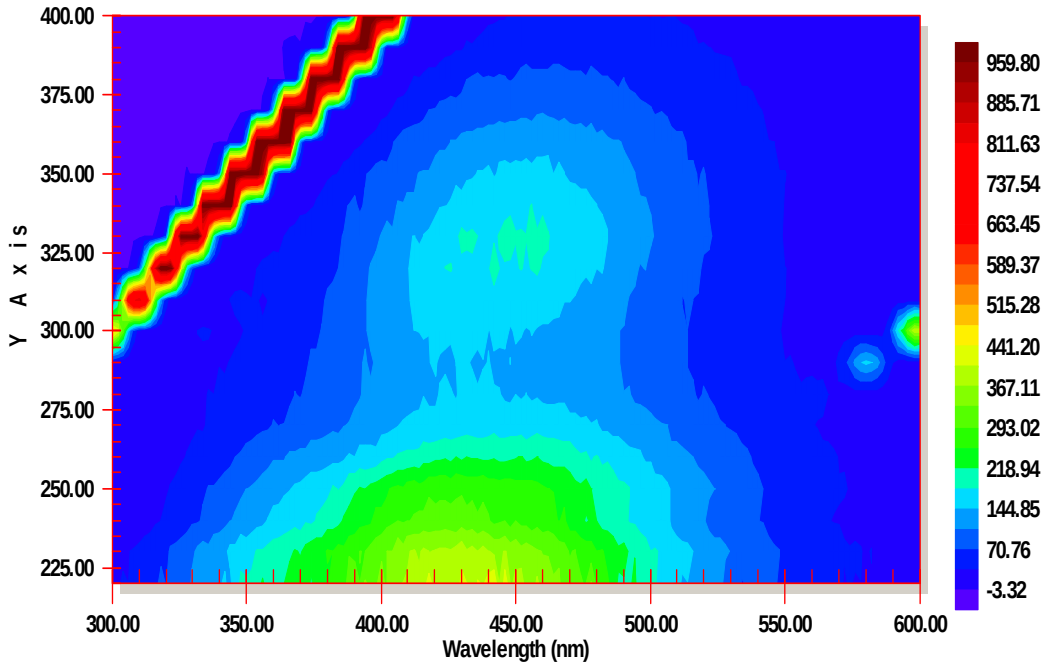

b

Figure 2.10 The contour plots of DOM at pH=5 by the procedure of pH 5(a)→2→5(b).

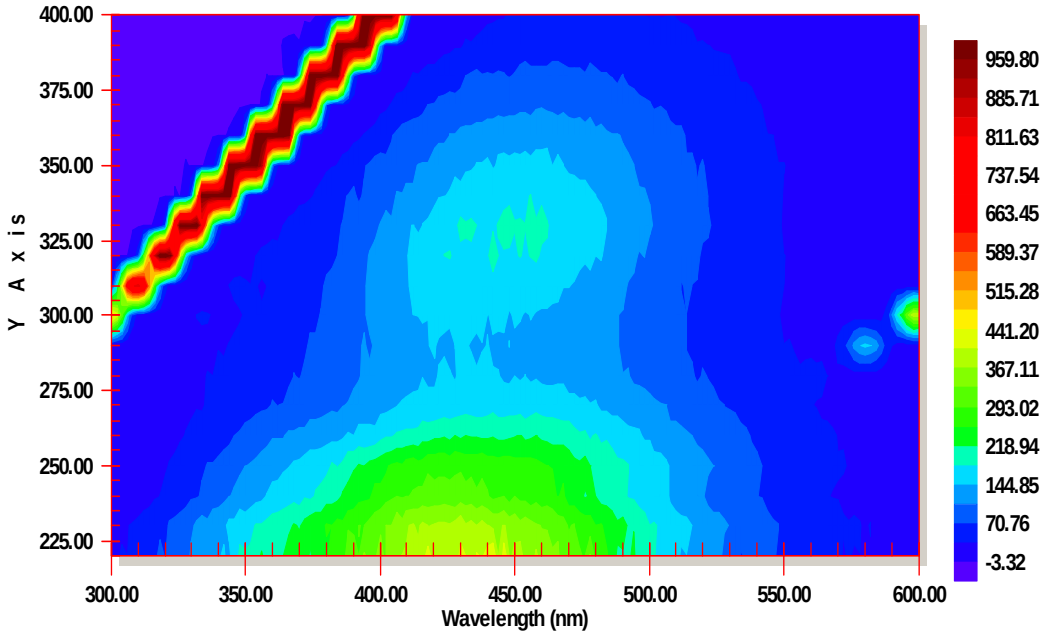

a

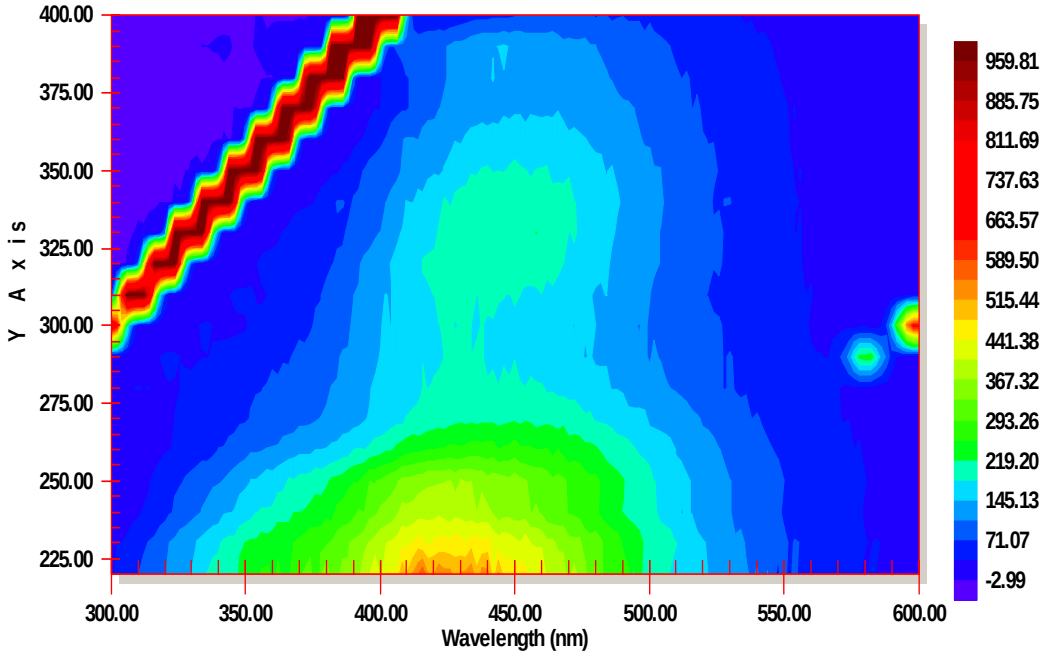

b

Figure 2.11 The contour plots of DOM at pH=5 by the procedure of pH 5(a)→10→5(b).

Comparing the maximum emission intensities between low and high pH values (Figure 2.11), it was observed that fluorescence intensities decrease a lot (about 300 au for peak A and 180 au for peak C) compare to its original intensity (pH~5) when pH decreased to 2, although pH value just decreased 3 units. The same results were obtained when pH increased to 12 (pH increased up to 6 units). Fluorescence intensities decrease at the extreme pH conditions, whether extreme acidic or basic conditions. But it seemed that extreme acidic condition had stronger adverse influence on the intensity than that of the basic pH.

D. Change in peak ratio

Fluorescence maximum emission intensities ratio of the fluorophores A and C, $r = I_A/I_C$, was described as a potential organic matter (OM) quality parameter and was examined according to the pH. If r is strongly pH-dependent, r ratio is proposed as a good indicator of OM maturing. By investigating r change in the whole pH range from 2 to 10, the results demonstrated that r responded in the same manner to pH. When pH increased, r increased too. However, r just increased a little bit (about 0.4) when pH value changed from 2 to 10.

2.3.3 The effects of ion-pairing reagent and solvents on partitioning

A. The effects of ion-pairing reagent on DOM partitioning

Because of the amphiphilic and negative charged characteristics of humic and fulvic acids, an ion-pairing reagent was applied to investigate if there is any possibility to separate humic substances from the matrix or separate humic acids from fulvic acids by

exploring the change of fluorescence. The results indicated that addition of ion-pairing reagent not only changed emission spectrum, but maximum emission intensity as well. The shapes of both visible humic-like (peak C) and UV humic-like (peak A) fluorescence changed from round to long elliptical shapes, especially peak C. More importantly, the peak emission wavelength (λ_{em}) blue-shifted from 450-460 nm to 400-430 nm for peak C and From 430-450 nm to 390-440 nm for peak A respectively when ion-pairing reagents varied from 0.1 g to 0.8 g. As the ion-pairing reagent concentration increased, the maximum emission wavelengths gradually shift to shorter values. Before the ion-pairing reagent was added, the peak excitation wavelength occurred at λ_{ex}= 210-230 nm, and the emission intensities at these three wavelengths were almost the same. After ion-pairing reagent addition, the peak excitation occurred at λ_{ex}= 230 nm, followed by excitation wavelengths of 220 nm and 240 nm. Moreover, the emission intensities of these three wavelengths were different and the sensitivities of these three wavelengths on the amount of the ion-pairing reagent were varied, 230 nm is the most sensitive.

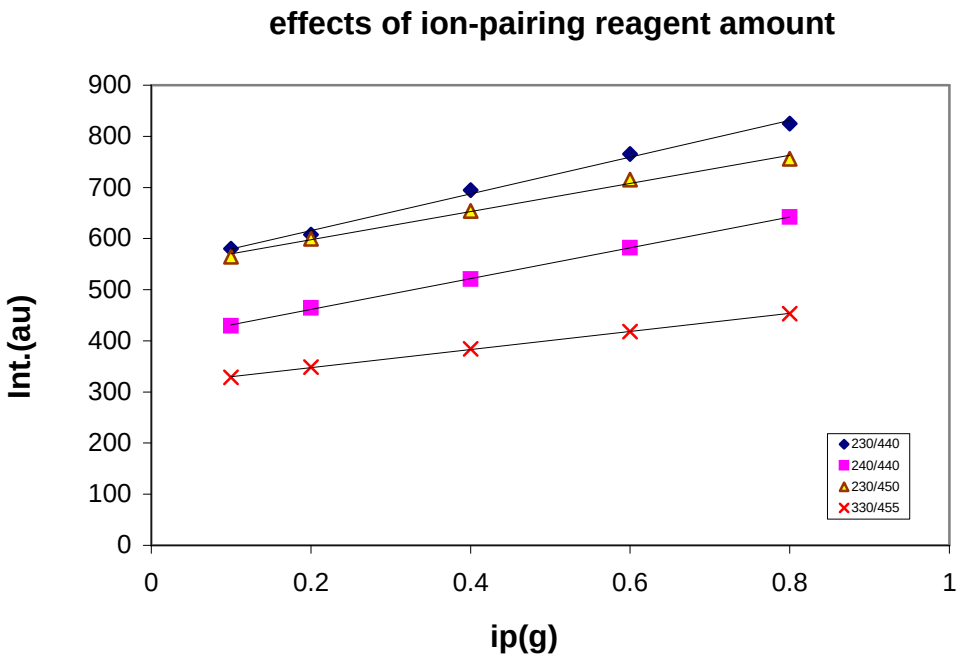

Figure 2.12 The linear relationship of ip (ion-pairing reagent) with the maximum emission intensity for peak A ($\lambda_{ex}/\lambda_{em}$ =230/440 nm, 240/440 nm, 230/450 nm) and peak C ($\lambda_{ex}/\lambda_{em}$ =330/455 nm).

There is a linear relationship between amount of ion-pairing reagent and emission intensity for peaks A and C (Figure 2.12). However, the ion-pairing reagent had an unexpected effect on emission intensity at low levels (Figure 2.13), the intensity decreased to below that of the original solution (before ion-pairing reagent was added) at all explored wavelengths. Then, after the amount of ion-pairing reagent reached a specific value (this value was named as critical value because it was a boundary to have contrary performances with ion-pairing reagent addition), the emission intensities were enhanced with increasing concentration of ion-pairing reagent --equal or higher than that of the original.

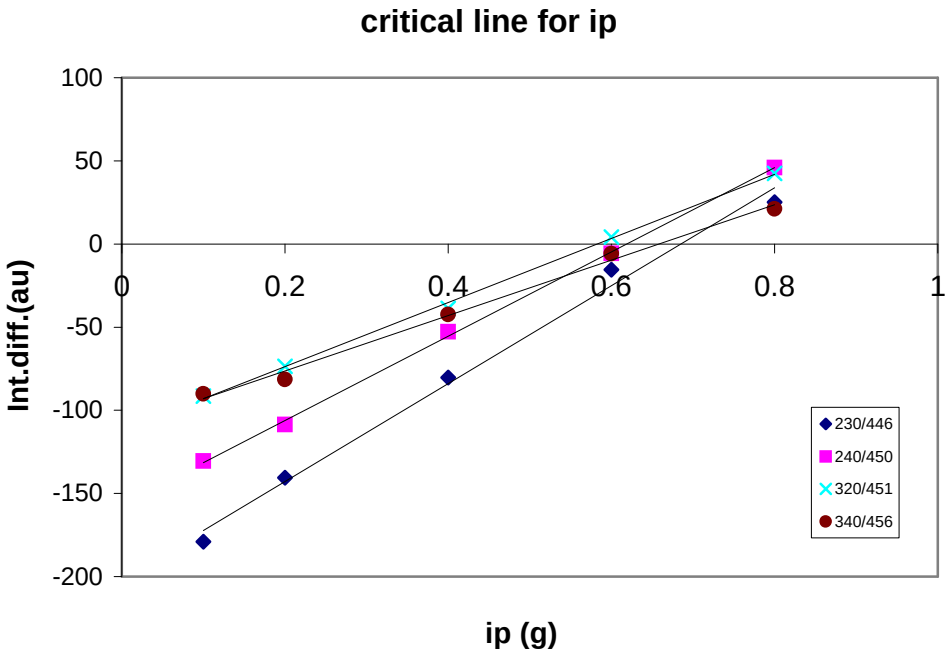

Figure 2.13 The critical values of ip at the maximum emission intensity for peak A ($\lambda_{ex}/\lambda_{em}$=230/446 nm, 240/450 nm) and peak C ($\lambda_{ex}/\lambda_{em}$=320/451 nm, 340/456 nm) (intensity difference=I_{DOM+ip}-I_{DOM}).

B. Extraction into organic solvents

In extractions without ion-pairing reagent, the fluorescence intensities of the organic phases were very weak. After ion-pairing reagent was added together with acetonitrile, 3DEEM showed oval plots of peaks A and C. $\lambda_{ex\ max}$ and $\lambda_{em\ max}$ didn't shift after addition of acetonitrile, they were still at $\lambda_{ex}/\lambda_{em}$= 230/430 nm for peak A and $\lambda_{ex}/\lambda_{em}$=320/430 nm for peak C. Because the acetonitrile miscible with the water, it was unable to extract the DOM from the mixture. Increasing the amount of acetonitrile only changed the fluoresence emission intensity, not $\lambda_{ex}/\lambda_{em}$ of peaks (Figure 2.14).

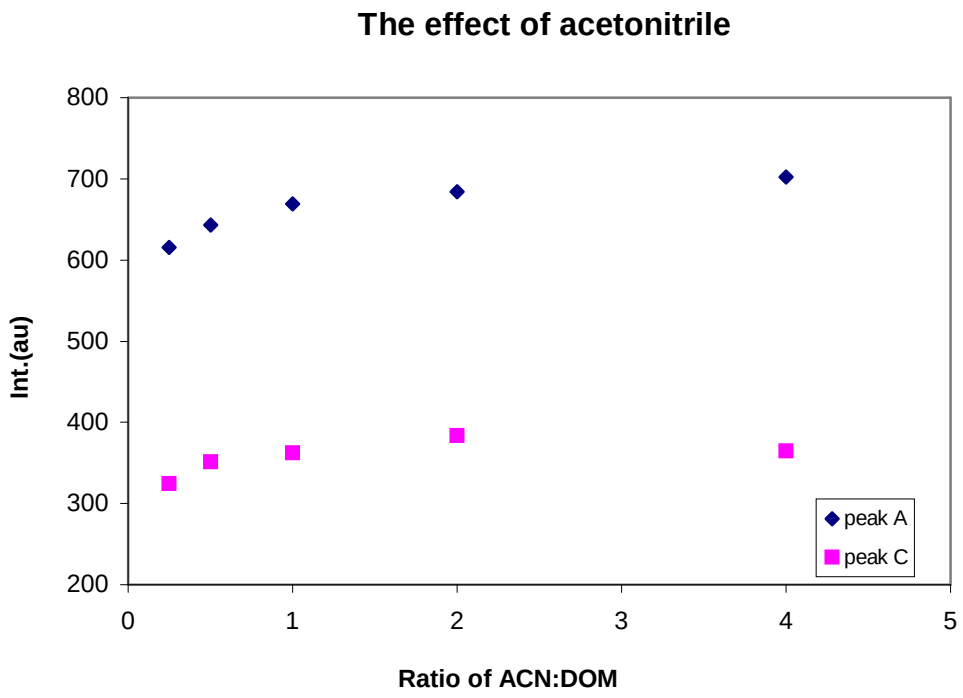

Figure 2.14 The maximum emission intensity of DOM changed as function of ACN:DOM ratio.

When DOM was extracted by diethyl ether with ion-pairing reagent added, the mixture was separated into two phases. After extraction, the aqueous phase intensities at excitation wavelengths were 230 nm>220 nm>240 nm>>250 nm. The maximum emission wavelength λ_{em} blue shifted from 440 nm to 420 nm for peak A and from 450 nm to 430 nm for peak C compared with DOM original solution; however, there was almost no shift occurring of the aqueous phase intensities after extraction compared with DOM and ion-pairing reagent mixture solution before extraction. The contour plots of the aqueous phase were similar to that of un-extracted DOM. In the ether phase, peak A fluorescence was very different (Figure 2.15). The excitation wavelengths showed an unusual contribution to peak A (Figure 2.16), totally differently from the Gaussian distribution maps. λ_{ex} occurred at 220 nm instead of usual 230 nm, while λ_{em} of peak A

shifted from 420 nm to a very short wavelength of 307. This remarkable blue shifting and distribution resulted in a very irregular shape for peak A. Although λ_{em} of peak C also blue shifted from 420 nm to 407 nm, the contour plots showed similar shape with that of the un-extracted DOM.

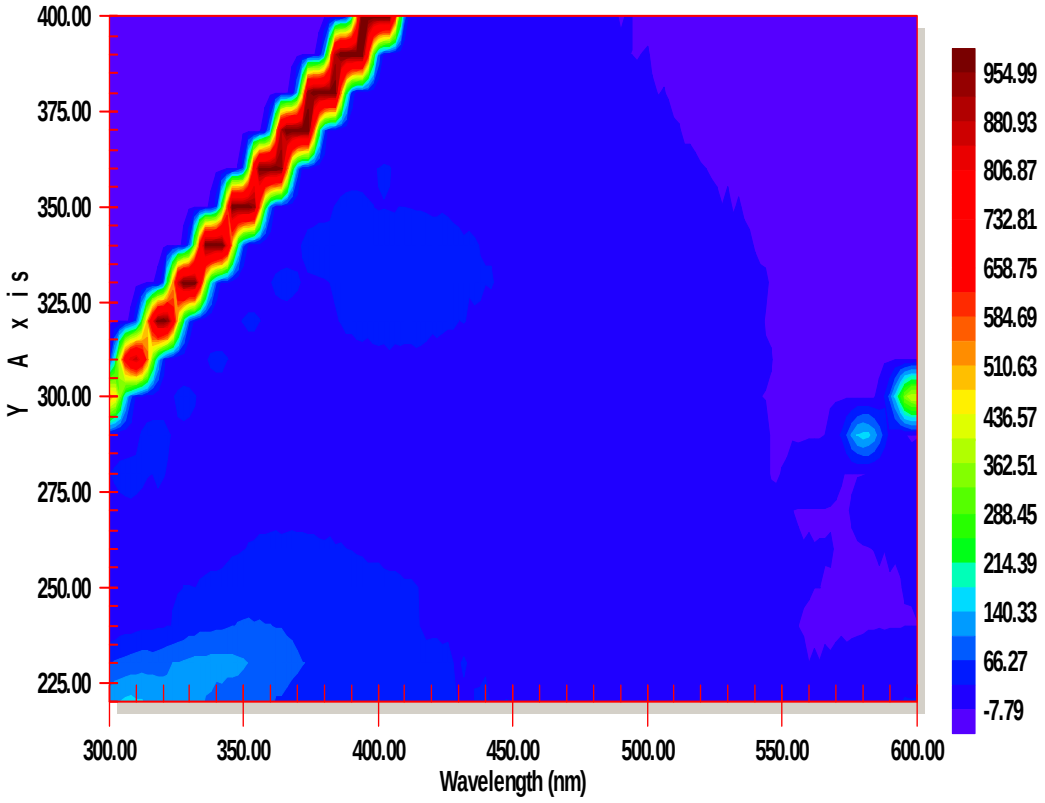

Figure 2.15 The contour plots of ether phases after extraction by diethyl ether with addition of ion-pairing reagent.

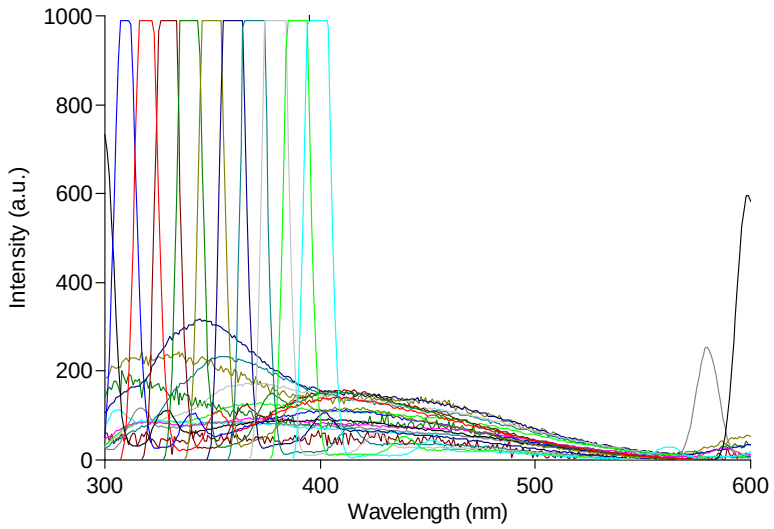

Figure 2.16 2-D emission spectrum of ether phase after extraction by diethyl ether with addition of ion-pairing reagent.

When diethyl ether was applied as extraction solvent, addition of ion-pairing reagent enhanced the maximum emission intensity a little bit of the peak A in the aqueous phase, but not for peak C. While in the ether phase, the emission intensities for both peaks were very weak even at high concentration of ip (1 g) was added.

Octanol is widely used as organic solvent for studying partitioning (octanol-water) of organic compounds between natural organic phase and water [Schwarzenbach, 2003]. After extraction by octanol (Figure 2.17), λ_{ex} of peaks in the aqueous phase don't shift, they are always at 230 nm. $\lambda_{em\ max}$ of peaks A and C shift very little, they still occur at the same wavelengths with those of the mixtures when ion-pairing reagents were added, and as ion-pairing reagent concentration increased, λ_{em} shift to shorter wavelengths gradually from 430 nm to 400 nm for peak A and from 440 nm to 410 nm for peak C respectively.

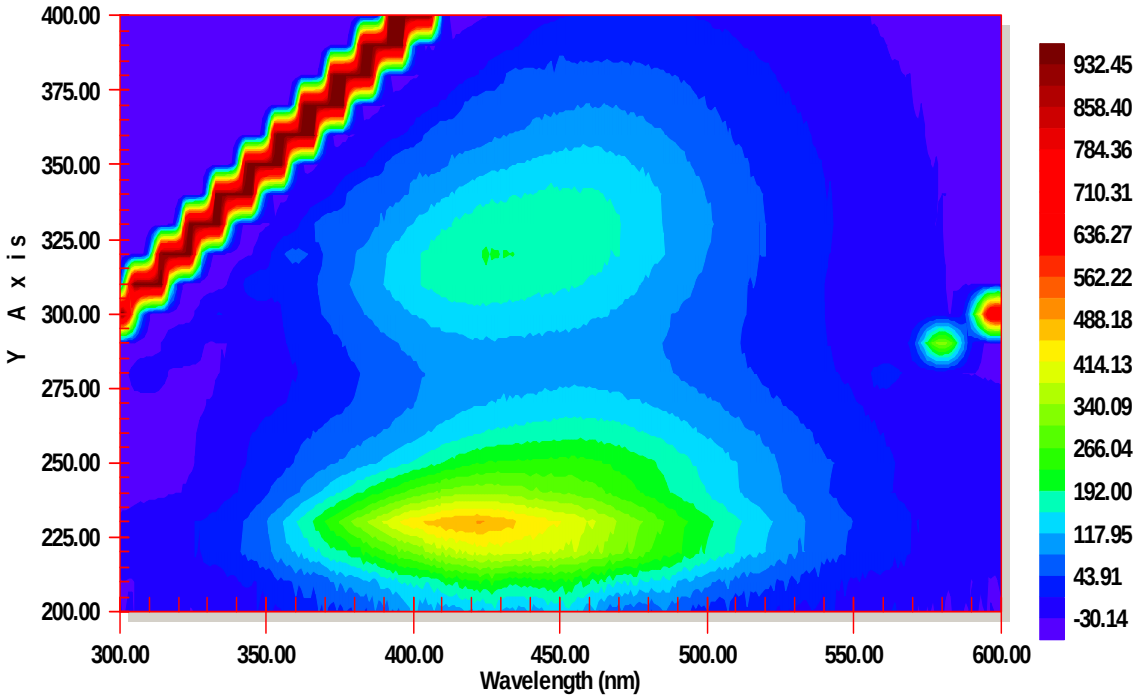

Figure 2.17 The contour plots of aqueous phase after extraction by octanol with addition of ion-pairing reagent.

For the organic phase, increasing ion-pairing reagent shifted the excitation maximum but not the emission one. λ_{ex} of peak C shifted from 320 nm to longer wavelengths, up to 340 nm when ion-pairing reagent was more than 0.1 g; while λ_{ex} of peak C shifted from 320 nm to shorter wavelengths at 300-310 nm when ion-pairing reagent was less than 0.1 g. The emission wavelength at which maximum emission intensity of peak A always occurred at 434 nm and peak C occurred at 410 nm no matter how much ion-pairing reagent was added.

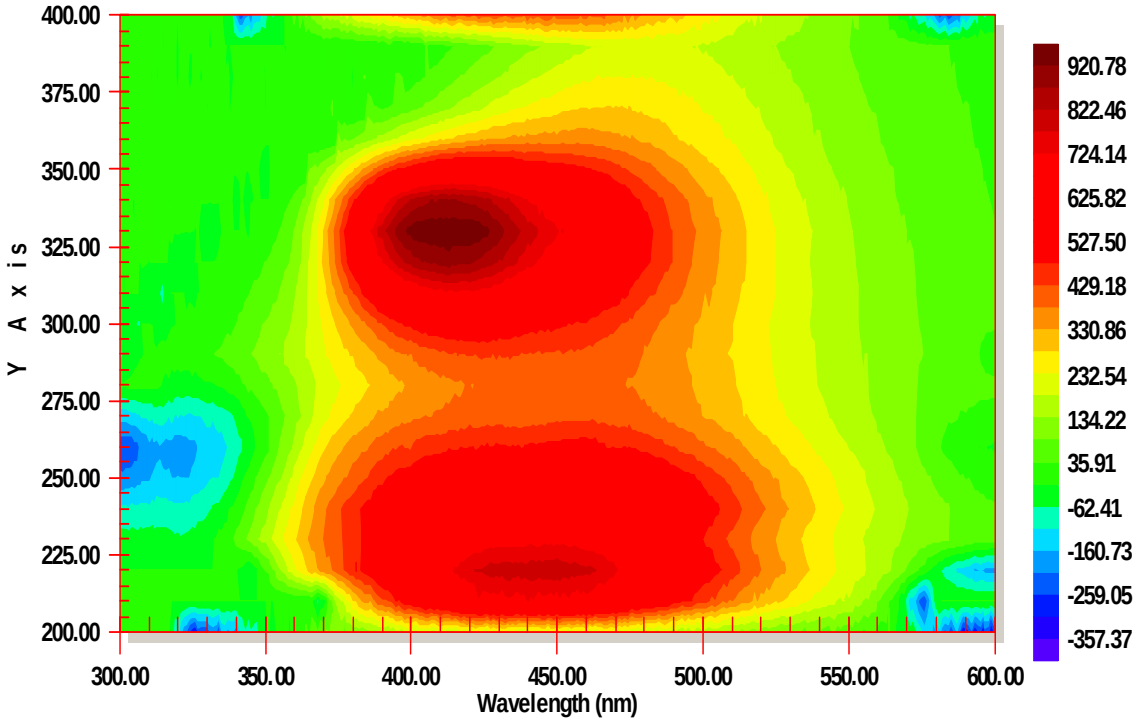

Figure 2.18 The contour plots of organic phase after extraction by octanol and ion-pairing reagent.

In the extracted octanol phase, emission intensities of peak C increased greatly and became stronger than those of the peak A once the ion-pairing reagent reached a limiting amount (>0.6 g). Generally, DOM emission intensities of peak A are always stronger than those of peak C. However, peak A is still stronger in the aqueous phase but weaker than peak C in the organic phase after extraction when a specific amount of ion-pairing reagent (>0.6 g) was added. Thus, octanol can extract DOM fractions highly enriched in visible humic-like fluorophores (peak C).

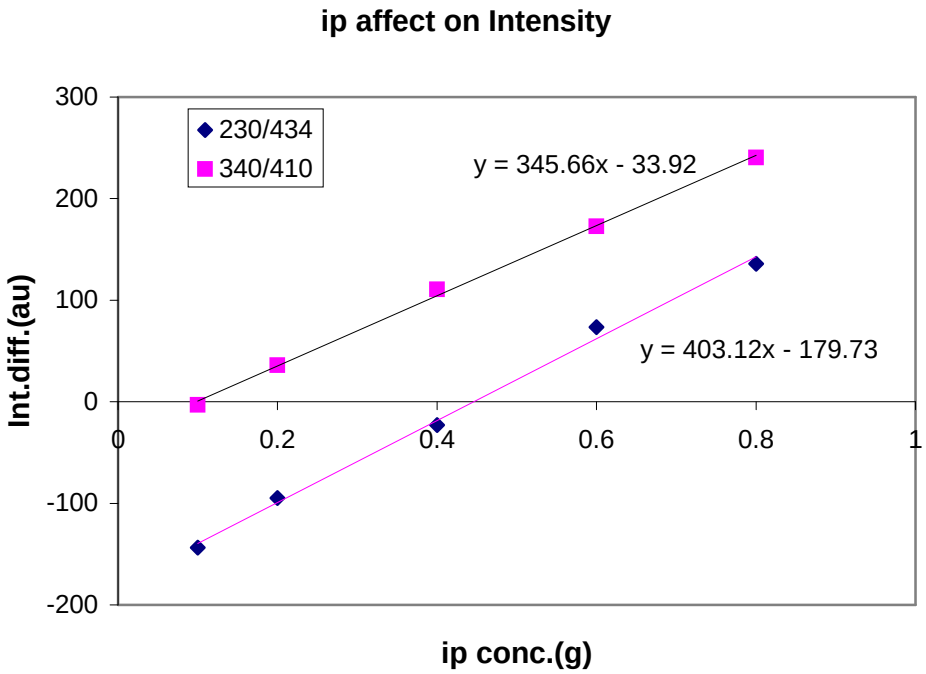

Figure 2.19 The critical line for ip at maximum emission intensity of DOM+ip before extraction (intensity difference=I_{DOM+ip}-I_{DOM}).

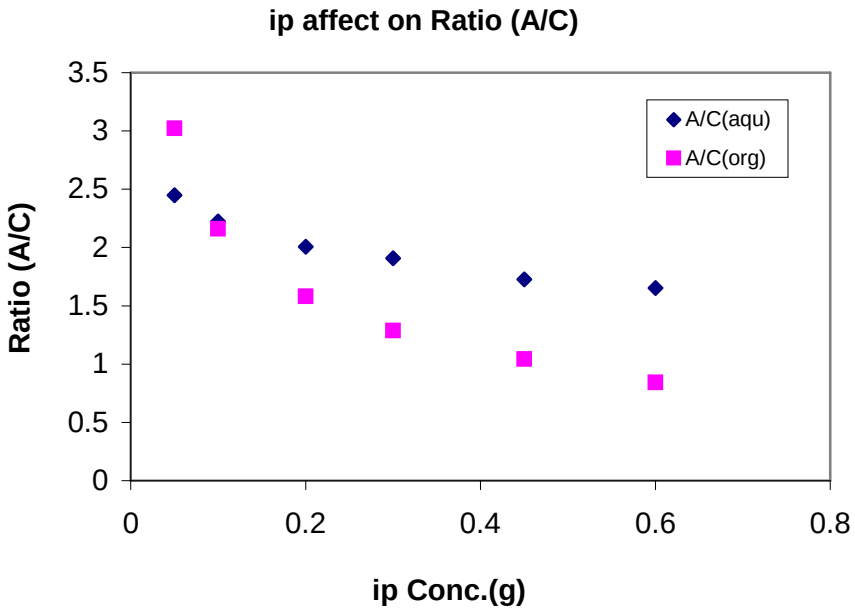

Figure 2.20 Intensity ratio ($r=I_A/I_C$) corresponding to ion-pairing reagent in organic (octanol) and aqueous phases.

The effects of ion-pairing reagent on emission intensity of peak A and peak C demonstrated a linear relationship (Figure 2.19), but on the intensity ratio r ($r=I_A/I_C$) (Figure 2.20), it demonstrated a non-linear correlation, whether in aqueous or in organic phases. In both phases, the intensity ratios of peak A and C decreased with the amount of ion-pairing reagent increased. The decrease trend was more obvious in the organic phase than aqueous phase. Because of the large blue shift of the λ_{em} in the octanol phase, even small amounts of ion-pairing reagent enhanced the emission intensity of peak C.

Emission intensities of both peaks A and C in the aqueous phase are weaker than those in the octanol phase. With the increasing of ion-pairing reagent concentration, the difference between them became smaller. When the concentration of ion-pairing reagent was lower, the intensities of peak C fluorescence in aqueous and organic phases were weaker than that of before extraction while the sum of emission intensity in both phases after extraction was much larger than that of mixture before extraction. For the peak A fluorescence, the intensities in aqueous and organic phases were weaker than that of mixture before extraction. However, the sum of emission intensity of aqueous and organic phases after extraction was much larger than that of mixture before extraction. This phenomenon was attributed to enhanced fluorescence intensity in a non-polar solvent.

Extraction efficiency %E decreased a little bit (about 5%) for the peak A when ion-pairing reagent increased from 0.05 g to 0.6 g (Figure 2.21). The effects of the ion-pairing reagent on the maximum emission intensity were much stronger than on extraction efficiency. Contrasted to the peak A, %E of peak C increased more than 20 % when ion-pairing reagent increased from 0.05 g to 0.6 g. Thus, addition of the ion-pairing

reagent improves the separation of these two groups of fluorophores. Increasing ion-pairing reagent enriches UV humic-like fluorophores (peak A) in the aqueous phase, while enriches the visible humic-like fluorophores (peak C) in the organic phase.

$$\text{efficiency of extraction (\%E)} = (I_{DOM+ip} - I_{aqueous})/ I_{DOM+ip} \quad (1)$$

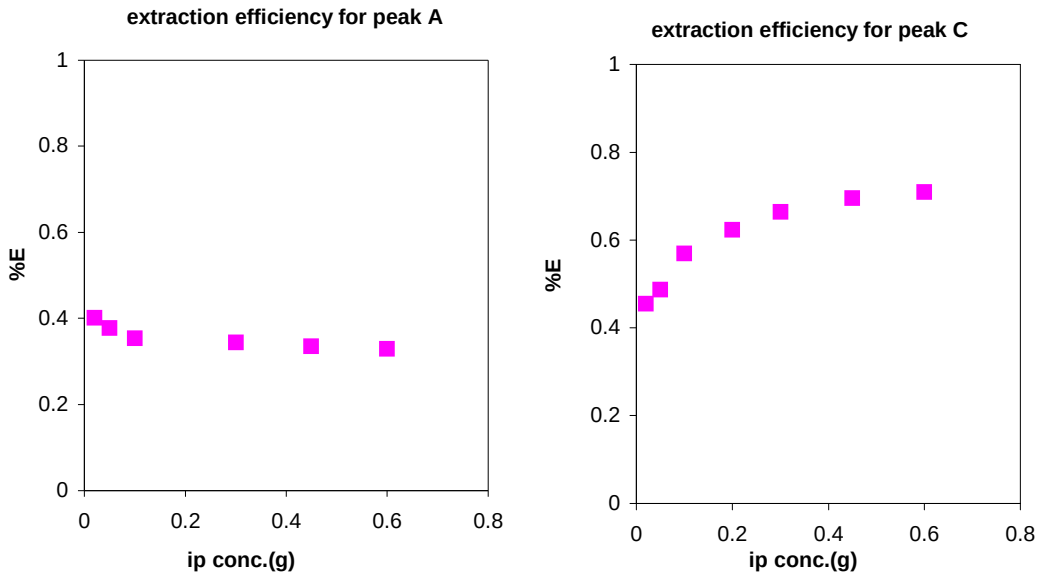

a b

Figure 2.21 Extraction efficiency of peak A (a) and peak C (b) by octanol as function of ip.

By investigating the efficiency of extraction for peak C and peak A fluorophores by octanol, experiments demonstrated that extraction efficiency for peak C increased while peak A declined with ion-pairing reagent concentration rising. It seemed that the ion-pairing reagent has greater effect on visible humic-like fluorophores and addition of ion-pairing reagent was favor for visible humic-like fluorophores separation from UV humic-like fluorophores.

Table 2.1 Summaries of fluorescence features

Peak	Property	DOM	Water+ip	ACN+ip	Diethyl ether+ip		Octanol+ip	
					organic	aqueous	organic	aqueous
C	λ_{ex} (nm)	320-330	320-330	320-340	330-340	320-330	300-340	330-350
	λ_{em} (nm)	450-460	410-430	410-450	400-420	420-440	410	410-430
	Intensity	423	369	397	158	361	>1000	226
	Shape	round	ellipse	ellipse		ellipse	ellipse	ellipse
A	λ_{ex}(nm)	210-230	230	230	230	230	230	230
	λ_{em} (nm)	430-450	400-430	400-440	340-350	410-430	434	400-430
	Intensity	808	655	670	314	880	822	519
	Shape	round	ellipse	ellipse		ellipse	ellipse	ellipse

Note: The concentration of DOM in all solutions was 20 mg/L.

Table 2.1 summarized fluorescence features of DOM in various solutions. Generally, λ_{ex} doesn't shift and λ_{em} blue shifts in cases. Because of the blue shift of the λ_{em} and broadening of peaks, the shapes of the contour plots change from round to ellipse or other irregular shapes. This ellipse shape suggested that the solution contains a mixture of fluorophores.

Therefore, ion-pairing reagent changed the partitioning of DOM (Table 2.1). The hydrophobic constituents were concentrated in organic phase and hydrophilic in aqueous phase when extracted with organic solvent. The results suggested that fractionation of DOM by HPLC with the addition of ion-pairing reagent should be feasible. Comparing acetonitrile, diethyl ether and octanol as extraction agents, acetonitrile was not able to fractionate DOM, and diethyl ether is the less effective to separate the hydrophobic from hydrophilic. So, octanol is the non-polar solvent of choice.

2.3.4 Ion-pairing reagent effects on DOM partitioning

Ion-pairing reagent enhances the partitioning of DOM into organic solvents. Once the ion-pairing reagent or organic solvent was added, the maximum emission wavelength blue shifts from 450 nm to as low as 400 nm for the peak C fluorescence. The maximum excitation wavelength change only slightly in most of cases, occurring at 320-340 nm.

The maximum emission wavelength of peak A is also blue shifted, but less than peak C. Since octanol has high absorbance below 230 nm (Figure 2.22), peak A fluorescence above 250 nm is chosen for comparison. The emission intensity changed after ion-pairing reagent or organic solvent was added.

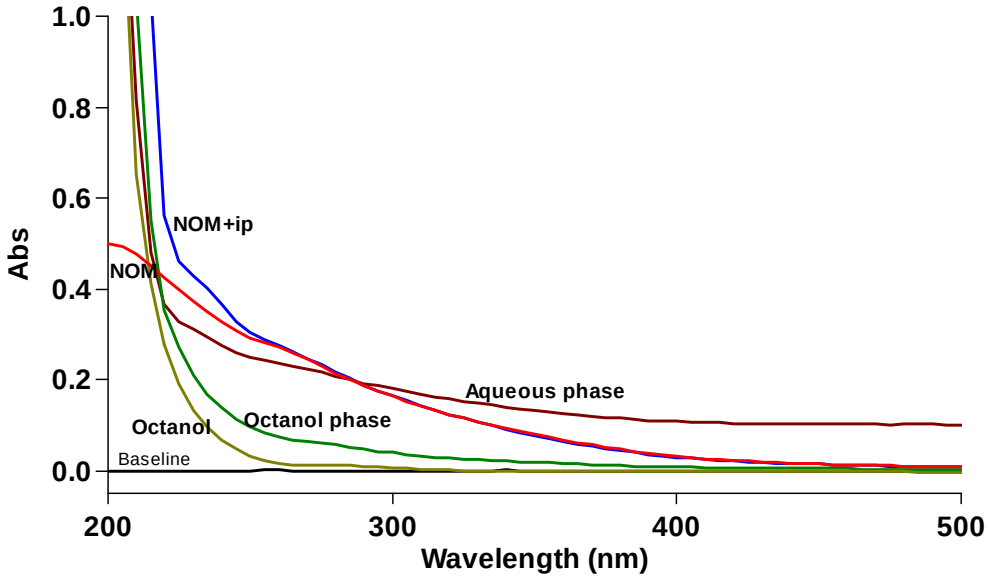

Figure 2.22 The absorbance spectra of DOM extracted by octanol with addition of ion-pairing reagent.

Besides the two dominant peaks of A and C, there is a third peak obscured by the two major peaks. This peak has a fluorescence maximum at $\lambda_{ex}/\lambda_{em}$= 250/460 nm (designated here as peak B, since it occupies a similar optical region with peaks A and C and statistic didn't resolve this peak from spectra [Stedmon and Markager, 2005]). Peak B overlaps with Peak A, but it is differentiated from peak A in some samples because it has more intense emission at excitation wavelengths of λ_{ex}= 250-290 nm. The peak B fluorophores are not well characterized in the literature perhaps because they are difficult to distinguish from the other two familiar peaks. Peak B could be observed from emission spectra of NOM, HA and FA samples. The maximum excitation wavelength at λ_{ex}= 250 nm has a very clear peak at emission of 460 nm, after ip was added, the emission

abundance of peak A was enhanced more than peak B, thus, the emission spectrum at λ_{ex}= 250 nm is flat from peak A to peak B.

The intensity of peak C is always less than that of peak A in the aqueous phase, but higher than peak A in organic phase if enough ion-pairing reagent was added.

The influence of ion-pairing reagent on fulvic acids (FA) and humic acids (HA) are similar to those on DOM. There are two interactions between ion-pairing reagent and humic acids (fulvic acids): hydrophobic and electrostatic interactions. Fulvic acid is more hydrophilic than humic acids, and may be less strongly affected by hydrophobic interaction.

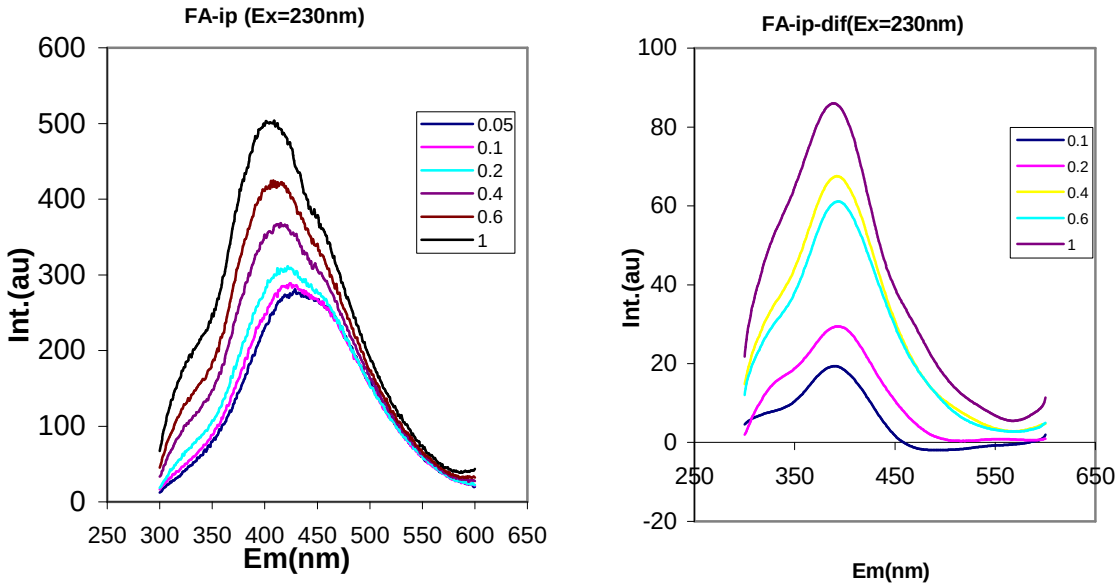

a b

Figure 2.23 The initial (a) and differential spectra (b) of fulvic acids + ion-pairing reagent before extraction at λ_{ex}=230 nm (differential spectrum 1 in b= spectrum 1-spectrum 0.6 in a, differential spectrum 0.6 in b= spectrum 0.6-spectrum 0.4 in a, etc. differential spectrum 0.1 in b= spectrum 0.1-spectrum 0.05 in a).

There are three peaks at λ_{ex}= 230 nm (Figure 2.23) after addition of ion-pairing reagent: the main peak occurred at λ_{em} = 410-420 nm for HA, FA and HA+FA, and the maximum emission wavelength blue-shifted 20-30 nm respectively when ion-pairing reagent increased from 0.05 g to 0.6 g. The other shoulder peaks appeared at λ_{em} = 330 nm and λ_{em} = 460 nm, and neither shifts with ion-pairing reagent. The latter peak overlaps with the main peak and broadens of the spectrum. In the differential spectra, there were only two peaks left and the shoulder peak at λ_{em}=460 nm disappeared. Meanwhile, the main peak appeared at λ_{em}=394 nm no matter what the amount of ion-pairing reagent were added for all HA, FA and HA+FA solutions. The results suggested that the shoulder peak at λ_{em}=460 nm does not change with ion-pairing reagent. Both peaks at λ_{em}=330 nm and λ_{em}=394 nm are attributed to hydrophobic structures, so their fluorescence intensity changes with the ion-pairing reagent. The blue-shifted λ_{em} results from overlapping of the main peak with the shoulder peak at λ_{em}=460 nm, because in the differential spectra, the main peak showed no shift. In the differential spectra, the same position of the maximum emission wavelength (λ_{em}=394 nm) of HA, FA and HA+FA indicated that the main peak at $\lambda_{ex}/\lambda_{em}$=230 nm/394 nm is assigned to UV humic-like fluorophores.

At λ_{ex}=310 nm, there are also three emission peaks (Figure 2.24). The maximum emission wavelengths of the main peaks gradually shifted to the shorter wavelengths when the concentration of ion-pairing reagent increased. However, this peak occurred at λ_{em}=410 nm and emission wavelengths don't shift with ion-pairing reagent in the differential spectra. The shoulder peaks at λ_{em}=460 nm disappeared in the differential spectra too. Another peak occurred at λ_{em}=360 nm and appeared not a shoulder peak but an obvious peak. Same with another shoulder at λ_{em}=460 nm, this peak disappear in the

differential spectra. Therefore the main peaks at λ_{em}=410 nm are visible humic-like fluorescence and emission wavelengths blue shifting is the result of overlapping with the shoulder at λ_{em}=460 nm.

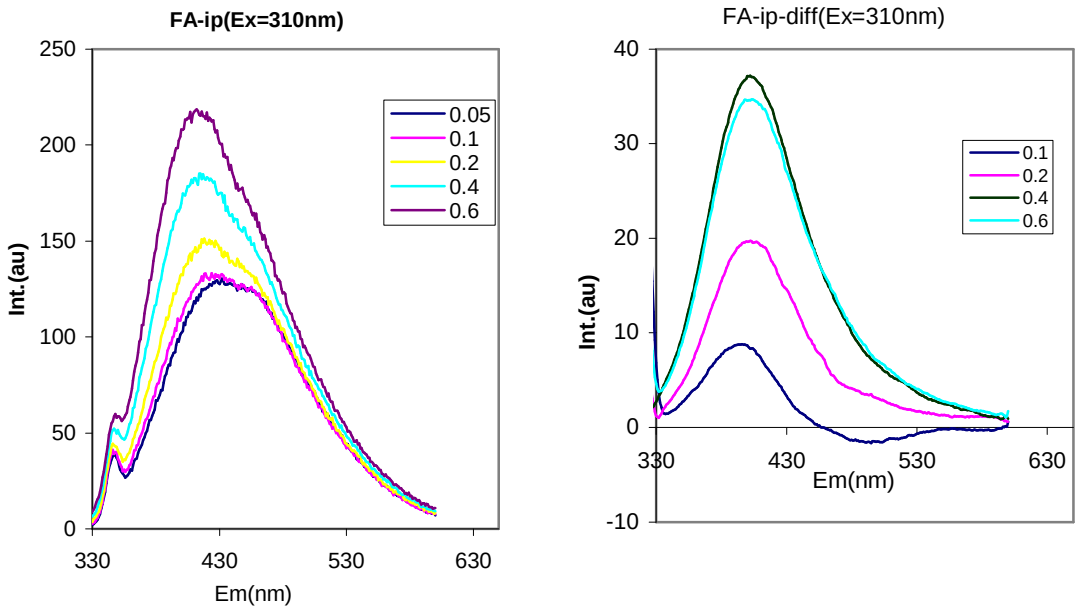

a b

Figure 2.24 The initial (a) and differential (b) spectra of fulvic acids + ion-pairing reagent before extraction at λ_{ex}=310 nm.

After octanol extraction, the aqueous phase at λ_{ex}=230 nm shows a wider emission peak at λ_{em}=430-415 nm in the initial spectra (Figure 2.25). However, in the differential spectra for all samples, this peak shows as the only peak at the same position λ_{em}=410 nm. The different maximum λ_{em} in the initial spectra is due to the main peak overlapping with the shoulder peak at λ_{em}=460 nm.

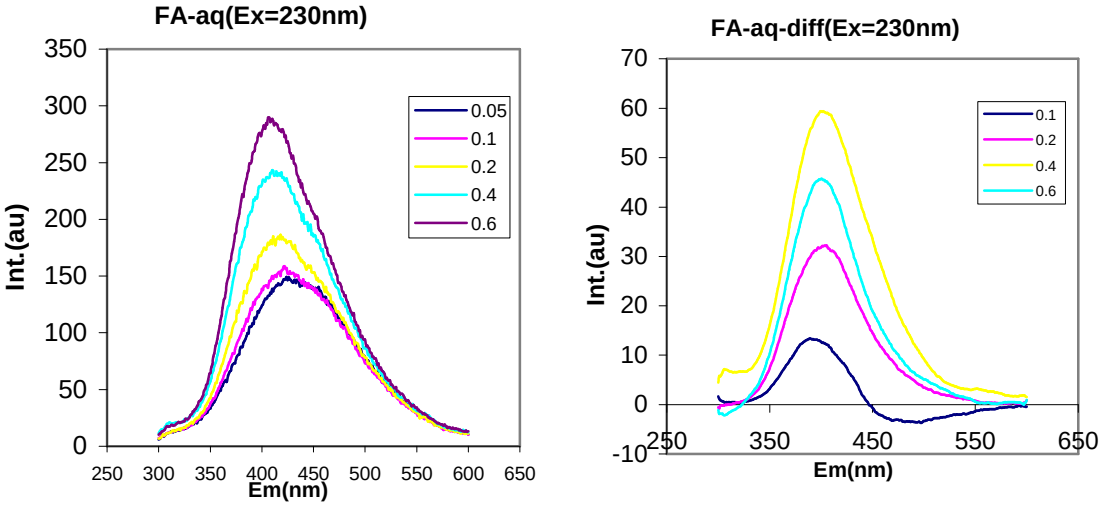

a b

Figure 2.25 The initial (a) and differential (b) spectra at λ_{ex}=230 nm of fulvic acids + ion-pairing reagent in the aqueous phase after extraction.

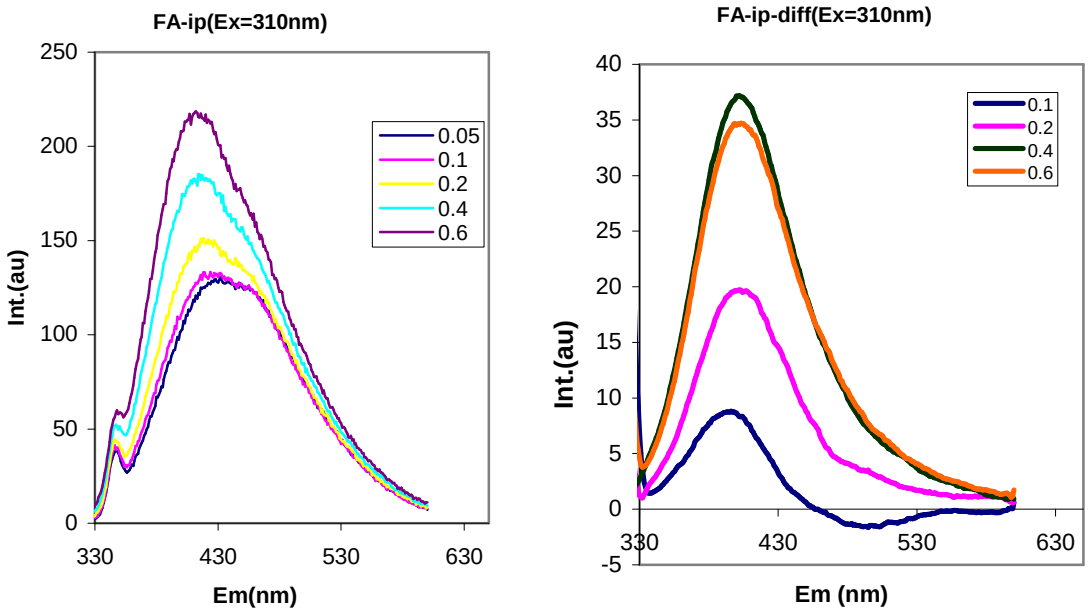

a b

Figure 2.26 The initial (a) and differential (b) spectra at λ_{ex}=310 nm of fulvic acids + ion-pairing reagent in the aqueous phase after extraction.

For λ_{ex}=310 nm, the initial and differential spectra of aqueous phase (Figure 2.26) are very similar to the spectra before extraction. The peaks at λ_{em}=350 nm and λ_{em}=460 nm appeared again in the initial spectra and disappeared in the differential spectra.

In the organic phase (Figure 2.27), the effect of background absorbance by octanol complicates interpretation at λ_{em}<350 nm. However, in the range from λ_{em}=300 to λ_{em}= 550 nm, there appear to be four peaks: the most intense one occurred at λ_{em}=435 nm belongs to the UV humic-like fluorophores and the less intense one at λ_{em}=410 nm is attributed to visible humic-like fluorophores. The other two are shoulders, occurring at λ_{em}=360 nm and λ_{em}=460 nm respectively. In the differential spectra, there are two peaks at λ_{em}=350 nm and c.a. λ_{em}=500 nm, the latter a very broad peak of very low intensity. Absence of the UV humic-like peak in the differential spectra indicated that this fluorophore is not enriched in the organic phase.

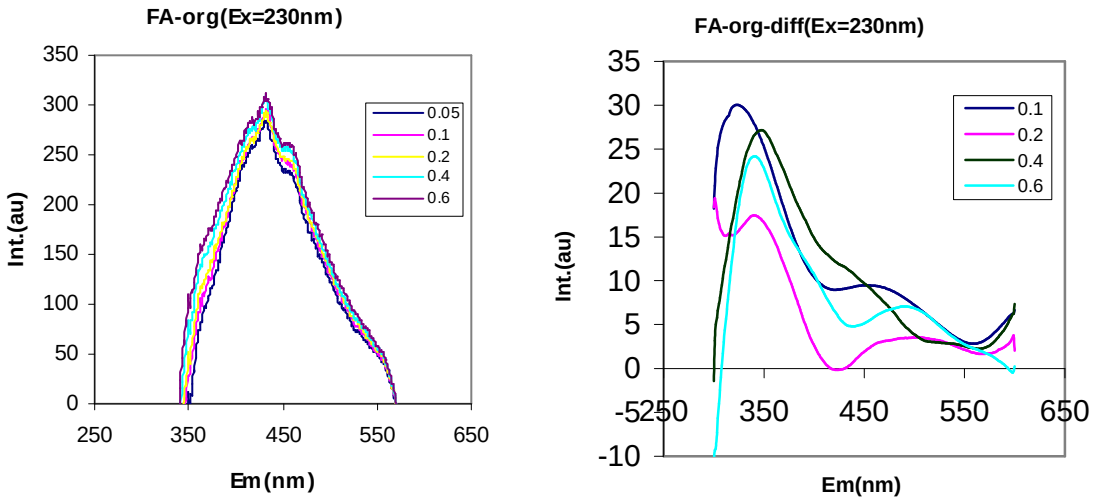

a b

Figure 2.27 The initial (a) and differential (b) spectra at λ_{ex}=230 nm of fulvic acids + ion-pairing reagent in the organic phase after extraction.

Comparing the effects of ion-pairing reagent addition spectra in the organic phase and aqueous phases, the emission intensity in the organic phase is stronger, but increased only slightly (<20 a.u.) as ion-pairing reagent increased. Enhancement of intensity in the aqueous phase is over 120 a.u. when ion-pairing reagent varied from 0.05 g to 0.6 g. The UV humic-like fluorescence in organic phase showed very low intenstity in the differential spectra, indicating that the effects of ion-pairing regent on the fluorophores are weak.

The peaks at $\lambda_{ex}/\lambda_{em}$=230 nm/330~360 nm are observed in the mixture solution and in the octanol phase, even in the differential spectra. But these peaks don't appear in the aqueous phase after extraction. The peaks at $\lambda_{ex}/\lambda_{em}$=310 nm/350 nm (Figure 2.28) are present in all spectra, but the maximum emission intensity in aqueous phase is much lower than in organic phase, indicated that this peak is more hydrophobic. In the differential spectra, the peaks disappeared in all conditions.

The shoulder at λ_{em}=460 nm is present in all mixture solutions, aqueous and organic phases, but are very weak in the aqueous phase. Only when the concentration of ion-pairing reagent is low, can they be discriminated from the spectra. The shoulder disappears completely in the differential spectra.

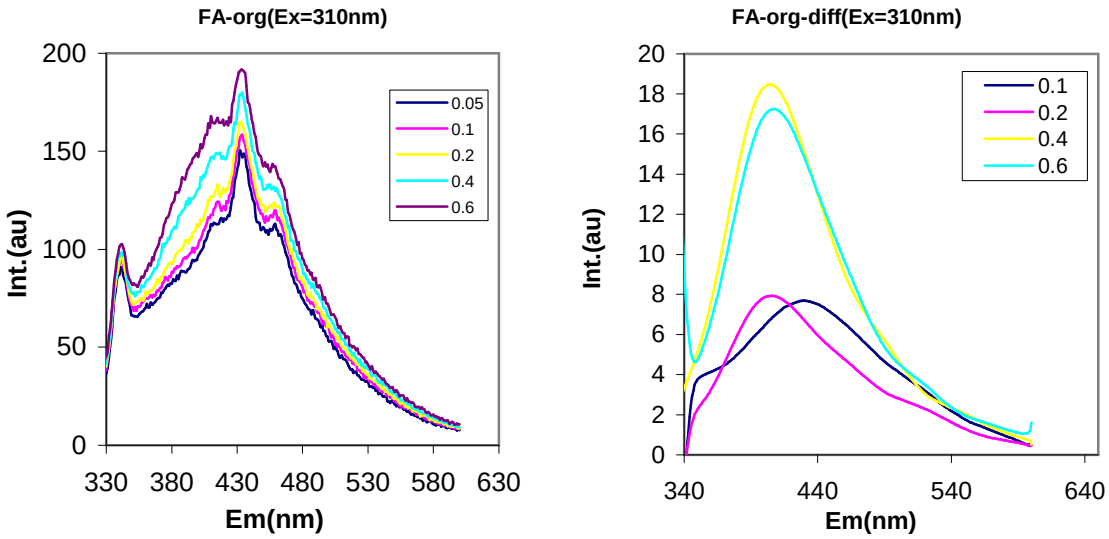

a b

Figure 2.28 The initial (a) and differential (b) spectra at λ_{ex}=310 nm of fulvic acids + ion-pairing reagent in the organic phase after extraction.

The maximum excitation wavelength of visible humic-like fluorescence red-shifted from λ_{ex}=310 nm in the water solution to λ_{ex}=340 nm in the octanol solution. Similarly, maximum λ_{ex} shifted from 310 nm to 340 nm when ion-pairing regent increased from 0.05 g to 0.6 g. At λ_{ex}=340 nm, there are three peaks in the original spectra and only one peak in the differential spectra (Figure 2.29), very similar to the spectra before extraction. The shapes and distribution of the spectra are very similar in both phases. The first shoulder occurred at λ_{em}=380 nm, while the secondary shoulder couldn't be located exactly.

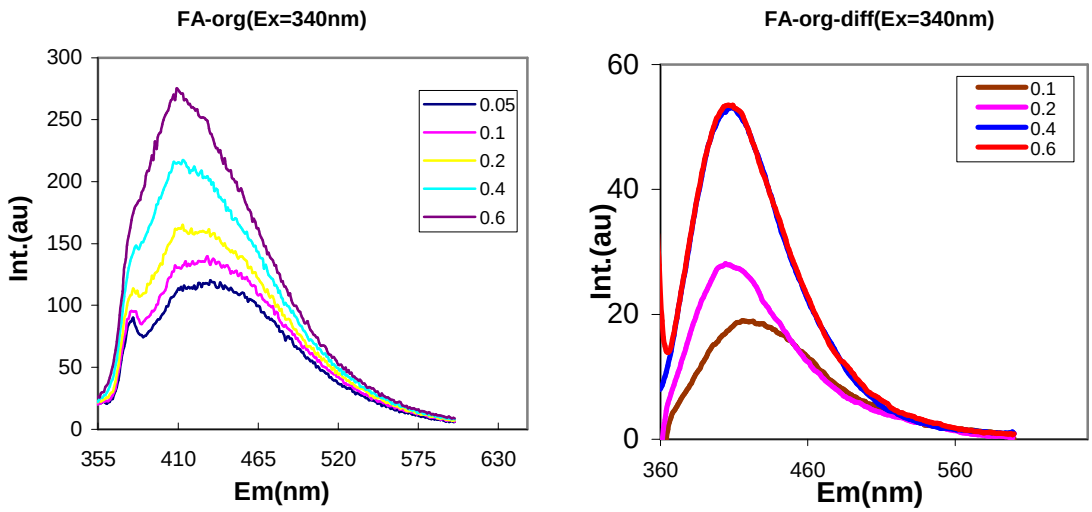

a b

Figure 2.29 The initial (a) and differential (b) spectra at λ_{ex}=340 nm of fulvic acids + ion-pairing reagent in the organic phase after extraction.

The shoulders at λ_{ex} =230 nm, λ_{em}=330-360 nm is present in the original (non-extracted) solutions, but disappears in aqueous phases and appears as a main peak at in differential spectra of organic phases when the ion-pairing reagent is varied. Therefore, the fluorophores responsible for this peak are probably hydrophobic. Another shoulder occurring at 460 nm appears in all solutions except the differential spectra of both initial mixed solutions and aqueous phase, but is very weak in the aqueous phase. Both are observed clearly in organic phases and are the only two peaks in differential spectra of organic phases. At λ_{ex}=310 nm, 330 nm and 460 nm are very obvious in all original mixed solutions but disappear in all differential spectra.

The maximum λ_{em} of peaks A and C occur at 390 ~ 410 nm in the differential spectra, and differential spectra show little shift in maximum λ_{em} indicating that the apparent shift in raw spectra is due to the overlapping with the sub-peaks.

In the different phases, the effects of ion-pairing reagent were different and also λ_{ex} and λ_{em} dependent (Figure 2.30). The maximum emission intensity increased about 80 a.u. for peak A and 150 a.u. for peak C when ion-pairing reagent increased from 0.05 g to 0.6 g. Compared to peak A, peak C is affected more strongly by the ion-pairing reagent in the organic phase. The intensities of peak A almost don't change in organic phase, but are enhanced in aqueous phase with ion-pairing reagent increasing; similarly, emission intensities of peak C are enhanced in organic phase but almost don't change in aqueous phase when increased the concentration of ion-pairing reagent. Therefore, in theoretically, visible humic-like fluorophores could be concentrated in the organic phase while UV humic-like fluorophores could be enriched in aqueous phase by addition of ion-pairing reagent. It seemed that visible humic-like and UV humic-like structures could be separated by ion-pairing reagent and octanol.

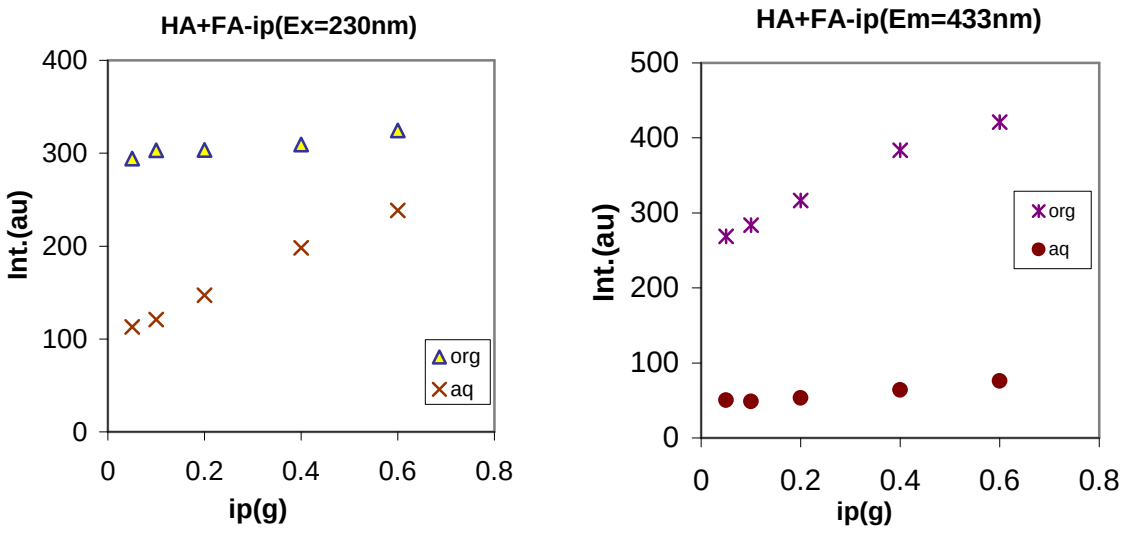

a b

Figure 2.30 The effects of ion-pairing reagent on emission intensities of peaks A and C in aqueous and organic phases.

The maximum emission intensities are enhanced by the ion-pairing reagent: the higher the addition, the higher the intensities. However, in all of the differential spectra, the addition of ion-pairing reagent of 0.4 g exhibits the maximum enhancement, coinciding with the critical value of the ion-pairing reagent to increase the maximum emission intensity.

The extraction efficiencies (%E) are excitation and emission wavelengths depend (Figure 2.31). At λ_{em}=420 nm, the extraction efficiencies increase when excitation wavelengths vary between 200 nm and 400 nm, but are stable for some range of λ_{ex} from 250 to 320 nm. In the range of selected λ_{em} by the instrument, the extraction efficiency decreases then increases with λ_{ex} varied between 300 nm to 600 nm and reach the lowest value at 420 nm when λ_{ex}=230 nm.

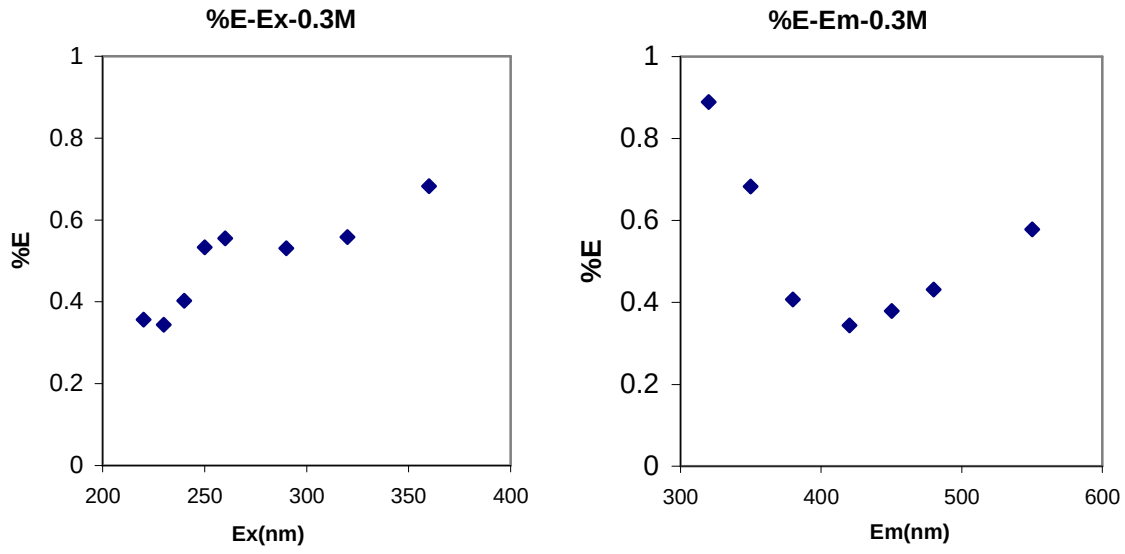

a b

Figure 2.31 Extraction efficiency were Ex dependent at λ_{em}=420 nm (a) and Em dependent at λ_{ex}=230 nm (b) when the concentration of ion-pairing reagent was 0.3 g.

Because there are two phases after separation by octanol, theoretically, the losing (missing) of the aqueous phase should be equal to the gaining of the organic phase. But the gaining is nearly two times higher than the losing (missing) for the both peaks.

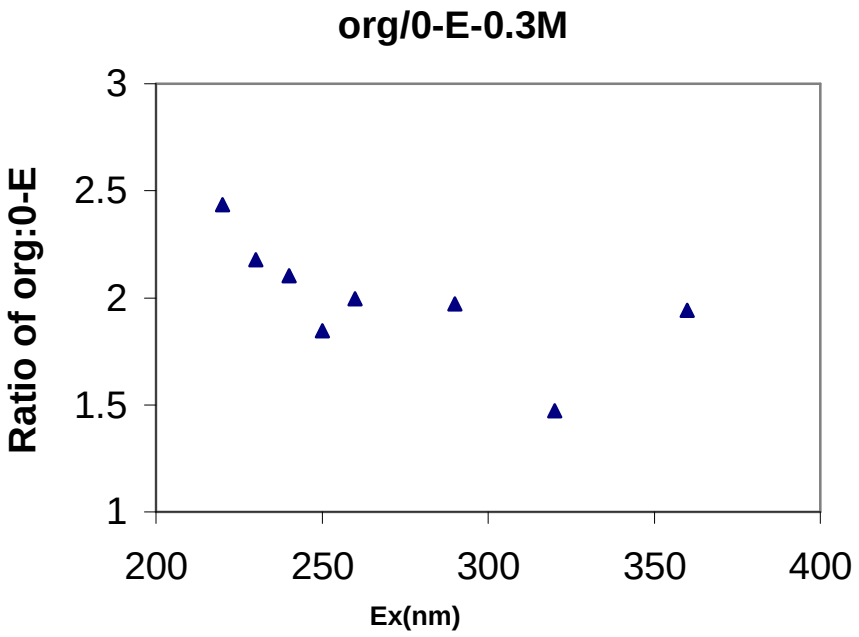

Figure 2.32 The ratio of different fractions partitioning into organic phase to aqueous phase at different excitation wavelengths (λ_{em}=420 nm).

2.4 DISCUSSION

Two principal hypotheses for the appearance of DOM optical spectra (absorbance and fluorescence) are: (1) the sum of many independent spectra from different chromophores/fluorophores; and (2) a continuum of coupled states formed through charge-transfer interactions of a few distinct chromophores, rather than from a superposition of many independent chromophores [Del Vecchio and Blough, 2004].

The spectral parameter that best characterizes fluorescent DOM composition is the position of fluorescence center for the fluorophores found in natural waters. The overall level of variability within groups having similar λ_{em} suggests that UV and visible humic-like peaks may vary independently of each other. The variation in the ratio of fluorescence intensity of peaks A:C (UV : visible humic-like fluorescence), it has been suggested that at least two separate fluorophores are responsible for humic-like fluorescence of DOM, because a single fluorophore would be expected to show a constant ratio. Of course, this type of analysis cannot be applied to samples which show variability in the position of λ_{ex} /λ_{em} for either peak.

2.4.1 The effect of pH

Fluorescence is a function of structure and functional groups in molecules. According to Laane [Laane, 1982], the change of fluorescent intensity with pH is probably due to ionization of the fluorescent molecules after modifications of pH. UV humic-like and visible humic-like fluorescence is mainly attributed to aromatic-carboxylic functional groups [Egeberg, 2002; Senesi, 1991]. Because DOM is not a strong acid (pH is 4.8 at 20 mg/L), increased pH deprotonated its acid groups, the higher

the pH, the more deprotonated. Some functional groups (e.g., phenols) become stronger acids on excitation, whereas others become more basic (e.g., carboxylic acids). The electron donating groups such as hydroxyl and methoxyl groups have also been reported to enhance fluorescence by increasing the transition probability between the singlet and ground state. The increase in emission intensity with pH may also be related to the increased ionization causing decreased association or decoiling of macromolecular structures (e.g. disrupt hydrogen bonds). The enhancement of emission intensity with increasing pH may result from reduced hydrogen bonding within and between humic molecules, and breakage of these hydrogen bondings would cause decrease in particle association and decoiling of macromolecular structures [Guo et al., 1987]. Although the electron-withdrawing carboxyl functional groups would weaken the fluorescence intensity, transforming from deprotonated carboxyl groups to electron-donating structure would increase the emission intensity of fluorescence [Sutton et al., 2005; Chen, 2002].

Another possible explanation could be related to the macromolecular configuration of humic substances: more rigid structures giving better fluorescent yields. This result could also explain that the fluorescence intensity increase with increasing pH. A spherocolloidal configuration could mask some fluorophores inside their structure. At higher pH, the configuration becomes linear, and some fluorophores are not masked anymore, they can fluoresce, therefore increase the fluorescence intensity [Patel-Sorrentino, 2002]. Surface pressure and viscosity measurements indicate that humic substances have linear structure at high pH and coil when pH decreased.

Very low pH and very high pH values are not favorable for strong DOM fluorescence signals. This is similar to the fluorescence of salicylic acid, a molecular

model of humic substances (Figure 2.33). For both acidic (H_2Sal) and basic (Sal^{2-}) structures, there are more vibration modes and thus weaker fluorescence. For $HSal^{-1}$, the intramolecular H-bonding limits vibration modes and fluorescence is strong (Figure 2.33). Another model humic structure (Figure 2.34) is catechol. At higher pH (like pH is 8), they are partially deprotonated (ionization), and form ring by H-bond, so absorb light and express deep color. At lower pH, they are protonated and do not absorb light and express light color (Figure 2.34).

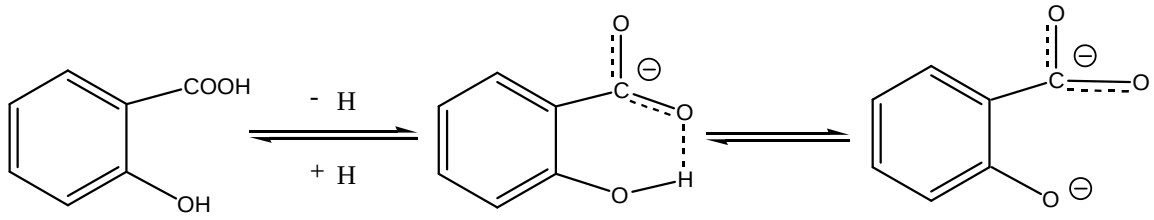

weak fluorophore good fluorophore weak fluorophore

Figure 2.33 Salicylic acid models at different pH.

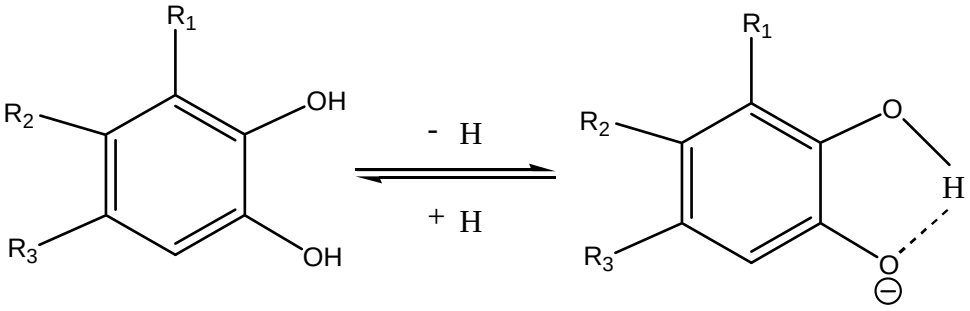

weak fluorophore good fluorophore

Figure 2.34 Catechol models at different pH.

For a single, simple fluorophore, contour plots are symmetrical. Elliptical emission plots may be attributed to a mixture of fluorophores. At pH =10, the contour plots of

visible humic-like fluorescence showed an obvious ellipse shape, indicating that the hydrolysis and breakage of Hydrogen bonding and/or strong ionization fractionated part or surface of the supramolecule structure building (or blocks) into sub-components or sub-fractions with similar fluorophores. Even after pH return to pH=5, the ellipse shapes didn't change back to round ones suggested the change was not reversible.

Aromatic esters hydrolyze at extremely acidic or basic conditions. NMR showed there are aromatic esters in the humic substances which were obtained by RO separation, not by XAD extraction, because XAD extraction used extremely basic condition. Base hydrolysis is faster than acid hydrolysis, and these hydrolyses are irreversible. Hydrolysis of H-bonding of humic substances may also be irreversible. Once these bonds are broken, hydrogen bonds between sub-fractions will rebuild in a different pattern. Therefore, recombination and/or rebuilding of molecular structure segments at high pH values can change fluorescent efficiency.

For UV humic-like fluorescence (peak A), contour plots at pH=10 didn't change shape indicating that even this pH did not decompose or fractionate UV humic-like fluorophores structures. The different performances of UV humic-like fluorophores (peak A) and visible humic-like fluorophores (peak C) at the strong basic condition suggested that UV humic-like fluorophores contain few ester structures, and they are more resistant to base.

2.4.2 The effects of ion-pairing and solvents on partitioning

The addition of ion-pairing reagent blue-shifts peaks A and C and the more ion-pairing reagent, the larger the shifting. The addition of ion-pairing reagent could alter the

relative proportion and contributions of the individual fluorophores, resulting in changes in the positions of the emission maximum and the shape of the spectra. Two possible explanations are counted for the changes: solvent effect and bond disruption.

Solvent effect: The addition of non-polar ion-pairing reagent altered the solvent environment of the fluorophores. The solvent changed from polar to less polar, shifting λ_{em} to shorter wavelengths. The more ion-pairing reagent, the more non-polar the environment around these fluorophores, and greater shift.

Bond disruption: In the aqueous solution, the ion-pairing reagent, tetrabutylammonium hydrogensulfate, has both of hydrophobic and charge-charge interactions with humic substances, and these interactions maybe result in the breakage or fractionation of the supramolecule into smaller sub-structures. These smaller sub-structures either continue as separate molecules or rebuild into new supramolecules. The more ion-pairing reagent added, the more breakage of hydrogen bonding, van der waals forces and/or hydrophobic interactions. No matter what the fractions (or “monomers”) or new suprastructures they are, the very similar fluorescence spectra with the original humic substances indicated that they have the similar structures and/or properties.

The peak sensitivities were different for peaks A and C. Peak A is the more sensitive one, and λ_{ex} shifted from 250 nm and/or 260 nm to 230 nm, with fluorescence intensities increasing due to spectra overlapping. When ion-pairing reagents were added, the environment became less polar, therefore increased the quantum yield, and resulted in the emission wavelengths blue shifting. To confirm shifts to lower λ_{ex} (<200 nm) would require vacuum optics.

Solvent effects with diethyl ether were problematic due to low extraction efficiency. Diethyl ether is less polar than water, and maximum λ_{em} of peak A in the ether phase had a large blue shift. Maximum λ_{em} of peak C also blue shifted, although less than peak A and the shape of its contour plots didn't change. The blue shifts of maximum emission wavelengths of both peaks were expected due to the polarity differences. Very weak intensities of both peaks in diethyl ether phase indicated that diethyl ether has limited capability to extract the hydrophobic structures from water solution due to its short aliphatic chain and less non-polar nature.

Octanol provided the best extraction. The aqueous phase after extraction exhibited very similar fluorescence spectra to the original mixture. In the octanol phase, λ_{em} were ion-pairing reagent independent for both peaks. The change of the solvent conditions made λ_{em} behavior differently in the aqueous and organic phases when the ion-pairing reagents varied. In the aqueous phase, humic substances were surrounded by the polar water molecules. Addition of less polar ion-pairing reagent gradually replaced the polar water molecules and changed the environment of humic substances, thus made the maximum λ_{em} blue shift. In the organic phase, ion-pairing reagent and octanol are non-polar, and there was little change in the fluorophores environment, therefore no wavelength shift. The opposite direction shifting of peaks A and C made the maximum emission wavelengths appear at the same location. The higher intensities of both peaks in the octanol phase are due to both extraction of a high fraction of fluorophores and higher quantum efficiency in the non-polar media.

The critical value of ion-pairing reagent for the fluorescence intensity suggested that different amount of ion-pairing reagent interacted with humic substances differently.

Because fluorescence intensity is strongly influenced by the molecular structures of DOM such as molecular weight (MW), degree of condensed aromatic moieties, and the intensity of the band increase along with decrease of MW. When the concentration of ion-pairing reagent was low, ion-pairing reagents may link with DOM macromolecule as bundle by hydrophobic and/or charge-charge interaction(s) because the huge surface area of DOM molecule, rather than break the supramolecule into fractions. Thus, the bundle increased MW of the supramolecule and resulted in fluorescence intensity decreased. Once the concentration of ion-pairing reagent was more enough, ion-pairing reagent couldn't bind tightly with the supramolecule any more because of fewer of the surface area. In order to get good in touch with these sub-structures, the supramolecule had to be broken into many simpler pieces. Comparing with the supramolecule, the MW of these bundles of ion-pairing reagent and sub-structures were small, therefore fluorescence intensity were enhanced. Although the breakage of supramolecule would decrease conjugated unsaturated bonds and increase fluorescence intensity, the final result indicated that the influence of MW was stronger than degree of condensed aromatic moieties. Actually, there were critical values to fluorescence intensity enhancement indicated that the solvent polarity effect was not as important as destruction and rebuilding for effect of the addition of ion-pairing reagent.

2.4.3 Fractionation DOM by ion-pairing reagent

Uncharged peak C structures are more hydrophobic than peak A structures and the ion-pairing reagent has greater effect on peak C. This allows peaks A and C to be separated partially from each other into different phases with addition of ion-pairing

reagent. This is the first indication of any possibility that humic substances could be fractionated into different fluorophores. Because this separation procedure doesn't need strong acid or strong base, the fractions display their native features.

The octanol extract has very high intensities because of higher quantum yield in the nonpolar solvent due to reduced interactions.

For peak A, fluorescence intensity in the aqueous phase increased with ion-pairing reagent while intensity in organic phase did not vary. The addition of aliphatic ion-pairing reagent did not change the polarity of the octanol, while the polarity of the aqueous phase decreased because of the less polar environment enhanced the quantum yields of the fluorophores of peak A.

For peak C, fluorescence intensity in organic phase increased with added ion-pairing reagent. while aqueous phase spectra did not change. Fluorophores of peak C had greater hydrophobic interactions with the aliphatic chains of ion-pairing reagent because these fluorophores are larger and less polar comparing with fluorophores of peak A. They were more easily extracted to the organic phase, and the quantum yields of these fluorophores in the octanol phase were higher than in the aqueous phase. As more ion-pairing reagent was added, more DOM was extracted into the octanol phase and the higher the quantum yield in that phase, while in the aqueous phase, the fluorophores concentration decreased but the polarity also decreased, resulting in increased quantum yield. Because of these two offsetting effects, there was almost no change in the aqueous phase for peak C fluorescence with the addition of ion-pairing reagent.

Extraction efficiency was excitation and emission wavelength dependent, suggesting that the interactions between ion-pairing reagent and different fractions or

sub-structures of DOM varied. In particular, peak C is extracted more efficiently than peak A, suggesting these fluorophores occur on different molecules.

2.5 CONCLUSIONS

The peak locations of humic substance fluorescence varied somewhat from sample to sample. Peak A occurred at $\lambda_{ex}/\lambda_{em}$=230 nm/430-450 nm (UV humic-like fluorophores) and peak C at $\lambda_{ex}/\lambda_{em}$=320-330 nm/450-460 nm (visible humic-like fluorophores). Peak B ($\lambda_{ex}/\lambda_{em}$=250-260 nm/460 nm) may be the same with peaks A and C that it may be the intrinsic structure of NOM. There is no definitely structure for this organic matter, which maybe an aggregation of smaller molecules with similar functional groups.

The results from pH and ion-pairing reagent support the hypothesis that humic-substances are collections of chemically diverse, relative low molecular mass components forming dynamic associations stabilized by hydrogen bonds, hydrophobic interactions and van der waals forces. These supramolecular associations are able to spatially segregate and decoil in different environments, or even disrupt the linked clusters.

No extraction of either peak A or C occurred without ion-pairing reagent. Alteration of the partitioning of these two fluorophores by ion-pairing reagent and non-polar solvents enriched peak A in the aqueous phase and peak C in the organic phase. Maximum excitation and emission wavelengths shifted with the addition of ion-pairing reagent were due to enhanced peak overlapping and solvent effects.

2.6 REFERENCES

Abbt-braun, G., and Frimmel, F.H. (1999) Basic characterization of Norwegian NOM samples - Similarities and differences. *Environ Int.* 25,161-80.

Aiken, G.R. (1984) Evaluation of ultrafiltration for determining molecular-weight of fulvic-acid. *Environ. Sci. Technol.* 18, 978-981.

Aiken, G.R. (1985) *Humic substances in soil, sediment, and water: Geochemistry, isolation, and characterization.* Wiley, New York, 363-385.

Aiken, G.R., (1988) *Humic substances and their role in the environment.* Wiley, Chichester, 15-28.

Chen, J., Gu, B., Leboeuf, E.J., Pan, H., and Dai, S. (2002) Spectroscopic characterization of the structural and functional properties of natural organic matter fractions. *Chemosphere* 48, 59.

Chen, J., Leboeuf, E.J., Dai S., and Gu, B. (2003) Fluorescence spectroscopic studies of natural organic matter fractions. *Chemosphere* 50, 639.

Chen, W., Westerhoff, P., Leenheer, J.A., and Booksh, K. (2003) Fluorescence Excitation−Emission Matrix Regional Integration to Quantify Spectra for Dissolved Organic Matter. *Environ. Sci. Technol.* 37, 5701-5710,

Christman, R.F., Norwood, D.L., Millington, D.S., Johnson, J.D., and Stevens, A.A. (1983) Identity and yields of major halogenated products of aquatic fulvic-acid chlorination. *Environ. Sci. Technol.* 17, 625.

Coble, P.G. (1996) Characterization of marine and terrestrial DOM in seawater using excitation-emission matrix spectroscopy. *Marine Chemistry* 51, 325.

Coble, P.G., Green, S.A., Blough, N.V., and Gagosian, R.B. (1990) Characterization of dissolved organic matter in Black Sea by fluorescence spectroscopy. *Nature* 348,432.

Collins, M.R., Amy, G.L., and Steelink, C. (1986) Molecular-weight distribution, carboxylic acidity, and humic-substances content of aquatic organic-matter-implications for removal during water-treatment. *Environ. Sci. Technol.* 20, 1028-1032.

Croué, J.P., DeBroux, J.F., Amy, G.L., Aiken, G., and Leenheer, J.A. (1999) Natural organic matter: structural characteristics and reactive properties. In: P.C. Singer, Editor, *Formation and Control of Disinfection By-Products in Drinking Water,* American Water Works Association, Denver,

Cunico, R.L., Gooding, K.M (Eds.). Wehr T. (1998) HPLC and CE of biomolecules,Bay Bioanalytical Laboratory, Richmond, VA.

Dejanovic, K. and Cabaniss, S.E. (2004) Reverse-phase HPLC method for measuring polarity distributions of natural organic matter. *Environ. Sci. Technol.* 38, 1108-1114.

Del Castillo, C.E., Coble, P.G., Morell, J.M., Lopez, J.M., and Corredor, J.E. (1999) Analysis of the optical properties of the Orinoco River plume by absorption and fluorescence spectroscopy. *Marine Chemistry* 66, 35.

Del Vecchio, R., and Blough, N.V. (2004) On the origin of the optical properties of humic substances. *Environ. Sci. Technol.* 38, 3885-3891.

Edzwald, J.K., Becker, W.C., and Wattier, K.L. (1985) Surrogate parameters for monitoring organic matter and THM precursors. *J Am Water Works Assoc.* 77(4), 122–32.

Egeberg, P.K., Alberts, J.J. (2002) Determination of hydrophobicity of NOM by RP-HPLC, and the effect of pH and ionic strength. *Water Res.* 36, 4997-5004.

Fettig J. (1999) Characterisation of NOM by adsorption parameters and effective diffusivities. *Environ Int.* 25, 335-346.

Hedges, J.I. (1992) Global biogeochemical recycle-progress and problems. *Marine Chemistry* 39, 67.

Her, N., Amy, G., and McKnight, D.M. (2003) Characterization of DOM as a function of MW by fluorescence EEM and HPLC-SEC using UVA, DOC, and fluorescence detection. *Water Res.* 37, 4295-4303.

Her, N., Amy, G., Foss, D., and Cho, J. (2002) Variations of molecular weight estimation by HP-size exclusion chromatography with UVA versus online DOC detection. *Environ. Sci. Technol.* 36, 3393-3399

Her, N., Amy, G., Foss, D., Cho, J., Yoon, Y., and Kosenka, P. (2002) Optimization of method for detecting and characterizing NOM by HPLC-size exclusion chromatography with UV and on-line DOC detection. *Environ. Sci. Technol.* 36, 1069.

Imai, A., Matsushige, K., and Nagai, T. (2003) Trihalomethane formation potential of dissolved organic matter in a shallow eutrophic lake. *Water Res.* 37,4284-4294.

Kitis, M., Karanfil, T., Kilduff, J.E., and Wigton, A. (2001) The reactivity of natural organic matter to disinfection byproducts formation and its relation to specific ultraviolet absorbance. *Water Sci. Technol.* 43(2), 9–16.

Kononva, M.M. (1961) Soil organic matter. *Its Nature, its role in soil formation and in soil fertility.* Pergamon Press, New York.

Laane, R.W.P.M. (1982) Influence of pH in the fluorescence of dissolved organic matter. *Marine Chemistry* 11, 395-401.

Leenheer, J.A, Huffman, E.W.D., (1976) Classification of organic solutes in water by using macroreticular resins. *J.Res.US Geol. Surv.* 4, 737-751

Leenheer, J.A. (1981) Comprehensive approach to preparative isolation and fractionation of dissolved organic-carbon from natural-waters and wastewater. *Environ. Sci. Technol.* 15, 578-587.

Liang, L. and Singer, P. (2003) Factors influencing the formation and relative distribution of haloacetic acids and trihalomethanes in drinking water. *Environ. Sci. Technol.* 37, 2920-2928.

Mant, C.T., and Hodges, R.S (Eds.). (1991) *High-Performance Liquid Chromatography of Peptides and Proteins: Separation, Analysis and Conformation*, CRC press, Boca Raton, Fl.

Mant, C.T., Hodges, R.S., and Gooding, K.M., Regnier, F.E (Eds.). (2002) HPLC of Biological Macromolecules. Marcel Dekker. New York, NY, pp433.

Mantoura, R.F.C., and Riley, J.P., (1976) The analytical concentration of humic substances from natural waters. *Anal. Chim. Acta.* 76, 97-106.

Marhaba, T.F., and Van, D. J. (2000) The variation of mass and disinfection by-product formation potential of dissolved organic matter fractions along a conventional surface water treatment plant. *Hazardous Material* A74, 133-147

Masami, F., Atsunori, K., Kenji, T., and Fumiko, T. (2006) Separation of fulvic acid from soil extracts based on ion-pair formation with a cationic surfactant. *Analytical Chemistry* 22,229-233.

Mcgarry, S.F., and Baker, A. (2000) Organic acid fluorescence: application to speleothem palaeoenvironmental reconstruction. *Quaternary Sci. Rev.* 19,1087.

McKnight, D.M., Boyer, E.W., Westerhoff, P.K., Doran, P.T., Kulbe, T., and Anderson, D.T. (2001) Spectrofluorometric characterization of dissolved organic matter for indication of precursor organic materials and aromaticity. *Limnol. Oceanography* 46, 38-48.

Miano, T.M., and Sposito, G. (1988) Fluorescence spectroscopy of humic substances. *Soil. Sci. Am. J.* 52, 1016.

Mobed, J.J., Hemmingsen, S.L., Autry, J.L., and McGown, L.B. (1996) Fluorescence characterization of IHSS humic substances: Total luminescence spectra with absorbance correction. *Environ. Sci. Technol.* 30, 3061-3065.

Mopper, K., and Schultz, C.A. (1993) Fluorescence as a possible tool for studying the nature and water column distribution of DOC components. *Marine Chemistry* 41,229.

Parlanti, E., Morin, B., Vacher, L. (2002) Combined 3D-spectrofluorometry, high performance liquid chromatography and capillary electrophoresis for the characterization of dissolved organic matter in natural waters. *Org. Chem.* 33,221.

Patel-Sorrentino, N., Moynier, S., and Benaim, J.Y., (2002) Excitation-emission fluorescence matrix to study pH influence on organic matter fluorescence in the Amazon basin rivers. *Water Research* 36, 2571-2581.

Perdue, E.M., and Ritchie, J.D. (2003) Dissolve organic matter in freshwater. *Surface and groundwater, weathering and soils (*ed. J. I. Drevor). Vol 5. *Treatise on geochemistry* (ed.H.D.Hollard and K.K. Turekian). Elsevier-Pergamon, Oxford. pp 273-318.

Pomes, M.L., Green, W.R., Thurman, E.M., Orem, W.H., and Lerch, H.E. (1999) DBP formation potential of aquatic humic substances. *J. Am.Water Works Assoc.* 91,103-115.

Pullin, M.J., and Cabaniss, S.E. (1995) Rank analysis of the pH-dependent synchronous fluorescence-spectra of six standard humic substances. *Environ. Sci. Technol.* 29(6),1460.

Reckhow, D.A., Singer, P.C., and Malcolm R.L. (1990) Chlorination of humic materials: byproduct formation and chemical interpretations. *Environ. Sci. Technol.* 24(11),1655–64.

Roccaro, P., and Vagliasindi, F.G.A. (2009) Differential vs. absolute UV absorbance approaches in studying NOM reactivity in DBPs formation. Comparison and applicability *Water Research* 43(3),744-750.

Schwarzenbach, R.J., etc (2003) *Environmental Organic Chemistry*, second edition, Wiley-interscience.

Senesi N. (1990) *Anal. Chem. Acta.* 23,277.

Senesi, N., Miano, T.M., Provenzano, M.R., and Brunettig. (1991) Characterization, differentiation and classification of humic substances by fluorescence spectroscopy. *Soil Sci.* 152(4), 259.

Shibu, M., Mant, C.T., and Hodges, R.S. (2005) Effects of anionic ion-pairing reagent hydrophobicity on selectivity of peptide separations by reversed-phase liquid chromatography. *Journal of Chromatography A* 1080, 68-75.

Sierra, M.M.D., Giovanela, M., and Parlanti, E. (2006) 3D-fluorescence spectroscopic analysis of HPLC fractionated estuarine fulvic and humic acids. *J. Braz. Chem.* 17(1), 113-124.

Smith, B., and Warwick, P. (1991) Analysis of fulvic-acids by ion-pair chromatography. *Journal of Chromatography* 547, 203-210.

Stedmon, C.A., and Markager, S., (2005) Tracing the production and degradation of autochthonous fractions of dissolved organic matter by fluorescence analysis. *Limnol.Oceanogr.* 50, 1415-1426.

Steinberg, C.E.W., Meinelt, T., Timofeyev, M.A., Bittner, M., and Menzel, R. (2008) Behavior of chemicals in water and their interactions with organisms. Humic substances, Part 2. *Env. Sci. Pollut. Res.* 15(2), 128-135.

Stevens, A.A., Slocum, C.J., Seeger, D.P., and Robeck, G.G. (1976) Chlorination of organics in drinking-water. *J. Am. Water Works Assoc.* 68,615.

Stevenson, F.J. (1994) *Humus chemistry: Genesis, composition, reactions.* John Wiley & Sons: New York. 59-95.

Sutton, R., and Sposito, G. (2005) Molecular structure in soil humic substances: the new review. *Environ. Sci. Technol.* 23, 9009-9015.

Swietlik, J., and Sikorska, E. (2005) Characterization of natural organic matter fractions by high pressure size-exclusion chromatography, specific UV absorbance and total luminescence spectroscopy. *Polish journal of environmental studies* 15(1),145-153.

Thurman, E.M. (1985) *Organic Geochemistry of Natural water*. M.Nijhoff and W. Junk Publishers. Dordrecht, the Netherlands.

Thurman, E.M., Malcolm, R.L. (1981) Preparative isolation of aquatic humic substances. *Analytical Chemistry* 15, 463-466.

Watt, B.E., Malcolm, R.L., Hayes, M.H.B., Clark, N.W.E., and Chipman, J.K. (1996) Chemistry and potential mutagenicity of humic substances in waters from different watersheds in Britain and Ireland *Water Res.* 30, 1502-1516.

Weber, J.H., and Wilson, S.A. (1975) Isolation and characterization of fulvic acid and

humic acid from river water. *Water Res.* 9, 1079-1084.

Whelan, T.J., and Kamali, K.G. S., and Wilson M. (2003) *Ind. Eng. Chem. Res.* 42, 6673-6681.

Wu, F.C., Evans, R.D., and Dillon, P.J. (2003) Separation and characterization of NOM by high-performance liquid chromatography and on-line three-dimensional excitation emission matrix fluorescence detection. *Environ. Sci. Technol.* 37, 3687-3693.

CHAPTER 3

Isolation and Characterization of River DOM by Solid Phase Extraction

3.1 INTRODUCTION

Interest in DOM isolation and fractionation lies in its ability to measure suspected problematic fractions. One of the present research challenges is extending DOM characterization from the compound-class level to the specific compound level. Molecular characterization of DOM will give specific information about its precursors, and about reactive structures in DOM such as DBP precursors, metal-binding sites, etc. [Leenheer, 2003]. Therefore, more selective and easy-to–use isolation and fractionation techniques are being developed.

Although liquid-liquid extraction has been known as the “gold standard” for sample work-up, SPE is becoming more popular for sample pretreatment for high throughput automation and benefits from the increased commercial availability of innovative SPE sorbents during the last decade. A whole series of packing materials is now being marketed, including apolar to polar, mixed-mode, ion-exchange and combinations of these. The SPE technique is considered one of the most powerful techniques currently available for rapid and selective sample preparation and purification. Compared to conventional liquid-liquid extraction methods, advantages of SPE include smaller sample

and solvent requirements as well as simplicity and ease of handling. It is also environment-friendly method because of the reduced usage of toxic solvents.

SPE has been applied not only for the isolation and enrichment of trace organic contaminants from environmental samples before their analysis but also for the removal of the interfering components of the complex matrices in order to obtain a cleaner extract containing the analytes of interest.

For very complex matrices, the ultimate way to optimize isolation is to use orthogonal separation modes in tandem. An orthogonal method is one in which a second separation mode based on different mechanism follows the primary mode. When two columns or cartridges have orthogonal separation modes, they are usually packed with two different stationary phases. For example, one of the columns can be a revers ephase comumn and the other could be a cation exchange column, an anion exchange column, an affinity column or a metal chelating column. In another example, the two columns can be selected independently from the group consisting of a cation exchange column, an anion exchange column, an affinity column, a metal chelating column, and a reverse phase column. The methods using C8 and C18 columns are expected to yield similar elution profiles and are not orthogonal. In contrast, a C18 and a polar-embedded phase (amide) column are orthogonal and expected to yield dissimilar profiles. The two columns having orthogonal separation modes can be connected through tubing and fittings, directly attached, or attached through nuts and fittings. Intelligent application-directed selection affords a powerful extraction tool which can be adapted to the particular needs of the analysis [Decaestecker et al., 2003, Bouvier, 1998, Franke, 1998, Huck, 2003].

Isolation and fractionation techniques are time and labor consuming, therefore there is a need to identify DOM fractions rapidly of source water characterization and optimization water treatment processes. 3DEEM fluorescence and UV-visble absorbance is the technique to meet these needs.

The aims of this study are (1) to test the ability of different types of SPE to extract the chromophoric humic substances from river water; (2) to find out which sorbent is the most appropriate with regard to extraction yield, cleanliness and preconcentration of the extracts from river water.

3.2 MATERIALS AND METHODS

3.2.1 Extraction protocols and procedures

SPE sorbents studied

Four SPE sorbents were studied: Sep-Pak C_{18} (Waters Corporation, catalog # WAT020515) and Em-Pore Disk (3M Center, catalog # 2215) were chosen as apolar sorbents, OASIS®HLB and OASIS®MAX sorbents (Waters, catalog # 186001880 and 186000865) as sorbents of organic polymers (Table 3.1).

Table 3.1 The properties of the apolar and organic polymers cartridges and disk.

Sorbent	Description	Particle size (μm)	Volume (mL/filled cartridge)	Source
Sep-Pak	Hydrophobic	80	1.60 mL	Waters
Oasis HLB	Hydrophobic and Hydrophilic balanced	30	3 mL	Waters
Oasis MAX	Mixed-mode	60	6 mL	Waters
Empore disk	Hydrophobic	12	500 mL	3M

Sep-Pak C18 cartridge Because of the strong hydrophobicity of its bonded-phase, C18 (Figure 3.1) cartridges are used to isolate hydrophobic species from aqueous solutions. Sep-pak is typically used to adsorb trace organic pollutants from environmental water samples.

EmPore C18 Disk The disk consists of end capped C18 hydrocarbon/silica material imbedded in an inert polytetrafluoroethylene (PTFE) fiber matrix. The disk format

provides a greater surface area and faster mass transfer to the C18 particles than the traditional cartridges. The nominal pore size of the disk is 60 Å.

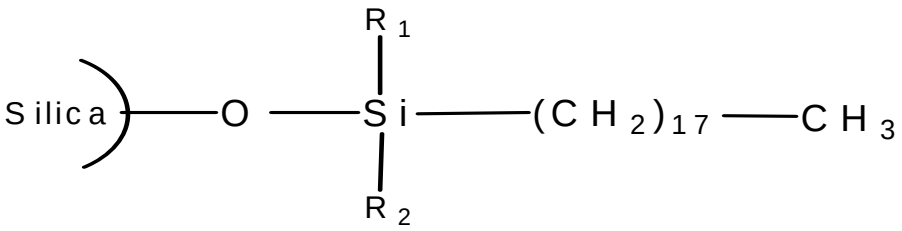

Figure 3.1 Chemical Structure of Sep-pak C18 and Em-pore C18.

Oasis®HLB HLB is a hydrophilic (N-vinylpyrrolidone)-lipophilic (divinylbenzene)-balanced reverse-phase sorbent (Figure 3.2), universal for acid, bases and neutrals. The manufacturer claims extraordinary retention of polar compounds, and a relative hydrophobic retention capacity (per volume) 3x higher than that of traditional silica-based SPE sorbents like C18 [Waters Corp.].

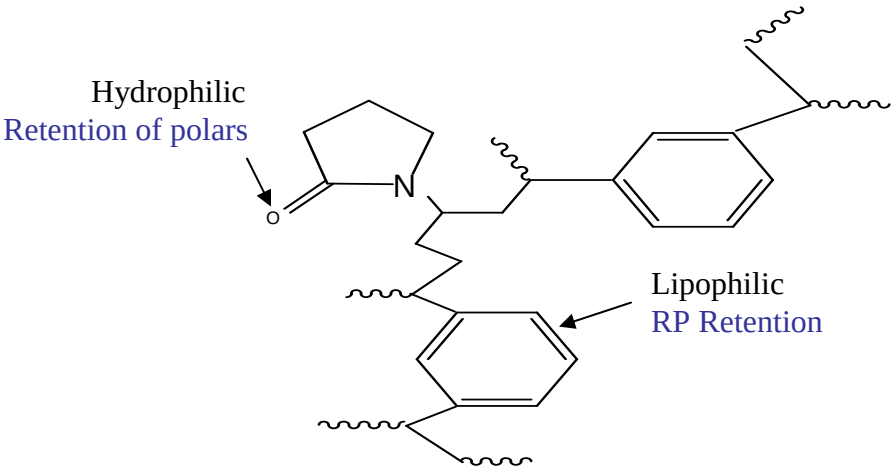

Figure 3.2 Oasis® HLB copolymer with hydrophilic-lipophilic (N-vinylpyrrolidone-divinylbenene) balance.

Oasis®MAX MAX is a mixed-mode anion-exchange reversed-phase sorbent. It has high selectivity and sensitivity for acidic compounds [Waters Corp.]. Since NOM is known to contain carboxylate and phenolate functional groups and behave as a polyanion, this specific sorbent was tried.

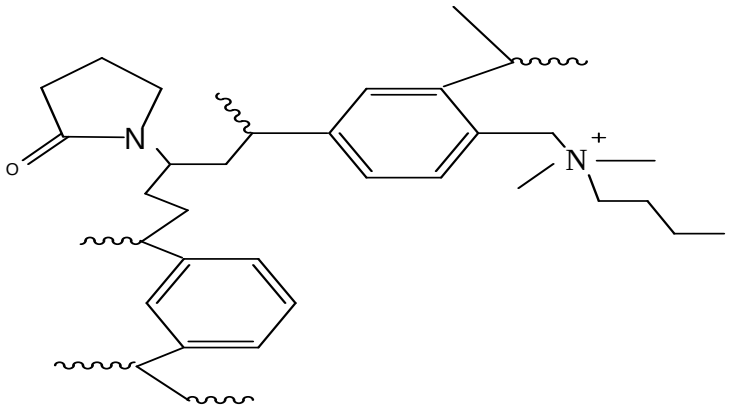

Figure 3.3 Oasis®MAX sorbent with reversed-phase retention and strong anion-exchange.

Sample preparation

Water samples

The Rio Grande River was sampled in July 14 of 2004 and August 13 of 2005 at Albuquerque, NM. Two water samples came from different sites on the Rio Grande, near the ABQ (Albuquerque) wastewater treatment facility (Figure 3.4). All water samples were collected near the surface, and were immediately filtered using a GFF (glass fiber filter) with a nominal pore size of 0.7 μm then stored in clean polyethylene bottles at -6 Celsius in the freezer.

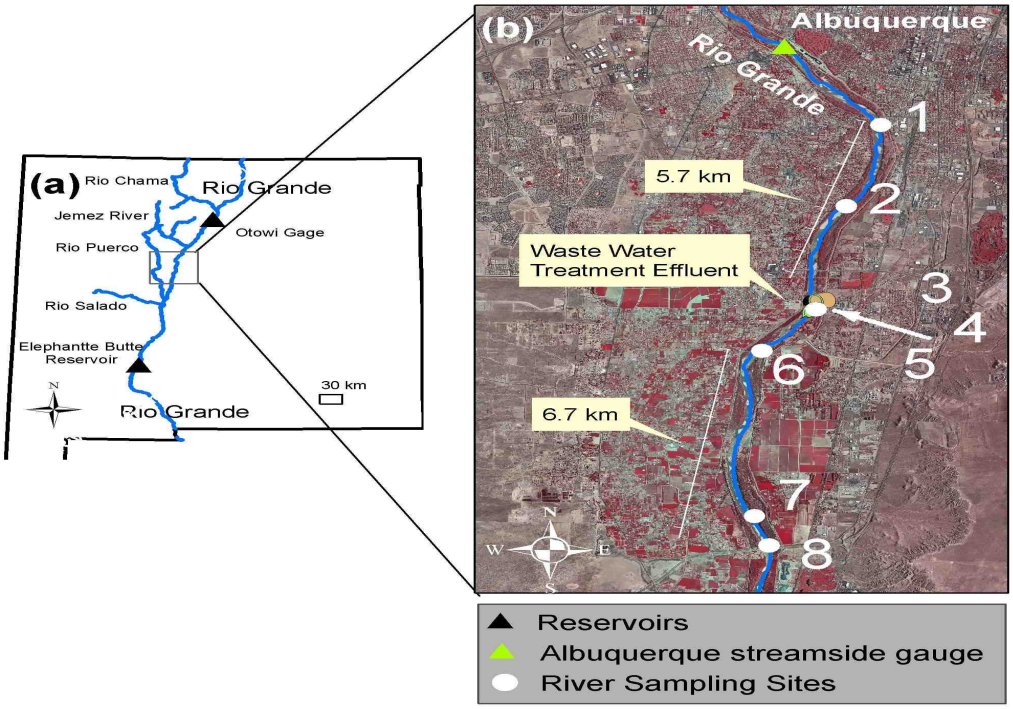

Figure 3.4 The site map of river water sampling.

The extraction of river DOM was performed by passing 5 mL or 30 ml of filtered water through pre-treated (30 mg-200 mg of packing) cartridges under gravity (without a vacuum system). Cartridges and disk were pre-treated following the procedure according to the manufacturer's manual (see the details below). All the elutes and the washes were nitrogen-dried and re-dissolved in 5 mL Milli-Q water and ready to run for the UV and fluorescence (Table 3.2).

Table 3.2 River water parameters.

Samples		DOC (mg/L)	UV_{254} (au)	SUVA (L/m.mg)
River water	7/2004	5.85	0.122	2.07
	8/2005	6.82	0.113	1.66

The general logical approach (Figure 3.5) for all of the protocols to extract DOM is

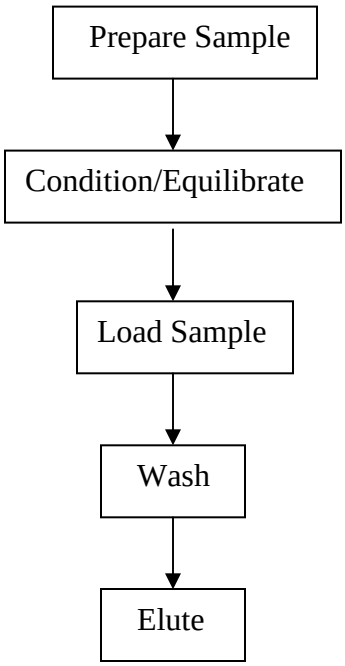

Figure 3.5 The approach to extract DOM from river water for all of the protocols.

Apolar Sorbents

Sep-Pak C18 cartridge Method (Figure 3.6) The cartridge was pretreated with 5 mL 0.3 mM HCl, then 5 mL methanol (MeOH), and finally 5 mL Milli-Q water. Just before loading, the C18 cartridge was conditioned with 3 mL methanol and 5 mL Milli-Q water. After loading with 5 mL sample, the C18 cartridge was washed with 1 mL Milli-Q water

before elution and then eluted with 1 mL methanol. Junk [Junk, 1988] showed that trace quantities of aliphatic, aromatic and silica compounds are eluted by organic solvents from a variety of reverse-phase extraction media. However, of all the solvents tested, methanol afforded the lowest amount of contamination.

If the sample flow rate is too high, components may not interact sufficiently with the SPE sorbent. The result is loss of resolution, analyte breakthrough, and poor recovery. Since the Sep-Pak C18 is a compact cartridge, the experiments were performed by using a flow rate 0.2-1 mL/min under gravity to condition, load and elute the cartridge.

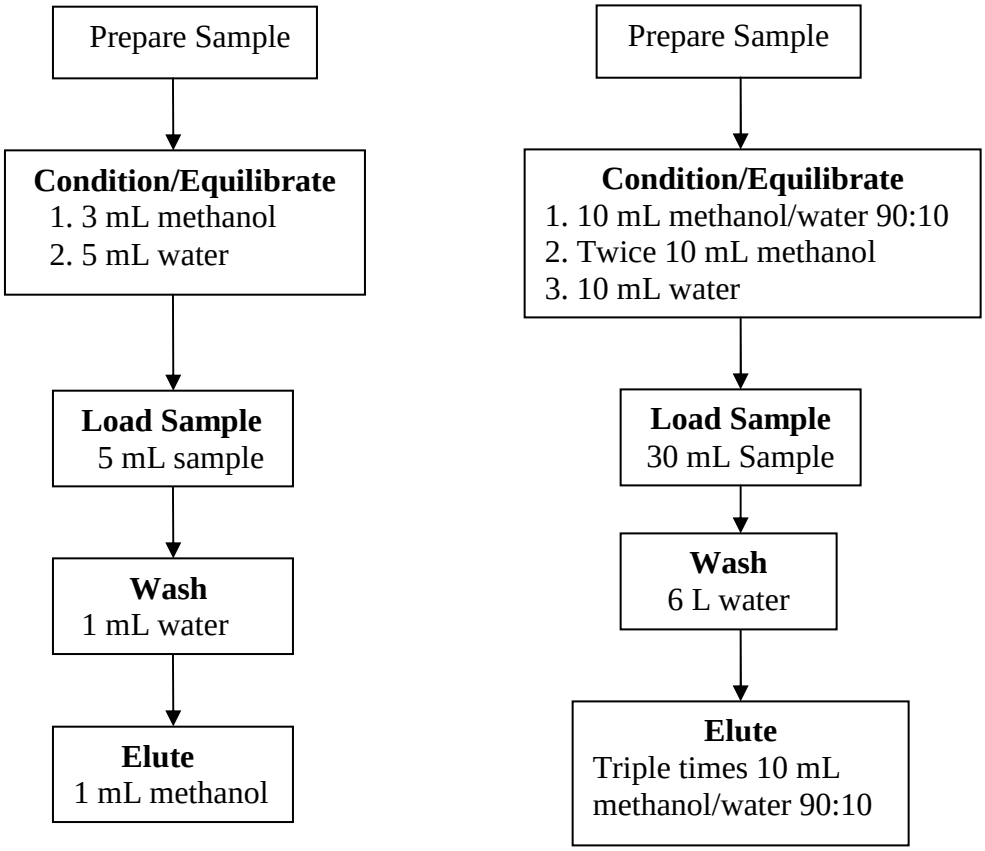

Extraction Method for Sep-Pak C18 Extraction Method for Empore disk

Figure 3.6 Extraction methods for Sep-pak C18 and Empore disk.

Empore C18 Disk Method (Figure 3.6) Solid-phase extraction was performed using Empore C18 disks and a borosilicate-glass 2 L vacuum-filtration unit with a coarse fritted glass holder to support the C18 disk.

The disk was activated and conditioned according to the manufacturer's manual. The disk was rinsed first with 10 mL of MeOH: H_2O (90:10), then twice with 10 mL methanol, and finally with 10 mL DI water. For complete mass-balance characterization of the disk and removal of the methanol, it was further rinsed with 6 L of DI water. The retention capacity of the C18 disk may be diminished by this extensive DI water rinse. To elute the sample from the disk, the disk was rinsed three times with 10 mL MeOH: H_2O (90:10). The eluates from the disk extraction were collected in a clean flask and dried with nitrogen gas at room temperature. Dried samples were re-dissolved in 5 mL DI water and were taken for UV and fluorescence analysis.

Oasis HLB Method (Figure 3.7) HLB cartridge was conditioned with 1 mL methanol followed by 1 mL water. After 5 mL sample was loaded, the cartridge was washed with 2 mL 5% methanol in water, then eluted sample with 3 mL methanol (Figure 3.7).

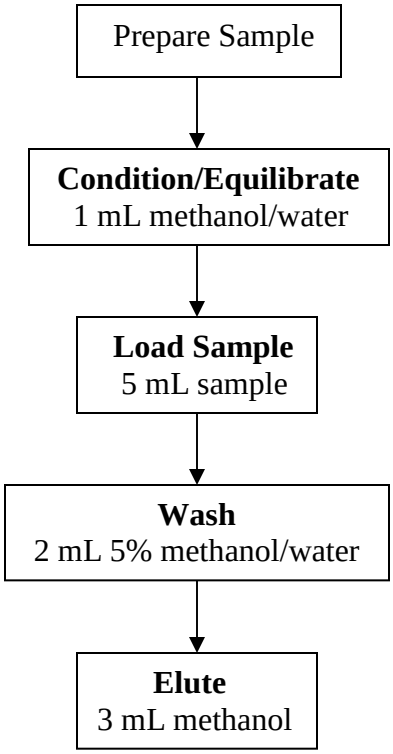

Figure 3.7 Extraction Method for HLB.

Oasis MAX Method In order to obtain high recovery for DOM from MAX cartridge, variable methods for conditioning, eluting were tried with different polarity solvents and those methods were modifications of protocol described below (Figure 3.8).

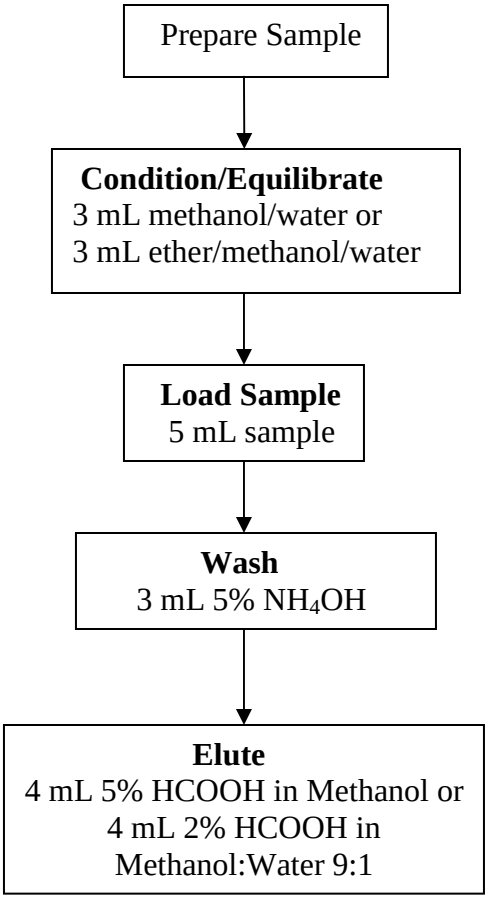

Figure 3.8 Extraction Method for MAX.

Tandem Oasis HLB-MAX Method (Figure 3.9) For the orthogonal separation modes in tandem, the procedure includes 4 stages: stage 1 was to condition, load and wash the Oasis HLB cartridge; stage 2 was to condition the Oasis MAX; stage 3 was to attach MAX cartridge to outlet of HLB cartridge, then elute from HLB into MAX (the final eluate from the first cartridge HLB was loaded directly into the second cartridge MAX). The final stage 4 was to discard the HLB cartridge and then wash and elute MAX cartridge.

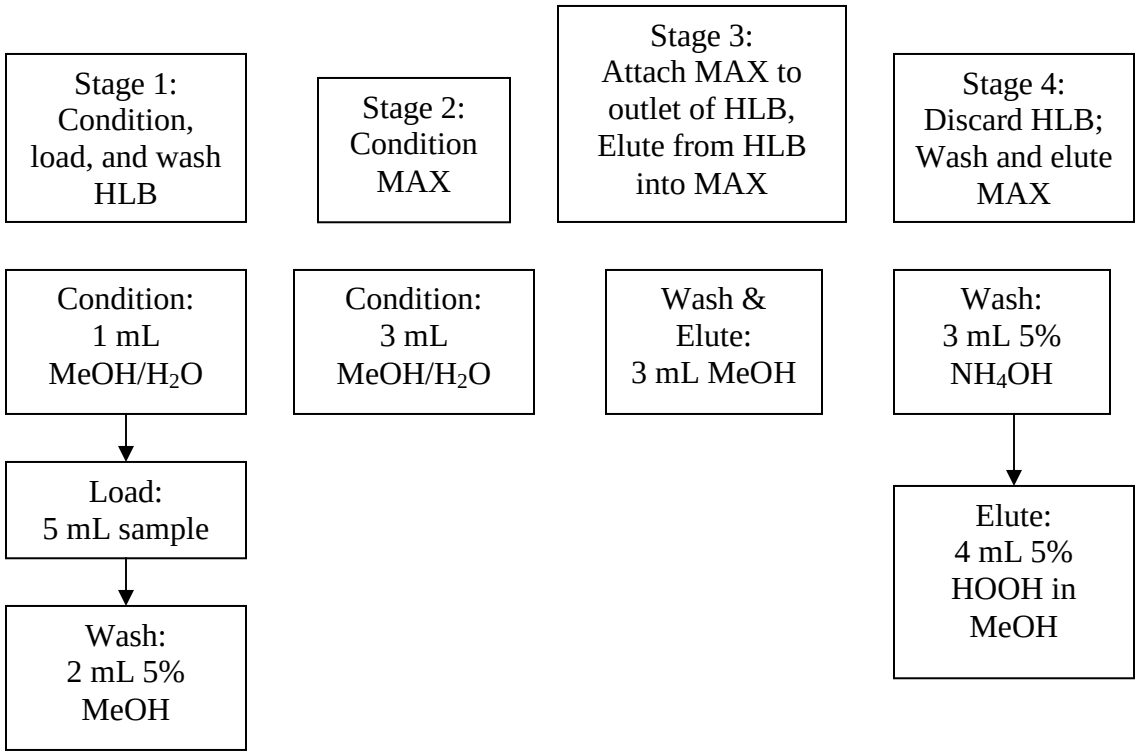

Figure 3.9 Extraction method for HLB-MAX mixed modes.

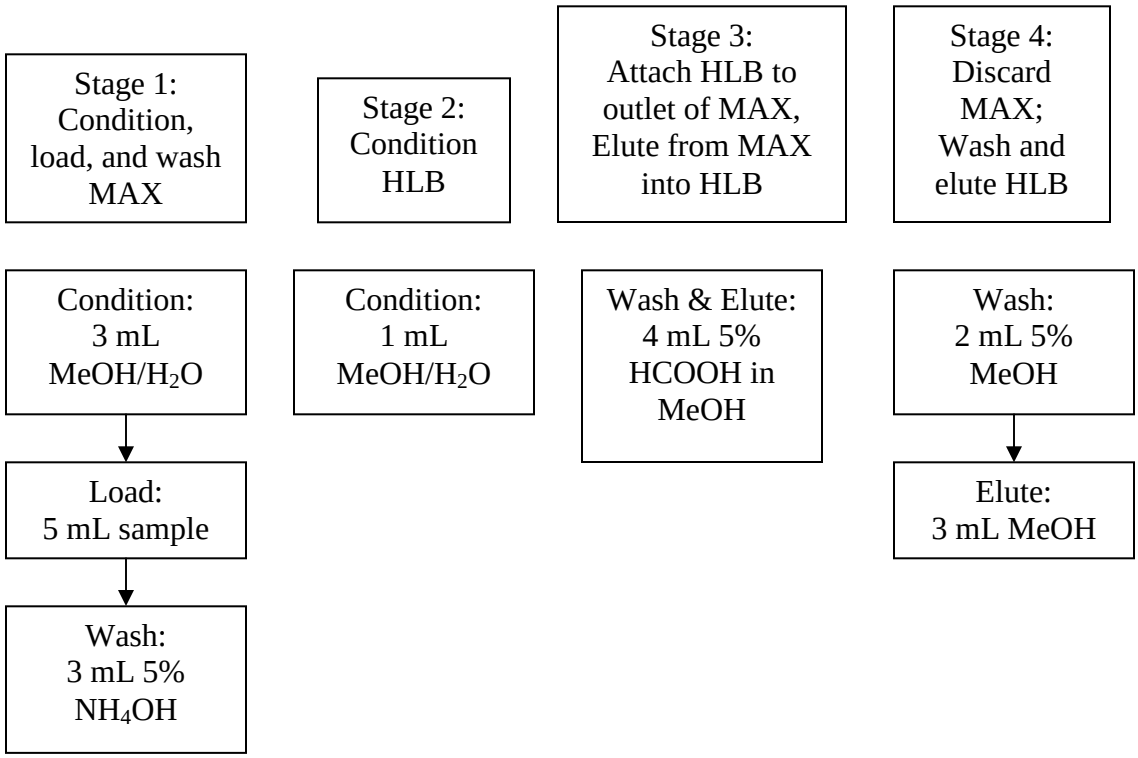

Figure 3.10 Extraction method for MAX-HLB mixed modes.

Tandem Oasis MAX-HLB Method (Figure 3.10) The protocol is similar to tandem oasis HLB-MAX method but reverses order of HLB and MAX. Stage 1 was to condition, load and wash the Oasis MAX cartridge; stage 2 was to condition the Oasis HLB; stage 3 was to attach HLB cartridge to outlet of MAX cartridge, then elute from MAX into HLB (the final eluate from the first cartridge MAX was loaded directly into the second cartridge HLB). The final stage 4 was to discard the MAX cartridge and then wash and elute the HLB cartridge.

The collected elutes from each cartridge were nitrogen air dried and re-dissolved in 5 mL milli-Q water for fluorescence and UV analysis.

3.2.2 Analytical methods

TOC was measured by TOC analyzer (Shimadzu high temperature Pt-catalytic oxidation).

Fluorescence spectroscopy and UV Spectroscopy

For procedural details on the fluorescence and UV spectroscopy refer to section 2.2.2.

3.3 RESULTS

3.3.1 Fluorescence and UV spectra features of river water and its isolates

The EEM fluorescence of the river water sample from August of 2005 is presented in Figure 3.11 and Figure 3.12. Two characteristic ranges of fluorescence can be distinguished: the most intense region is centered at $\lambda_{ex}/\lambda_{em}$= 230/424 nm (peak A) and the less intense one at $\lambda_{ex}/\lambda_{em}$=320/420 nm (peak C). The fluorophores responsible for these two main signals have been recognized as belonging to typical components—UV and visible humic-like fluorophores, having received individual designations as Peak A and C respectively [Coble 1990, Coble, 1996]. Besides these two main peaks, the samples present another two signals at shorter emission wavelengths. Coble and others [Coble, 1996; Yamashita and Tanoue et al., 2003; Parlanti et al., 2002] assigned the fluorescence signals at 275/340 and 220-230/340-350 to tryptophan-like fluorophores as peak T. Fluorescence maximum of the more intense signal is located at $\lambda_{ex}/\lambda_{em}$=230/350 nm, which usually is attributed to protein derived components and which is designated here as Peak T_1. The other signal identified around $\lambda_{ex}/\lambda_{em}$=260-270/340 nm is designed as T_2. Although fluorescence spectra of peak T_1 were observed to extend to shorter excitation and emission wavelength, it is difficult to be certain if another type of protein-like fluorescence, tyrosine-like fluorescence, is present due to spectral overlap with peak T_1. Tryptophan-like fluorophores are known to exhibit fluorescence signals in pairs with another maximum at $\lambda_{ex}/\lambda_{em}$ = 270-280/340-360 nm as peak T_2.

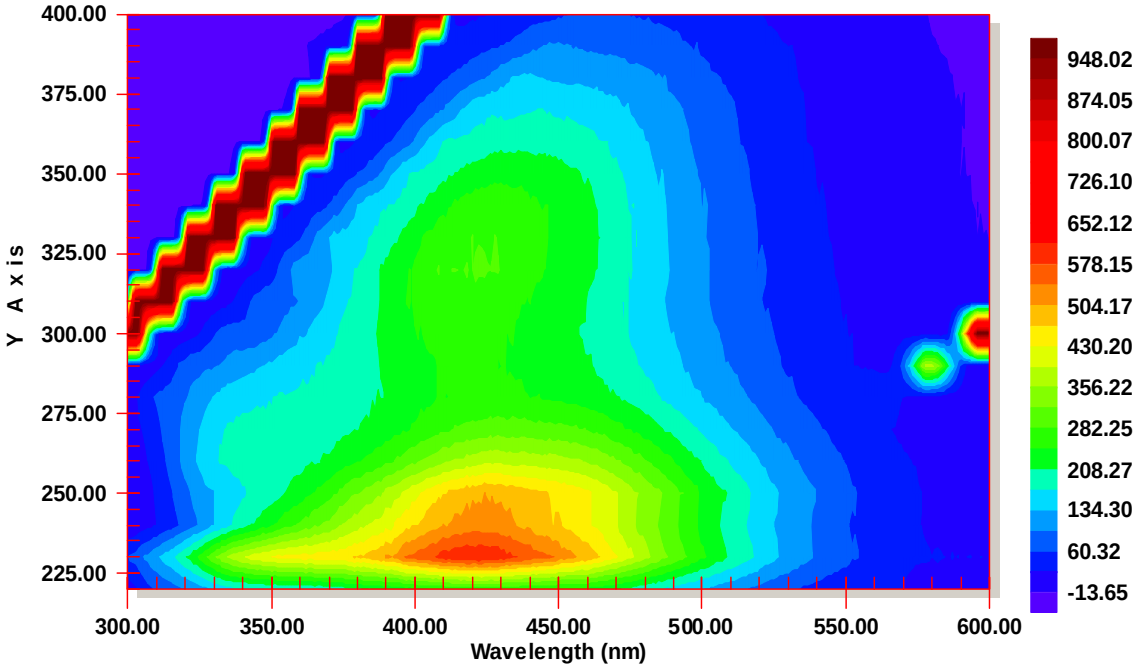

Figure 3.11 Contour plots of river water bulk samples in August of 2005.

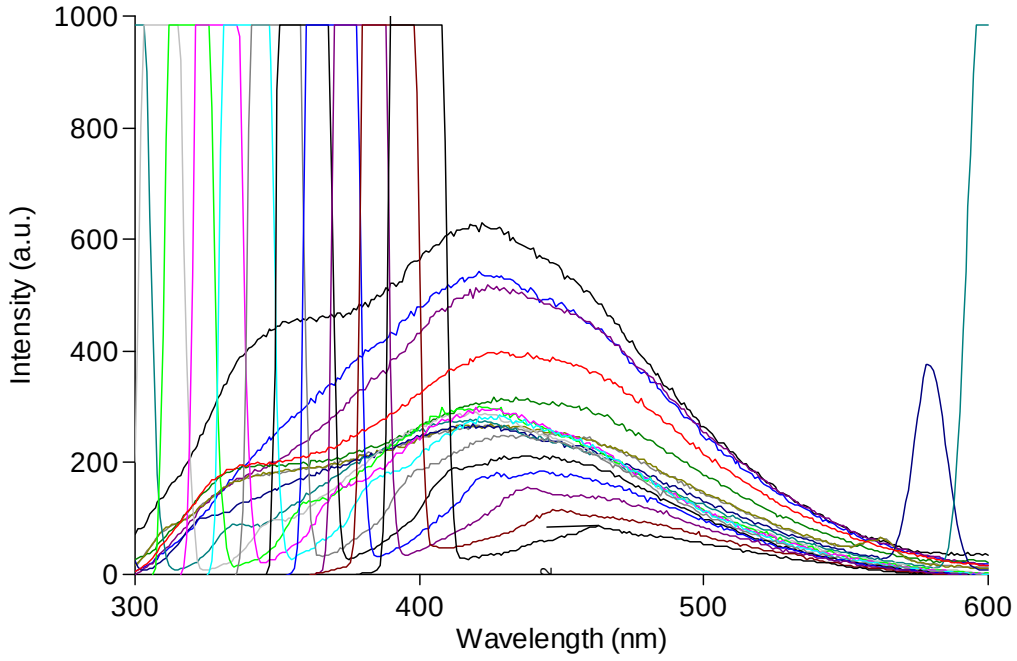

Figure 3.12 Emission spectra of bulk river water in August of 2005.

Comparing the August of 2005 sample to the fluorescence features of July 2004 (Figure 3.13, 3.14), they are similar except the sample from July, 2004 lacks fluorescence signals at $\lambda_{ex}/\lambda_{em}$=260-270/340 nm present in the sample from August of 2005. However, peak T_2 is identified at $\lambda_{ex}/\lambda_{em}$= 280/356 nm in the sample from July of 2004. Therefore, the fluorescence signal at $\lambda_{ex}/\lambda_{em}$= 260-270/340 nm in 2005 is defined here as peak D. Previous work may have missed this peak due to the consequence of fluorescence signals overlapping between peak T_2 and other unknown fluorophores. In addition, a poorly resolved peak but perceptible shoulder at around 250/460 nm was observed in both spectra from July of 2004 and August of 2005.

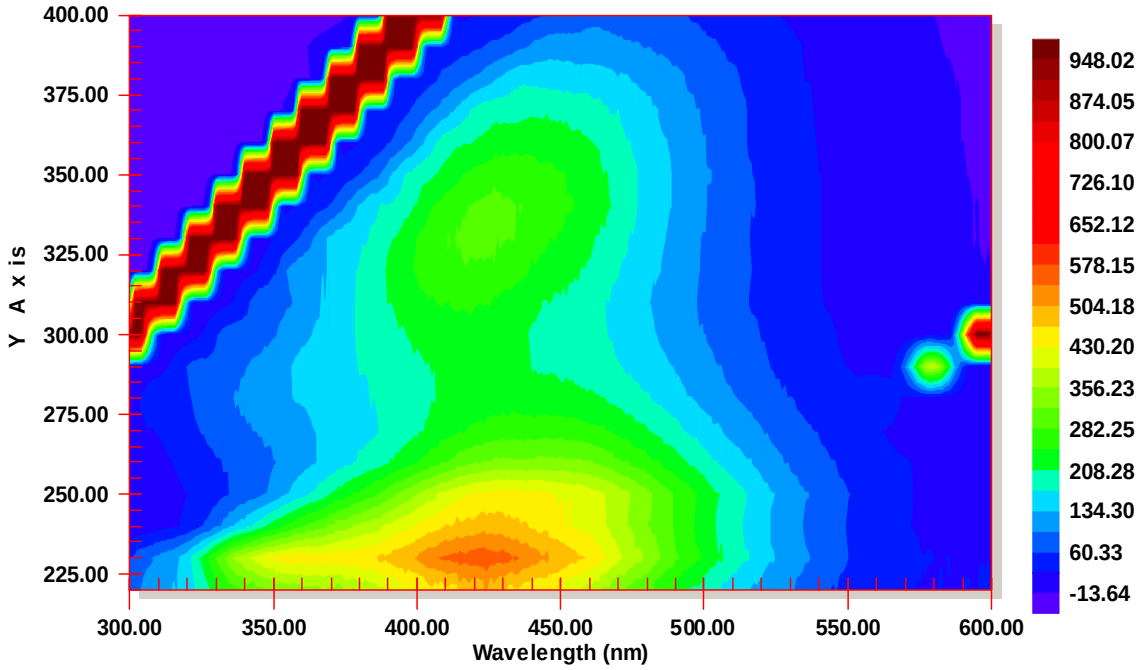

Figure 3.13 Contour plots of river water bulk samples in July of 2004.

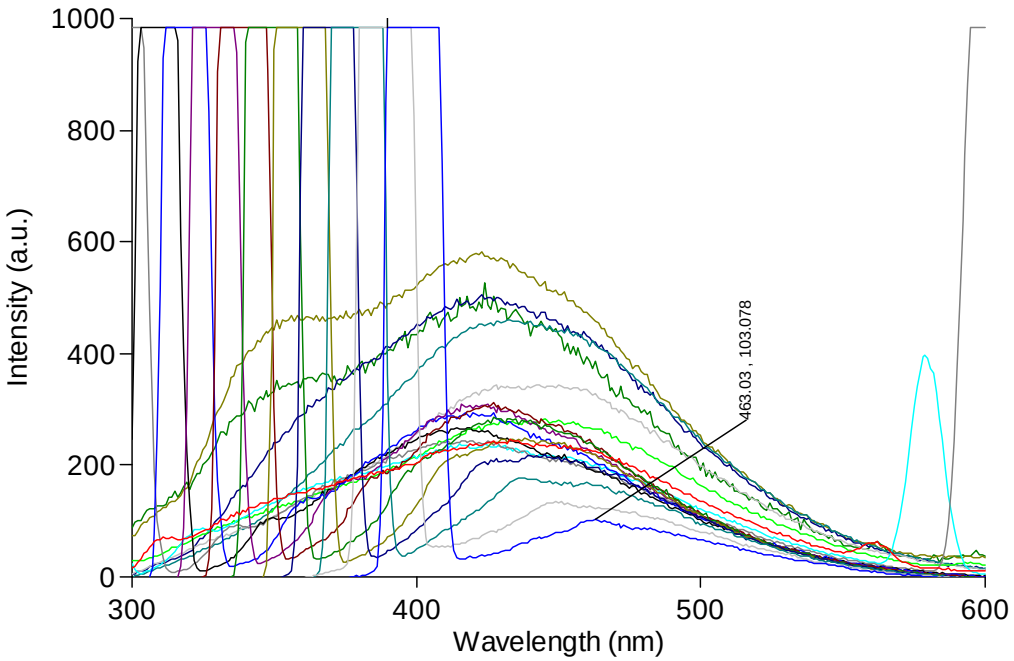

Figure 3.14 Emission spectra of bulk river water July of 2004.

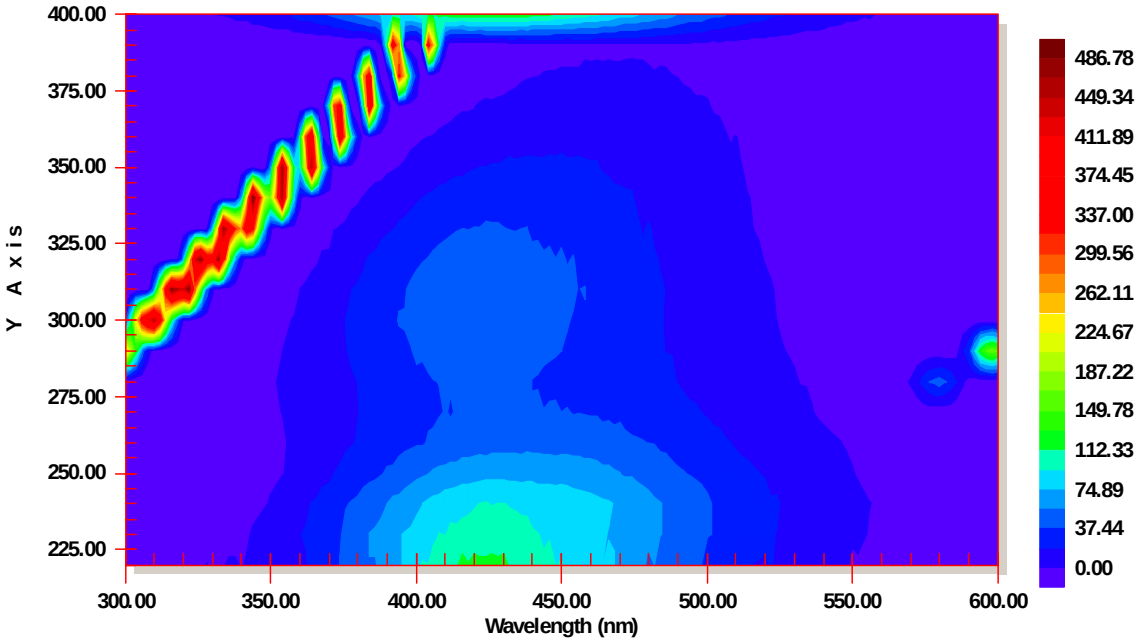

Figure 3.15 Contour plots of river water portion eluted from Sep-Pack C18 cartridge in August of 2005.

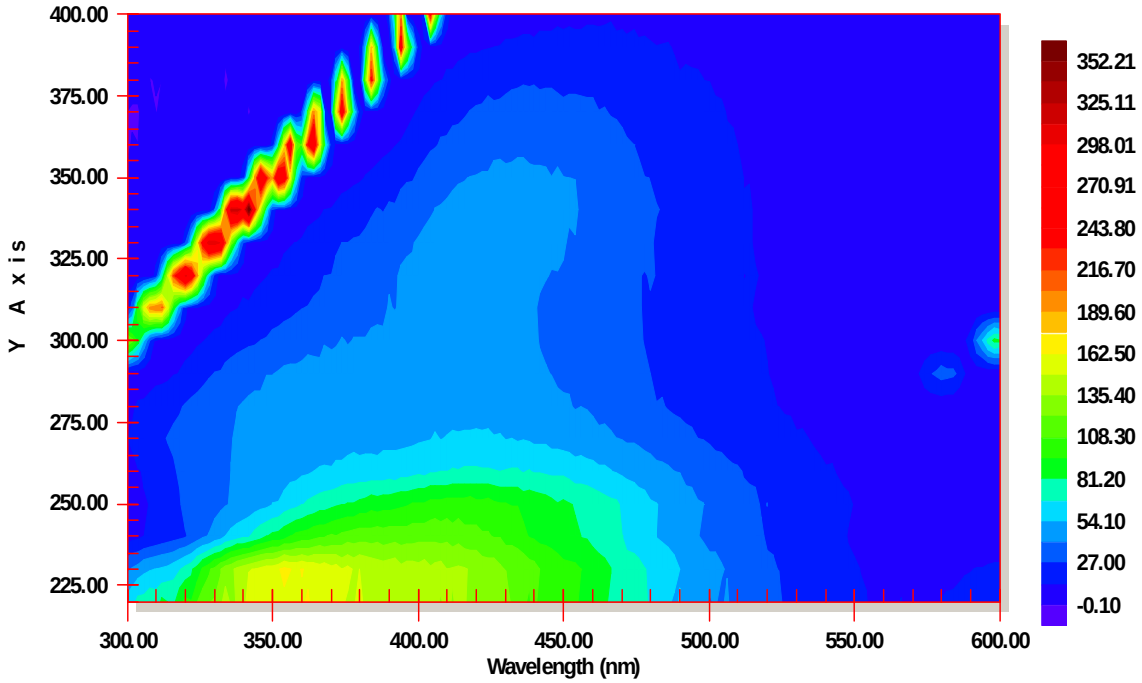

Figure 3.16 Contour plots of river water portion washed by Sep-Pack C18 cartridge in August of 2005.

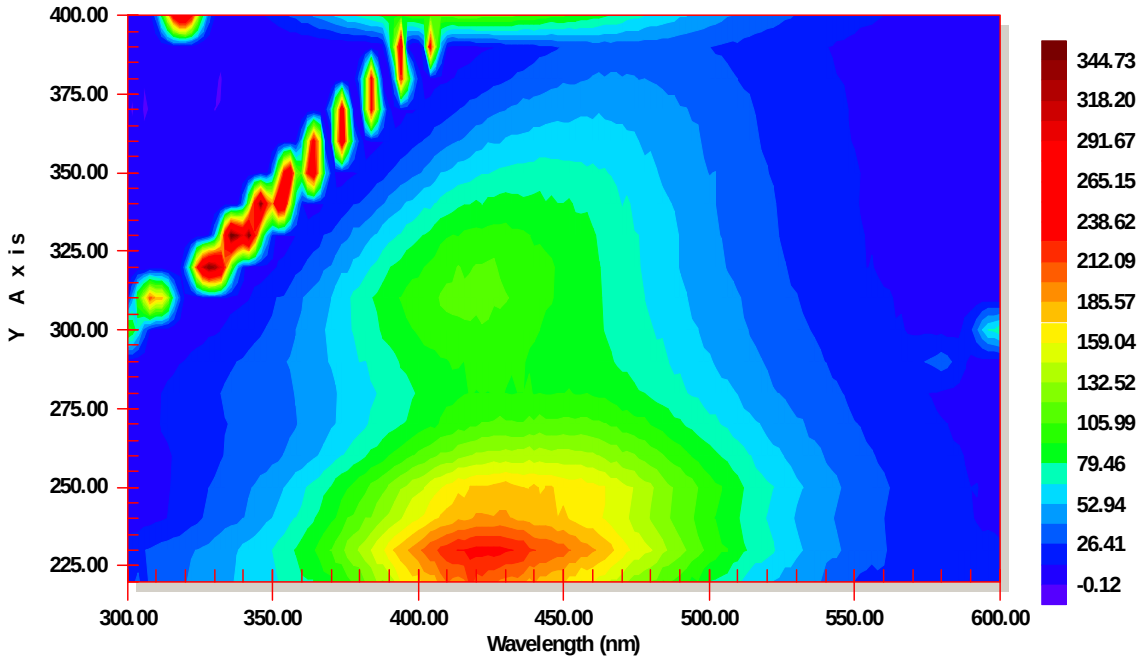

Figure 3.17 Contour plots of river water portion eluted from HLB sorbent in August of 2005.

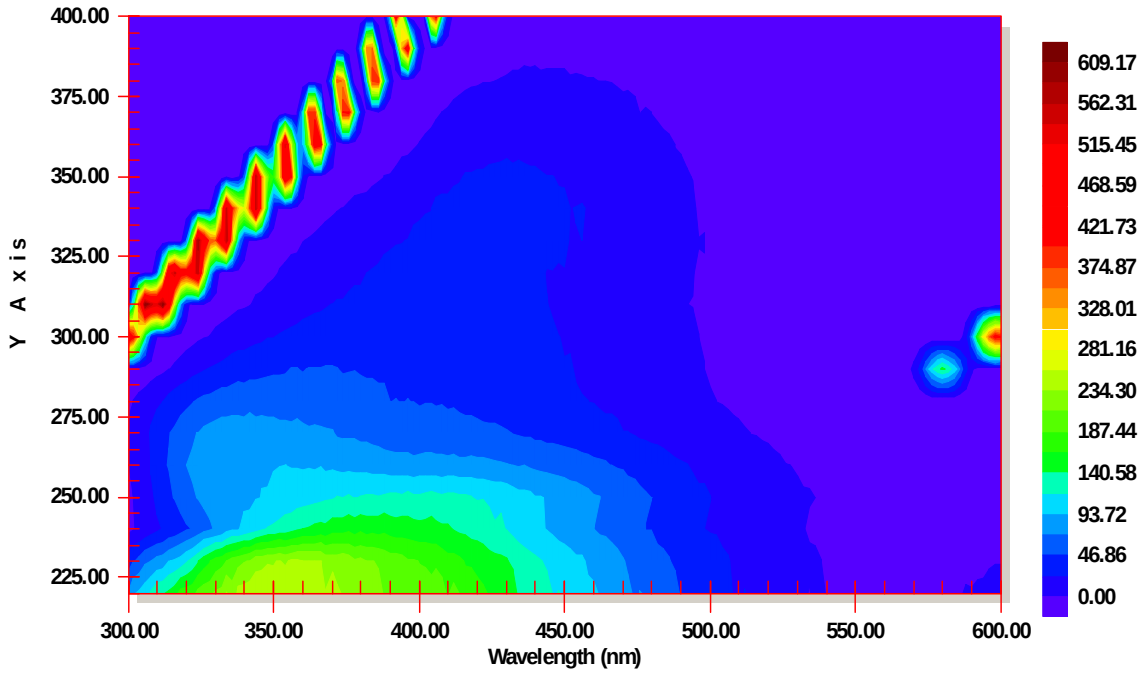

Figure 3.18 Contour plots of river water portion washed by HLB sorbent in August of 2005.

A comparison of EEMs (Figure 3.15-3.18) from eluted portions of river water shows no change in peaks' maximum wavelengths ($\lambda_{ex}/\lambda_{em}$) and little variation of overall peak shapes between Sep-pak C18 and HLB cartridges. For example, EEM spectra of the eluted isolates revealed two major fluorescence centers located at $\lambda_{ex}/\lambda_{em}$=230/424 nm (Peak A) and $\lambda_{ex}/\lambda_{em}$=320/420 nm (Peak C) respectively. These isolates from Sep-pak and HLB present no wavelength shift for their fluorescence maxima compared to raw water before extraction, only intensity decreases. Presence of humic-like fluorescence and absence of protein-like fluorescence demonstrate that both Sep-pak and HLB sorbents preferentially isolate humic-like fluorophores. Overall EEM shapes of these isolates resemble those of NOM from McDonalds Branch and HA, FA samples from IHSS (Figure 2. 2)

EEMs of the washes from Sep-pak C18 and HLB, closely resembled each other with four fluorescence peaks each. The most intense peak was Peak T_1 centered at $\lambda_{ex}/\lambda_{em}$=230/356 nm while the less intense peak was Peak T_2 with location difficult to determine. Peak A was observed as a clear shoulder with its fluorescence maximum around $\lambda_{ex}/\lambda_{em}$=230/420 nm by Sep-pak C18 method, while peak A was barely perceptible from fluorescence emission spectra by HLB method since it was obscured by Peak T_1. However, peak A still could be differentiated from the contour plots. Meanwhile, Peak C occured at around 310-340/420-430 because it overlapped seriously with the signals which inhibit its fluorescence center at 260/330 nm by both extraction methods. Maximum emission wavelength varied with maximum excitation wavelength for peak C (λ_{em} depends on λ_{ex}) implying that peak C is a mixture of multiple fluorophores.

EEMs of eluate and washes by Empore C18 Disk method (Figure 3.19 and Figure 3.20) are fairly identical to the HLB eluate and washes except that the fluorescence maximum of peak T_1 occurred at 230/350 nm. They have the same types of the peaks, same peak locations and same contour shapes.

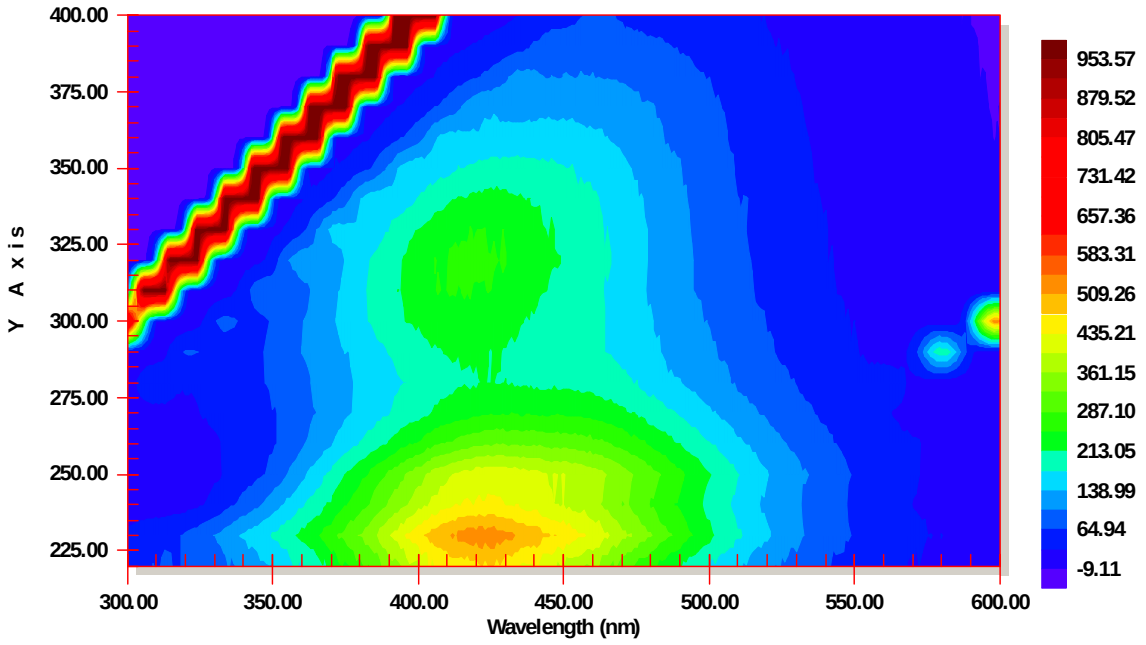

Figure 3.19 Contour plots of river water portion eluted from Empore C18 Disk in August of 2005 sample.

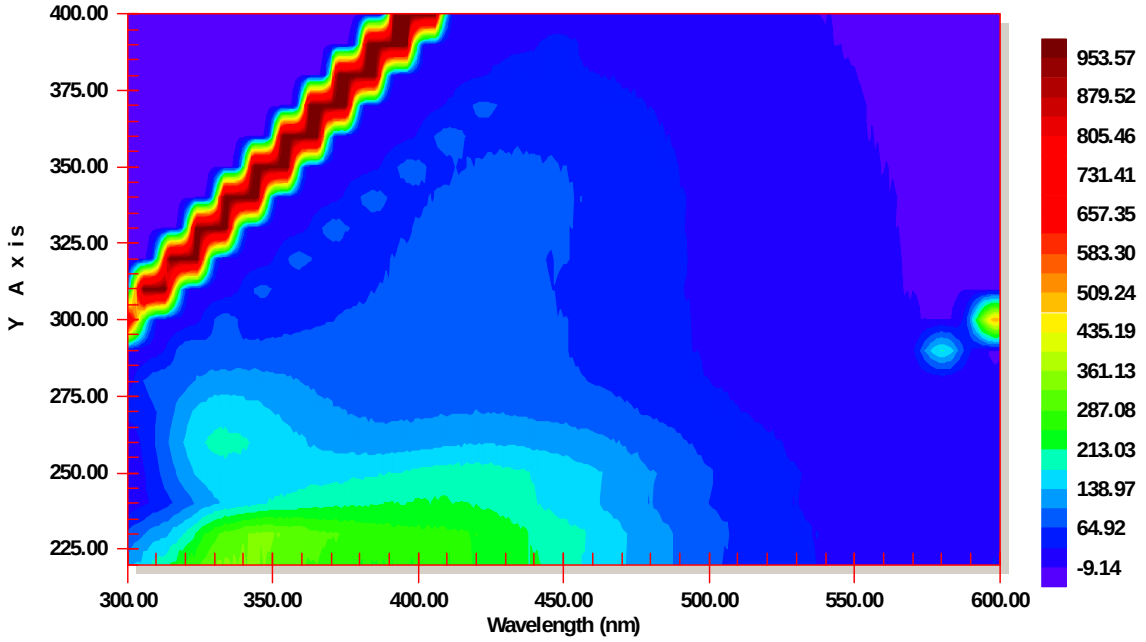

Figure 3.20 Contour plots of river water portion washed by Empore C18 Disk in August of 2005 sample.

Fluorescence spectra (Figure 3.21 and Figure 3.22) of washed fraction from the MAX cartridge showed nothing except water scattering lines for the sample of August 2005. On the other hand, three clear fluorescence signals were observed in the EEM maps of MAX eluted fraction with maxima at $\lambda_{ex}/\lambda_{em}$=240-250/410 nm (Peak A), 330/400 nm (Peak C) and 250-260/330-350 nm (peak D). Peaks A and C appear very well resolved ones because of the absence of near-by peaks; both peaks appear as complete shapes. Compared with original river water, fluorescence maxima of peaks A and C shifted, with λ_{ex} red shifting for 20 nm and λ_{em} blue shifting for 20 nm respectively. Moreover, contour plots of peak A exhibit oval shapes due to spectra overlapping, although peak C didn't distort along the first order Raman scattering line.

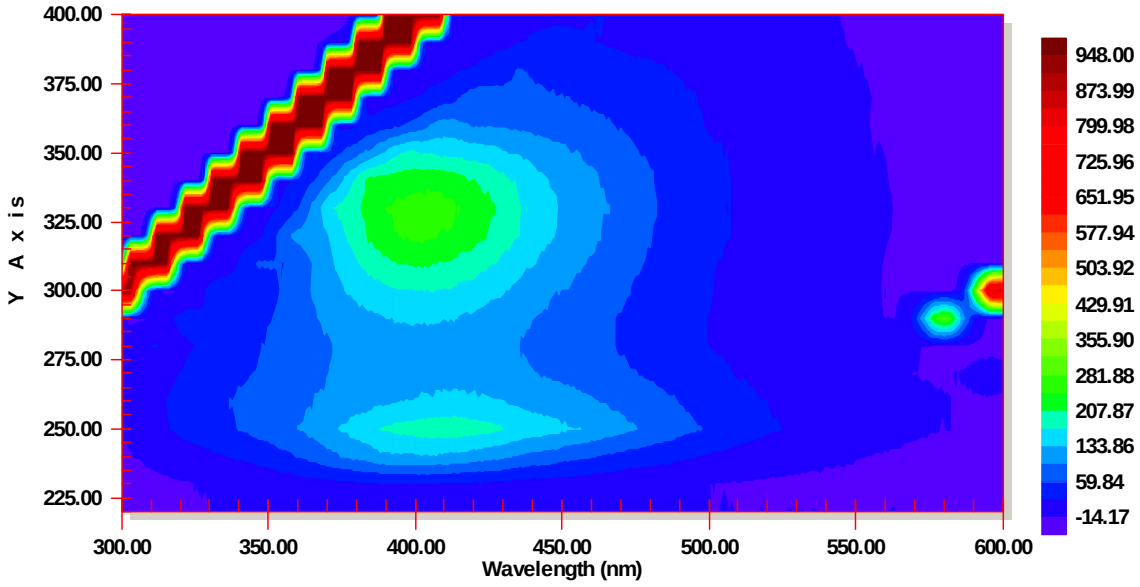

Figure 3.21 Contour plots of river water portion eluted from MAX sorbent in August of 2005.

Interestingly, the intensity of peak C is very close to or even higher than peak A with various polarity elution solvents. Peak B is not observed, and only peaks A and C are detected. The third peak appear as a shoulder between peaks A and C with excitation wavelengths from 250 to 290 nm and emission wavelengths from 320 to 360 nm (peak D). Although peak D occupies a similar region of optical space as tryptophan-like fluorescence (peak T_2), it could not be attributed to protein-like signal because the former maximum excitation wavelengths occurred at 250-260 nm, while the latter at 220-230 nm. If it is peak T_2, then it should have a more intense fluorescence signal at shorter excitation wavelength. Only one fluorescence center is observed in the EEMs, indicating that peak D is a different signal from peak T_2. In contrast, tryptophan-like fluorescence is not observed in either the eluate or the washes EEMs.

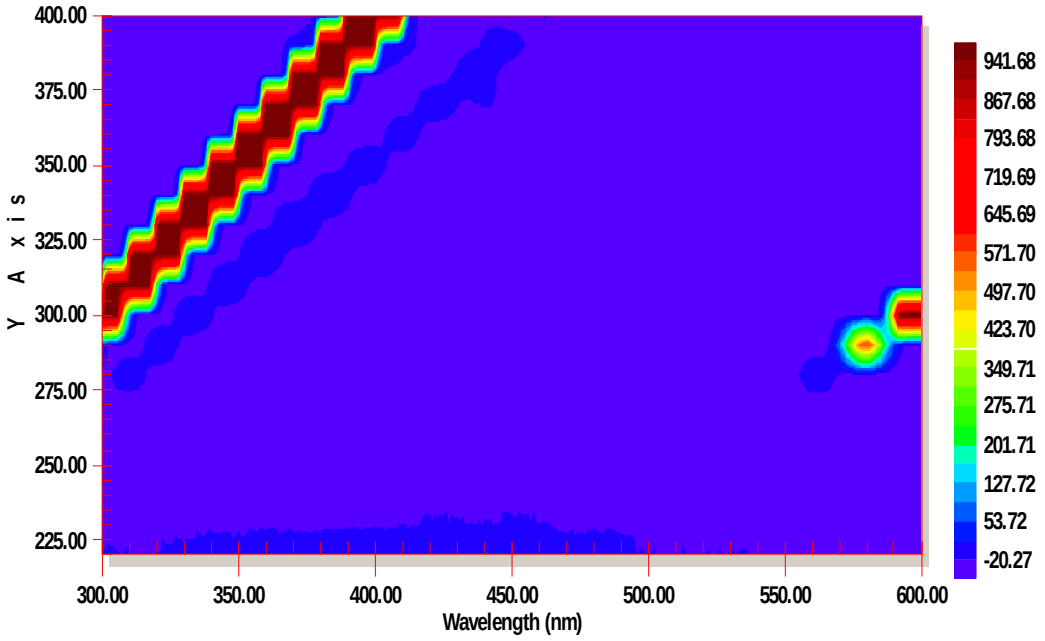

Figure 3.22 Contour plots of river water portion washed by MAX sorbent in August of 2005.

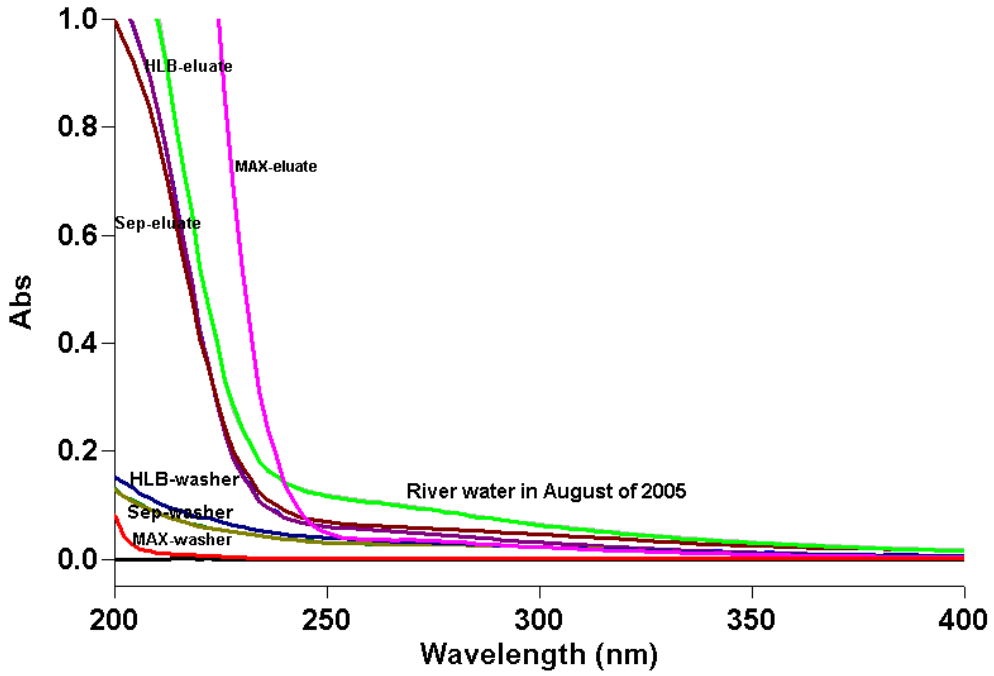

Figure 3.23 UV absorbance spectra of river water (August of 2005) and its isolations.

HLB and MAX cartridges were connected and optimized to investigate tandem performance on DOM extraction. Loss of fluorescence was observed in both EEMs' of eluates of both modes. The fluorescence spectra of washes by HLB-MAX mode show only peaks A and C with maxima located at 240/408 nm and 320/409 nm respectively. These are blue shifted for about 10 nm in both excitation and emission wavelengths in relation to the original river water ($\lambda_{ex}/\lambda_{em}$=230/424 nm for peak A and $\lambda_{ex}/\lambda_{em}$=320/420 nm for peak C) except for maximum excitation wavelength of peak C. Relative to MAX eluate ($\lambda_{ex}/\lambda_{em}$=250/410 nm for peak A and $\lambda_{ex}/\lambda_{em}$=330/400 nm for peak C), fluorescence maxima of these two signals are red shifted about 10 nm except for emission wavelength of peak A. In comparison, five fluorescence regions are identified in MAX-HLB mode and are associated with peak A, C, T_1, T_2 and D respectively. Weak fluorescence signals

of peak T_1 and T_2 were observed in the spectra, suggesting that small amounts of tryptophan-like fluorophores were retained by the MAX-HLB method.

3.3.2 Recovery by various methods

The recoveries for the sorbents based on UV absorbance at 254 nm and fluorescence are shown in Table 3.3. The criteria used to evaluate the extraction efficiency included the removal of UV-visible absorbance and removal of fluorescence.

Table 3.3 Recovery based on fluorescence and UV_{254}.

Samples		Peak A	Peak C	Peak T_1	UV_{254}**
Sep-pak	eluate*	34.2	33.2	0	57.8
	washes*	29.7	20.7	53.2	25.8
Disk	eluate	87.8	90.0	0	55.9
	washes	41.2	31.1	75.1	21.1
HLB	eluate	53.3	53.9	0	50.7
	washes	41.3	26.1	85.8	33.5
MAX(Aug)	eluate	35.0	66.0	0	69.0
	washes	0	0	0	0
MAX(Jul)	eluate	24.6	20.0	16.5	31.3
	washes	0	0	0	0
HLB-MAX	eluate	15.0	18.7	13.0	22.3
	washes	0	0	0	0
MAX-HLB	eluate	7.4	9.8	3.5	3.1
	washes	23.6	19.1	20.9	18.5

*Recovery (based on fluorescence) = fluorescence intensity in eluates (or washes)/fluorescence intensity in initial sample (river water)

**Recovery (based on absorbance) = absorbance at 254 nm in eluates (or washes)/ absorbance at 254 nm in initial sample (river water)

The recoveries based on absorbance were calculated by UV absorbance of isolates divided by the absorbance of the initial sample. Overall, the total recoveries calculated from absorbance range from 22% to 84%. Sep-pak C18, Empore C18 Disk and HLB methods have similar total recoveries around 80%, 50-60% for eluates and 20-34% for washes respectively. Mixed modes of polymeric sorbents account for the lowest recovery at around 20%. MAX and HLB-MAX methods have recovery only in retained fractions.

Extraction recoveries based on fluorescence were recorded as fluorescence intensity of isolates divided by that of the initial sample. Unlike the absorbance recoveries that are fairly consistent for Sep-pak, Disk and HLB extraction methods, the fluorescence extraction efficiencies for humic-like fluorophores vary between 30% for Sep-pak to 90% for Disk. Furthermore, the fluorescence extraction recoveries for protein-like fluorophores based on fluorescence are much higher than the yields based on absorbance. Most of the protein-like fluorophores were found at the washed portions by these three methods, and HLB produced recovery as much as 85%. Similar to absorbance recoveries, fluorescence efficiencies for mixed modes present worst yields as about 20%, which are close to the values of recoveries based on absorbance. Efficiency of eluate for MAX method is 0, while around 66% for visible humic-like fluorophores and 35% for UV humic-like fluorophores were washed off. Elution and wash from MAX yield no protein fluorescence.

3.4 DISCUSSION

3.4.1 Fluorescence features

Fluorescence maximum excitation and emission wavelengths of fluorophores in both eluates and washes by Sep-pak, Empore Disk and HLB methods occur at the same wavelength as raw river water except for peak A in the HLB wash fraction by HLB method. Absence of wavelength shift before and after extraction suggests that no transformation or selective retention occurs within peaks. Although Sep-pak was conditioned by strong acid (pH<2) before loading sample, acidification didn't alter the fluorescence features except for emission intensity (refer to chapter 2). Eluates and washes by the Sep-pak method show virtually the same features as those of the Disk and HLB, also indicate that there was no structure alteration since both Disk and HLB lack the procedures of cartridge acidification. Similarity of the fluorescence spectra indicates that these three methods isolate river water equally and they produce mixtures with similar structural composition.

Conversely, both excitation and emission wavelengths shift isolations by the MAX method. Only peaks A and C were observed in the eluate by the MAX method, and maximum emission wavelengths shift to lower values. Blue shifting of fluorescence indicated that the compounds retained by the MAX sorbents may have simpler structures or lower molecular weight comparing to the bulk compounds in raw river water. This blue shift may be caused by separation the peaks A and C fluorophores from the protein-like fluorophores. Proteinaceous moieties form part of the humic building block structure and are not solely associated with humic substances. The same case for peak B. Strong exchanges between the humic substances hydrophobic domains and the MAX sorbent

during fractionation, however, disrupt the associations between protein-like fluorophores, peak B and humic-like fluorophores, leading to the separation of the blocks, and consequently of the fluorophore assemblages simpler and decreasing apparent molecular weight, resulting in a blue shift of the fluorescence signal.

Table 3.4 Fluorescence peaks and their locations for the raw river water and the isolations.

Samples		**Peak A**	**Peak C**	**Peak T_1**	**Peak T2**	**Peak B**	**Peak D**
River water	7/2004	230/423	330/420	230/356	NR	250/460	ND
	8/2005	230/424	320/420	230/356	280/356	250/460	260/338
Sep-pak	eluate	230/424	320/420	ND[a]	ND	NR[b]	ND
	washes	230/420	310-340/420-430	230/356	NR	NR	260/330
Disk	eluate	230/424	320/420	ND	ND	250/460	ND
	washes	230/413	320/420	230/350	NR	250/460	260/330
HLB	eluate	230/424	320/420	ND	ND	NR	ND
	washes	220/413	310-340/420-430	220/356	NR	NR	260/330
MAX(Aug)	eluate	250/410	330/400	ND	ND	ND	250-260/330-350
	washes	ND	ND	ND	ND	ND	ND
MAX(Jul)	eluate	230/410	320/420	NR	NR	NR	NR
	washes	ND	ND	ND	ND	ND	ND
HLB-MAX	eluate	240/408	330/410	ND	ND	ND	ND
	washes	ND	ND	ND	ND	ND	ND
MAX-HLB	eluate	230/424	330/410	ND	ND	ND	ND
	washes	220/418	330/424	220/356	280/350	NR	~270/330

[a]ND: non-detected
[b]NR: non-resolved

Nothing similar to peak D has been noted in previous environmental fluorescence work. According to the results from apolar sorbents such as Sep-pak C18 cartridge and Empore C18 disk and polar sorbents such as HLB and MAX cartridges, peak D is present in fluorescence spectra of August river water samples and their isolates. Peak D is not tryptophan-like fluorescence, since maximum excitation wavelength occurred at 260 nm for peak D rather than 230 nm. Peak D is a separated fluorescence signal presented together with peak A, C, T_1 and T_2 in these samples. This fluorophore is not characterized in the literature perhaps because it occupies a similar fluorescence position to peak T_2, and therefore superposition of these two signals makes it difficult to discriminate peak D from peak T_2. Only when tryptophan-like fluorescence is absent could peak D be identified without being mistaken for peak T_2. Since peak D only occurs together with peak T_1 and it is absent when peak A and C exhibit as the only signals in fluorescence spectra by Sep-pak, Disk and HLB methods suggested that the polarity and/or separation properties of peak D are similar to tryptophan-like fluorescence. Since tryptophan-like fluorophores are more hydrophilic and humic-like fluorophores are more hydrophobic, therefore, peak D fluorophores are hydrophilic since it was not retained by the hydrophobic sorbents. This conclusion is also consistent with the result that fluorophores responsible for peak D were retained by hydrophilic sorbents. Peak D is present with peak A and C by MAX method implied that this fluorophores are negative charged because either positive charged or neutral hydrophilic material will not be retained by the MAX sorbent like protein-like fluorophores. The only difference between HLB and MAX stationary structure is MAX has highly selective retention for negative charged compound by its strong anion-exchange mode. Since peak D was missing in fluorescence

spectra generated by July's river water samples, the fluorophores associated with this peak might be specific to August rather than ubiquitous in river water. As a consequence of peak D serious overlapping with peak T_2, potential interference between T_2 and D may lead to mis-identification.

3.4.2 Extraction efficiencies of Sep-pak, Empore Disk and HLB methods

Absorbance recovery of eluates are much higher than washes for Sep-pak, Disk, HLB methods suggested that more chromophoric material was retained by these sorbents than washed.

Fluorescence features of eluates and washes by Sep-pak, Empore Disk and HLB methods are similar because the partitioning mechanisms of these three sorbents are mainly controlled by hydrophobic interactions between humic-like fluorophores and stationary phases of sorbents. High extraction efficiency of Empore Disk for both protein-like and humic-like fluorophores relative to Sep-pak is related to its larger surface area and faster mass transfer due to the short sample path and small particle size. All three methods demonstrated almost 2-fold greater recovery in washes for protein-like fluorophores than for humic-like fluorophores. HLB is 10% and 30% higher than Disk and Sep respectively to extract protein-like fluorophores due to the introduce of a neutral polar hook for HLB sorbent to enhance retention of more polar fraction. HLB didn't show any significant advantage over C18 sorbents as anticipated in terms of extraction efficiency and extracting recovery. Irreversible adsorption might account for a loss of total 20% and up to 50% recovery based on absorbance and fluorescence respectively. Taking into account recovery and isolating types, Sep-pak would be the last choice

because of its washes containing considerable amount of humic-like fluorophores besides protein-like fluorophores and the lower recovery due to the strong interaction between the interested fluorophores and the sorbents. The Empore C18 disk more efficiently separates different types of fluorophores with high recovery.

The tandem modes had lower recoveries based on absorbance and fluorescence to about 20%, much lower than individual mode of HLB or MAX. Moreover, tandem modes didn't present any advantages to isolate or fractionate compared to the individual modes. Maybe the extraction method such as wash and elute solvents need to be investigated intensively in order to optimize applications of mixed modes.

3.4.3 MAX method

Peaks T_1, T_2 and peak B fluorescence are lost in both eluate and washes, only peaks A, C and D are observed in the fluorescence spectra in eluate indicated that MAX sorbent preferentially enrich humic-like fluorophores from river water rather than anything else. The peaks inhabiting the similar optical regions and resulting in peak overlap and superpose with peaks A and C are eliminated by MAX method, in this regard, MAX method have higher selectivity to separate NOM components than C18 and HLB sorbents. Ruling out the effects of solvent, MAX sorbent differs from HLB by its anion in its backbone structures while HLB is neutral. Quaternary amine functional groups act as ion-pairing reagents to provide strong anion-exchange with acidic humic-like fluorophores, therefore, generation of ion pairs between anionic fluorophores in water sample and cationic functional groups on MAX may dominate over hydrophobic interactions. Perception of changing polarity distribution of organic matter by ion-pair formation in the

MAX sorbent is the same with separation idea employed in chapter 2 with addition of ion-pairing reagent. The advantages of MAX sorbent over procedures conducted in chapter 2 are MAX combines ion-pair formation and separation at one sorbent without addition of ion-pairing reagent. Meanwhile, reverse-phase sorbent enhances its ability and capacity to extract hydrophobic fraction from the complex. More importantly, the used sorbent can be reused after reconditioning. The procedures using MAX enable separation of negative charged humic-like fluorophores from river water and removal of neutral and positive charged compounds such as protein-like fluorophores. Recoveries of peak A and C are different and they are related to polarity of eluting solvents based on this method. Generally, recovery of peak A is less than that of peak C and the less polar, the more acidic of eluting solvent, the higher of recovery for peak C. The results that less polar and lower pH favor eluting peak C from sorbents suggest that visible humic-like fluorophores (peak C) are more hydrophobic and more pH sensitive relative to UV humic-like fluorophores (peak A). So, compared with C18 and HLB methods, MAX would be the best option to enrich humic-like fluorophores with high recovery without any interference from protein-like fluorophores or other unidentified compounds.

3.4.4 Extracting ability to UV- and visible humic-like fluorophores

The recoveries of UV and visible humic-like fluorophores depend on the polarity of elute solutions and sorbents (Table 3.5).

Table 3.5 Fluorescence intensity ratio of peaks A, C and T_1 and recoveries of peaks A and C based on fluorescence.

Samples		Ratio T_1/A	Ratio C/A	Recovery (Fl.)[c] (%)	
				Peak A	Peak C
river water (August of 2005)		0.73	0.49		
river water (July of 2004)		0.78	0.49		
Sep-pak	eluate	0	0.46	34.2	33.2
	washes	1.26	0.33	29.7	20.7
Disk	eluate	0	0.50	87.8	90.0
	washes	1.28	0.37	41.2	31.1
HLB	eluate	0	0.48	53.3	53.9
	washes	1.50	0.30	41.3	26.1
MAX (August)[a]	washes	ND	ND	0	0
MAX (August)[a*]	eluate	ND	*0.85*	*40.7*	*73.5*
MAX (August)[b*]	eluate	ND	*1.25*	*39.5*	*97.6*
MAX (July)	eluate	NA	0.41	24.0	20.1
HLB-MAX	eluate	0.67	0.63	15.0	18.7
	washes	NA	NA	0	0
MAX-HLB	eluate	0.68	0.41	23.6	19.1
	washes	0.36	0.68	7.4	9.8

[a] was eluted with 2% HCOOH in methanol and Milli-Q water mixture (Meth:H_2O=9:1);
[b] was eluted with 5% HCCOH in methanol solvent;
[c] recovery was based on the fluorescence;
*data based on their new fluorescence centers.

Fluorescence intensity ratios between C and A for eluates by Sep-pak, Disk and HLB are very similar and these ratios are very close to that in the raw river water. This implied that peaks C and A were extracted from initial water with the same efficiency by these three methods. Fluorescence recoveries for peak A are nearly identical to peak C in the eluates for Sep-pak, Disk, and HLB indicating that these three methods extracted both fluorophores with similar ability. However, fluorescence recoveries of peak A are on average 10% higher than peak C in the washes and the ratio of C/A vary and are less than that of the initial sample. The variation in peak ratios may be the result of peaks superposing between peak A and peak T and/or decrease of peak C recovery due to the irreversible adsorption between peak C and sorbents because the procedures and solvents polarity for these three methods are very similar.

For MAX, fluorescence intensities of peak C are close to or higher than those of peak A. The contour maps of peaks A and C by MAX method are dramatically distinct from those obtained by other methods and from initial water. Therefore, the observed peak A is the sum of a mixture of fluorophores with different subunits. MAX method separated those subunits and removed some of them such as peak T_1, B and low-wavelength fluorophores, with only some of the UV humic-like fluorophores remaining. In addition, peak C has less peak overlap with other peaks, thus extraction had much less effect on it. The consequence of elimination of building subunits from peak A made its fluorescence intensity less than peak C. Furthermore, recovery of peak C appears to be more complete than that of peak A, while other peaks (T, B) are not recovered at all. Therefore, in the initial river water, emission intensity of UV humic-like fluorophores is greater than visible humic-like fluorescence may be the artifacts of $(A+B+T_1+\ldots) > C$.

3.5 CONCLUSIONS

Fluorescence peak A can be attributed to a mixture of several UV humic-like fluorophores. Peak C fluorophores are more hydrophobic and pH sensitive than peak A fluorophores. Peaks T fluorophores are present on neutral or positively charged and more hydrophilic molecules. Peak D fluorophores molecules are negatively charged but more hydrophilic than peaks A and C fluorophores molecules.

The extent of extraction of various fluorophores from river water with hydrophobic solid phases differed with the type of bonded phases. Empore C18 disk is the best choice for ensuring the highest recovery. Take into account of selective isolation of specific components, MAX is good for isolating humic-like flurophores and discarding protein-like fluorophores, while HLB is better suited for extracting protein-like fluorophores. Sample preparation by MAX method requires neither pretreatment for aqueous samples nor the use of ion-pair regents. The mix-mode polymeric SPE cartridges have both reversed-phase and ion-exchange characteristics, and eliminate the need for ion-pairing reagent, providing a simple and rugged alternative for liquid-liquid separation.

The SPE procedures still need to be more extensively optimized in order to obtained greater recoveries of DOM pool and representative fluorescence subunits.

3.6 REFERENCES

Amador, J.A., Milne, P.J., Moore, C.A., and Zika R.G. (1990) Extraction of chromophoric humic substances from seawater. *Marine Chemistry* 29, 1-17.

Bouvier, E.S.P., Iraneta, P.C., Neue, U.D., McDonald, P.D., Philips, D.J., Capparella, M., and Cheng, Y. F. (1998) Polymeric reversed-phase SPE sorbents - Characterization of a hydrophilic-lipophilic balanced SPE sorbent. *LC GC-Magazine of Separation Science* 16, 53.

Coble, P.G. (1996) Characterization of marine and terrestrial DOM in seawater using excitation-emission matrix spectroscopy. *Marine Chemistry* 51(4) 325-346.

Decaestecker,T.N., Coopman, E.M., Van peteghem, C.H., and Van Bocxlaer, JF. (2003) Suitability testing of commercial solid-phase extraction sorbents for sample clean-up in systematic toxicological analysis using liquid chromatography - (tandem) mass spectrometry. *Journal of Chromatography B* 789, 19-25.

Franke, J.P., and de Zeeuw, R.A. (1998) Solid-phase extraction procedures in systematic toxicological analysis. *Journal of Chromatography B* 713, 51.

Huck, C.W. and Bonn,G.K. (2000) Recent developments in polymer-based sorbents for solid-phase extraction. *Journal of Chromatography A*. 885,51.

Junk, A., Avery, M.J., and Richard, J.J. (1988) Interferences in solid-phase extraction using C-18 bonded porous silica cartridges. *Anal.Chem*. 60, 1347-1350.

Leenheer, J. A. (2003) Characterization aquatic organic matter. *Envir. Sci.Technol*. 18A-23A.

Parlanti, E., Morin, B., Vacher, L. (2002) Combined 3D-spectrofluorometry, high performance liquid chromatography and capillary electrophoresis for the characterization of dissolved organic matter in natural waters. *Org. Chem*. 33,221.

Waters Corp. (2006) Oasis$^{@}$ Sample Extraction Products.

Yamashita,Y., and Tanoue, E. (2003) Chemical characterization of protein-like fluorophores in DOM in relation to aromatic amino acids. *Marine Chemistry* 82, 255-271.

CHAPTER 4

Characterization Wastewater Treatment by Membrane Filtration Using 3DEEM

4.1 INTRODUCTION

With the increasing demand of water supply and stricter regulation of water quality, water reclamation and wastewater reuse is booming. Wastewater reuse is increasingly seen as an essential strategy for making better use of limited freshwater, and a means of preventing deterioration in the aquatic environment from wastewater disposal. The main challenges of water reuse projects are to ensure that the water produced can be effectively distributed and safely used. Although secondary- and tertiary –treated wastewater can be discharged into waterways, it cannot be used even for non-potable purposes without further treatment. Across all industries, the practice of water reclamation and reuse is gaining momentum. This practice has a two-fold impact: not only is total water usage dramatically reduced, but potential pollutants are prevented from being released via the wastewater stream. Water recycling has become one of the key factors in moving toward zero discharge [Mcllvaine, 2008].

Advanced wastewater reclamation and treatment for industrial and potable purposes include biological wastewater treatment and can be followed by pre-treatment of secondary effluent with MF (colloidal & suspended), then reverse osmosis (RO) filtration, and finally UV for disinfection. Recently, the increasing need for improved water intake quality for potable supplies for human and industrial purposes has resulted

in the emergence of new water reuse technologies. Application of membrane technology to water treatment offers many advantages such as strict solid-liquid separation, ease of operation and small footprint. The use of membrane bioreactors (MBR) in combination with RO is one example of new treatment options. Used upstream of the RO system, MBR provide an efficient, cost-effective tool for removing biological contaminants from wastewater streams [Mcllvaine, 2008]. The average COD (Chemical Oxygen Demand) from MBR effluent is around 20 mg/L, while the RO effluent had a COD less than 2 mg/L and DOC lower than 1 mg/L. Besides high removal of ions, organic matter and pathogens, MBR-RO sequential system are capable of removing specific substances such as DBPs or endocrine disrupting substances [Dialynas, 2008].

Microfiltration membranes have been widely applied for its significant removal of particles, turbidity, and microorganisms from surface water and groundwater as an alternative to conventional water treatment processes (coagulation, sedimentation and sand filtration). The greater removal of particles and microorganisms is of particular interest in meeting the more stringent requirements of the surface water treatment rule (SWTR) and DBPs regulations [Yuan, 1999]. Relative to conventional treatment, MF offers several advantages including superior water quality, easier control of operation, lower maintenance, and reduced sludge production. A module-less MF membrane promises better fouling control and can hybrid with other treatment processes.

MF processes are a good choice of pre-treatment for RO systems because of the (a) consistency of treated water quality with variable feed water quality; (b) non-sensitivity to chemical reactions and adjustments to achieve good results; (c) stable membrane operations; (d) higher fluxes compared to conventional pretreatments; (e) longer RO

chemical cleaning intervals, and extending membrane lifespan; (f) less land area needed for the plant; (g) lower energy consumption; and (h) lower operating and maintenance costs [Ujang et al., 2007].

RO plays a key role in desalination, water reclamation, and process-stream purification, and minimizes industrial and domestic wastewater streams. In 2007, according to market research conducted by the Mcllvaine Co., the size of the market for industrial and municipal RO systems was estimated at $3.4 billion worldwide [Mcllvaine, 2008]. Expanding markets and new developments are assuring a place for RO systems well into the future [Ujang et al., 2007]. RO membranes recently have provided better water quality than other alternatives. The reverse osmosis process has been widely applied for water reclamation of treated used water (secondary effluent) due to its affordable cost and reliability. RO membranes have been involved in wastewater reuse processes to tackle water shortage problem, especially in arid areas. Crossflow systems allow continuous filtration and are used in conjunction with various pre- and post-treatment steps, depending upon the specific application and relative purity of the source water. High quality permeates suitable for indirect potable or direct non-potable use after disinfection are produced from RO process, and, RO (or equivalent) is currently required for indirect potable reuse because RO membrane shows significant contaminant rejection to meet and exceed drinking water standards.

Despite the advantages and booming market, one of the critical factors limiting the use of membrane filtration is membrane fouling, the irreversible loss of system flux over time caused by interactions between the membrane and the various components in the process stream. Mallevialle et al. showed that the structure of the fouling layer formed

during microfiltraion of natural river waters was determined largely by the organic matrix which served as a “glue” for inorganic constituents (e.g., ion, aluminum, silicon and calcium) in the fouling layer. [Yuan et al.,1999; Mallevialle et al., 1989; Bersillon et al.,1988]

Most authors agree that dissolved organic matter (DOM) is a principal cause of fouling. In biologically wastewater treatment, effluent organic matter (EfOM) has been implicated as the most important foulant. EfOM contains polysaccharides, proteins, amino-sugars, nucleic acids, organic acids, humic materials, and cell components [Baker et al., 2000]. EfOM is composed of NOM from source water, synthetic organic compounds (SOCs) from human activity and SMPs (soluble microbial products). The majority of EfOM in the secondary wastewater effluent is made of SMPs, which are derived from substrate metabolism in the biological wastewater treatment process. NOM is a heterogeneous mixture of humic and fulvic acids, lignins, carbohydrates, and proteins of various molecular sizes and functional group compositions. Therefore, an understanding of NOM as a membrane foulant and the behavior of NOM components in low-pressure membrane fouling are needed to provide a basis for appropriate selection and operation of membrane technology for water treatment.

Organic matter properties such as hydrophobicity, molecular weight, charge density and molecular shape are expected to affect membrane fouling [Lee et al., 2004]. Solution chemistry and membrane type also influences the charge and conformation of NOM macromolecules and, thus, the structure and hydraulic resistance of the foulant deposit layer. However, most researches have focused on the influence of hydrophobicity and molecular weight of organic matter.

There are still debates on which polarity-based fraction(s) of organic matter is (are) most important in the field of membrane treatment. Yuan et al [Yuan, 2000] suggested that the humic fractions of natural organic matter, which are largely hydrophobic, control the rate and extent of fouling. Shon agreed [Shon et al., 2006] that hydrophobic fractions were the main foulants, because hydrophilic fractions included mainly the small MW compounds which were much smaller than the membrane pore size of 17,500 Da and would have passed through the membrane pores. The high flux decline by hydrophobic may be due to the pore blocking, cake/gel layer and/or pore constriction by the large MW compounds present in the hydrophobic fraction. Further, there was a strong adsorption of hydrophobic compounds on the membrane surface [Shon et al., 2006]. However, recent studies have reported that hydrophilic (non-humic) organic matter might be the most significant foulant. For example, Gray et al. reported that neutral and basic hydrophilic components of organic matter lead to continuous flux decline [Gray and Bolto, 2003]. Lin [Lin et al, 2000] stated that hydrophilic fraction of humic acids caused most serious flux decline by using Aldrich humic substances as feed water solution, and, for the wastewater, they got the same results. Hydrophilic fraction in the wastewater used by them contained a significant amount of colloidal and macromolecular organic matter of non-humic properties. Fan [Fan et al., 2001] reported the effect of potential foulants as the following order: hydrophilic neutral > hydrophobic acid > transphilic acids. This may be related to: (1) the MW fraction in the colloidal range (>30 KDa) and (2) less charged/non-charged and less aromatic/non-aromatic fractions were the major components of the adsorbed materials leading to significant and long-term flux decline. Jarusutthirak et al. [Jarusutthirak, 2002; Shon et al., 2006] found that the colloidal

fraction consisted mainly of large MW of hydrophilic character, and this was the fraction that contributed the most to fouling when BTSE (biological treated sewage effluent) was used as the feed. Polysaccharides, which were hard to remove by pre-treatment such as coagulation or adsorption, are hydrophilic neutral. The absence of electrostatic repulsion among macromolecules and between DOM and membrane may increase deposition on the membrane to cause fouling [Lee, 2006]. These authors found the adsorption tendency of the polysaccharides (hydrophilic) in the membranes was approximately three times of that of humics.

Other authors have suggested that molecular size and shape are more significant predictor of fouling than polarity. Similarly, there is still no any agreement on what size(s) dominate membrane fouling. Howe et al. [Howe, 2002] found particulate matter (larger than 0.45 μm) was relatively unimportant in fouling of UF and MF membranes as compared to dissolved organic matter. The fraction smaller than 3 nm, included about 85-90% of the total OM, also caused very little fouling. Very small colloids, ranging from about 3-20 nm in diameter, appeared to be important. They concluded that the greatest degree of fouling was caused by smaller-MW molecules due to adsorption of small molecules in the membrane pore wall and pore blockage by colloidal organics (>30,000 Da). In addition, they also attributed greater fouling by the neutral hydrophilic fraction to the smallest MW distribution. On the other hand, Lin et al. [Lin et al., 2000] indicated that the highest-MW components (6.5-22.6 kDa) for both hydrophobic and hydrophilic fractions caused the greatest flux decline, whereas the smallest MW fraction (160-650 Da) exerts little effect on flux decline.

The effects of polarity and size were inconsistent on membrane fouling based on the literature review. This could be explained by the reason that most of researches had different operation conditions such as type of membrane, fractions of organics tested and the pre-treatment process employed, and also data were insufficient for comparison among them. In addition, experimental artifacts associated with extraction procedures could also cause these inconsistent results. So far, it is still unclear which fraction of organic matter causes the irreversible membrane fouling. Some conclusions were derived from results obtained from very shorterm filtration tests, therefore it is uncertain whether their results apply to the actual irreversible fouling that may occur over long-term operations.

Understanding the fouling mechanisms is essential to developing strategies for fouling control. In order to optimize the performance of the membrane filtration BTSE, it is important to identify the membrane fouling effect with different fractions in the wastewater. A detailed characterization of membrane fouled with different fractions will also help to select a suitable membrane and the optimum range of operating parameters [Shon et al., 2006]. Characterization of EfOM has been attempted by different techniques, including basic measurements such as dissolved organic carbon (DOC) and ultraviolet absorbance (UVA). More elaborate characterization methods include molecular weight distribution by high-performance size exclusion chromatography (HPSEC), fractionation using non-ionic macroporous resins, “fingerprinting” the organic groups by excitation-emission matrix (EEM) fluorescence spectroscopy, identifying organic functional groups of the fouling layer in the membrane surface using attenuated total reflectance Fourier transform infrared spectroscopy (ATR-FTIR), and determining the morphological

characteristic of foulants by environmental scanning electronic microscopy (ESEM) [Fan, 2008].

The gross parameter of DOC was often used in most membrane studies to evaluate DOM removal efficiency. DOC is an aggregate parameter and does not provide information on the organic character of NOM in water. The separation and fractionation methods such as HPLC and resin are time and labor consuming. The measurement method as FTIR needs removal of membrane and sample drying.

Fluorescence spectroscopy has potential for the rapid qualitative and quantitative measurement of the problematic DOM fractions for source water characterization/assessment and water treatment process optimization [Taha, 2000]. Distinctive fluorescence signatures have been determined for the refresh water samples [Taha, 2000; Baker et al., 2004; Reynolds, 2002; Chen et al., 2003], and it has been proven to be a useful technique to differentiate changes and transformations of organic mater in natural environments. However, EEM fluorescence has not been used broadly to characterize and identify EfOM during wastewater treatment. Characterization of EfOM fluorescence could provide information concerning the structure, functional groups, configuration, heterogeneity and dynamics of its components.

Fluorescence excitation-emission matrix (EEM) spectroscopy has proved to be a valuable tool to investigate DOM in river, estuarine waters and marine for almost two decades [Coble, 1996; Wu et al, 2003]. This method has been applied to explore and characterize organic matter in wastewater [Hudson, 2007; Kuzniz, 2007]. Because wastewater exhibits more complex behavior than natural waters and its complicated matrix effect, fluorescence technique may encounter more challenges to interpreting its

spectra. Attempts [Hudson, 2007; Reynolds, 2002; Baker et al.,2004] have been made to use fluorescence spectroscopy to monitor and control water quality, and provide information about wastewater treatment behavior. In water recycling schemes, proper monitoring and characterization of residual DOM in treated effluents is essential for estimating the potential of DOM to contaminate transport. Therefore, there is need for careful and on-going management to ensure reliability of water treatment performance to maintain full protection of public health [Henderson, 2009]. It is also important to implement real-time on-line monitoring technology in water quality management.

3DEEM fluorescence spectroscopy has been investigated to be used as a monitor tool to assessment of process performance and water quality because it is a rapid, sensitive, selectivity and reagentless technique which no sample pretreatment prior to analysis is required.

In order to provide a continuous, safe and reliable water supply, membranes were applied to increase capacity in a cost-efficient manner instead of having to build several new trains to meet local water supply. RO membranes were combined with other membrane protocols such as MBR and MF in three pilot sites of wastewater treatment processes: (1) MBR process that incorporates nitrogen removal at Rio Del Oro (RDO) WWTP in Los Lunas, NM; (2) Aerated lagoon of high strength concentrated domestic waste at Albuquerque Metropolitan Detention Center (MDC) WWTP; (3) Activated sludge process that incorporates nitrogen removal at Albuquerque Southside Water Reclamation Facility.

Since 3DEEM is a sensitive fingerprint technique, the overall goal of this chapter was to develop this fluorescence methods, combined with other analytical methods, to

monitor and characterization the change of organic matters in the wastewater treatment processes during reverse osmosis process, thus provide information to aid in figuring out the major components of foulants and disclosing fouling mechanism. Experiments were thus designed to: (1) characterize and discriminate fluorophores in the wastewater samples and their influence on fouling by 3DEEM fluorescence spectroscopy; (2) control water quality when TOC concentration is very low which is under detection limit (DL) with UV detector; (3) correlate fluorescence intensity with typical water quality parameters; and (4) use these results to obtain insights into the underlying physical phenomena governing membrane fouling during RO.

4.2 Methodology

4.2.1 Pilot plants and operation

The pilot plants for this study were set up at three existing wastewater treatment facilities, Rio Del Oro, Albuquerque wastewater treatment plant and Albuquerque metropolitan detention center.

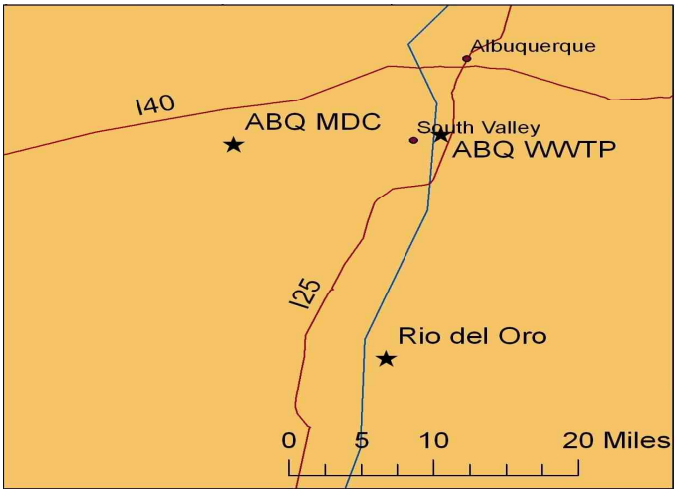

Figure 4.1 Site map for wastewater sampling.

Site I: Rio Del Oro (RDO) Wastewater Treatment Plant

The first site was Rio Del Oro (RDO), located in the Rio Del Oro area between Los Lunas and Belen. This facility used a membrane bioreactor (MBR) process followed by three sequential reverse osmosis (RO) membranes. The schematic diagram of cross-flow membrane set-up and sampling locations are shown in Fig 4.1. The MBR membrane configuration of the plant consists of flat sheet micro-filtration membranes (Kubota) with pore size 0.4 μm and an area of 14.6 ft^2. Prior to the pilot operation described in this part, the membrane module has been used as a biofilm-membrane reactor. In order to

investigate the RO membrane that suffered from irreversible fouling caused by constituents in wastewater source, a total run time of approximately 1000 hrs (42 days) (between April 24th and June 19th 2007) was continuously carried out.

Crossflow filtration was applied for the membrane filtration. Crossflow filtration as a semi-permeable membrane over which feed water flows under pressure, parallel to the membrane surface. A portion of the feedwater permeates (or filters) through the membrane, forming the permeate (or filtrate) stream, and leaving the majority of dissolved solids and organics filtered behind to form higher concentrations in the feedwater stream. The balance of feedwater becomes enriched with dissolved solids and organics as more permeate is formed. The balance of concentrated feed flows tangential to the membrane surface, forming the concentrate (reject) stream. For the separation process to take place, feedwater pressure should greater than the sum of feed-concentrate stream osmotic pressure, the permeate backpressure and any system pressure drops. Because the feed and concentrate flow parallel to membrane surface instead of perpendicular to it, the process is called "Crossflow" or "Tangential Flow". Concentrate is recycled back to the feed tank and the mixture of concentrate with feed water is Recycle water.

Samples from the pilot RO unit were collected at least twice a week. These included feed, recycle, permeates and concentrate samples. Flow and pressure measurements were collected and reviewed on a weekly basis. All samples were refrigerated at 4°C in dark. Milli-Q water was used for all dilutions, solution preparation, and final glassware washing.

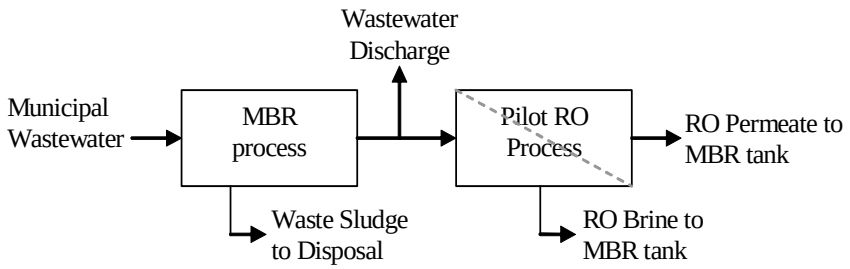

Figure 4.2 Schematic diagram of wastewater treatment by membranes [Field et al., 2008].

New membranes were installed at the beginning of the experiment and one cleaning sequence was performed during the fifth week of operation. The membranes were cleaned using a surfactant followed by a citric acid solution.

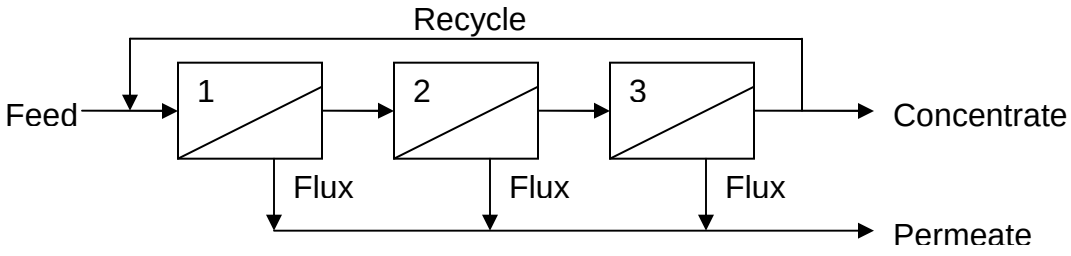

Figure 4.3 Sampling sites at RDO.

Site II: ABQ Metropolitan Detention Center (MDC) Wastewater Treatment Plant

In this study, the pilot plant was set up at the ABQ metropolitan detention center (MDC) wastewater treatment plant intake, pumping from the aerated lagoon of high strength domestic waste. Figure 4.4 shows the schematic diagram of the pilot plant used in this study. The pilot-scale was equipped with micro-filtration membrane (0.2 μm

polypropylene PP hollow fiber module) followed by RO membrane.

At this site, the wastewater came from a pond which receives the effluent of wastewater from MDC. Feed water was taken from the effluent of the microfiltration and the influent of the RO. Six samples—permeate, feed, recycle, and concentrate--were still collected approximately once per week from the pilot RO unit (Figure 4.4).

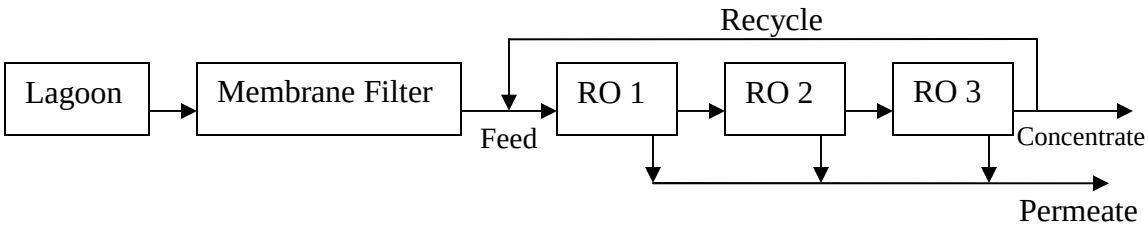

Figure 4.4 Sampling sites at MDC.

Site III: ABQ Southside water Reclamation Wastewater Treatment Plant (ABQWWTP)

The raw water taken from the primary clarifier of Albuquerque's wastewater treatment plant was connected to activated sludge basin and secondary clarifier. Then the effluent from the secondary clarifier was divided into two lines (Figure 4.5). One line flowed into the RO units with a MF membrane as the pretreatment. The other line was connected to a sand filter followed by RO units. Samples were collected once a week.

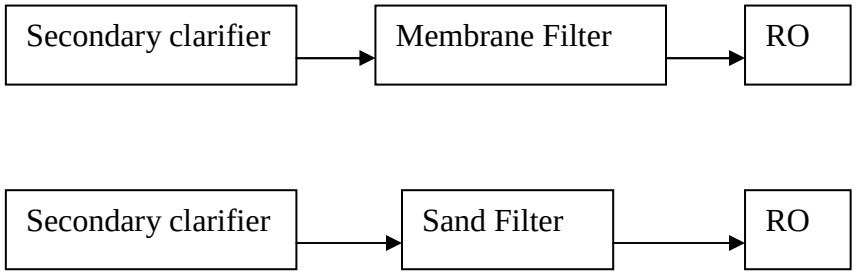

Figure 4.5 Two lines for wastewater treatment at ABQWWTP.

4.2.2 Analytical methods

Fluorescence spectroscopy

To obtain information on organic matter from different aspects, the fluorescence excitation-emission matrices (EEMs) of the samples were generated by using a fluorescence spectrophotometer (Varian).

Since the intensities of many samples were over range, in order to get quantitative information of intensity changes, dilution was required. All samples (feed, recycle and concentrate) except permeate were diluted with phosphate buffer so that the highest density was <1000 a.u. Therefore, the dilution factors range from 2.5% to 20%.

Phosphate buffer solution preparation. A phosphate buffer for optical measurement, pH =7, was prepared according to the Standard Methods for the examination of water and wastewater, 20th Edition, 5-66. Fluorescence of phosphate buffer and Milli-Q were very similar, with very weak intensity (less than 10 au) at DOM fluorescence regions.

Addition of Mercuric solution Because the water samples were not treated with disinfectants, the microorganisms in the samples could active even at 4°C in the dark. Therefore, in order to insure the fluorescence of the stored samples as the same with fresh

ones, saturated mercuric sulfate solution was added to stop the microorganism metabolism of the samples.

TOC and Protein analysis TOC were analyzed by TOC analyzer (persulfate-ultraviolet oxidation method). Protein concentration was determined by Lowry method [Lowry, 1951; Dunn,1992].

UV and fluorescence spectroscopy

A UV/vis spectrophotometer (Varian, Cary 50 Bio) was used to measure absorbance from 200 to 600 nm of water samples. All samples were measured without dilution using Milli-Q water as blank.

The procedure details on the fluorescence and UV spectroscopy refer to 2.2.2. Phosphate buffer was used as blank for fluorescence measurement.

4.3 RESULTS

TOC, UV_{254}, SUVA and protein content of feed and concentrate samples from three sites are shown in Table 4.1.

Table 4.1 Wastewater parameters

Samples	TOC mg/L	UV_{254} cm^{-1}	SUVA, $m^{-1}L/mg$	Protein mg BSA/L	S[a]
RDO permeate	0.09(±0.11)[b]	0.0023	NA[c]	NA	NA
RDO feed	4.90(±0.19)	0.12(±0.005)	2.57(±0.11)	7.1(±0.77)	-0.011
RDO concentrate	12.20(±2.16)	0.29(±0.02)	2.57(±0.15)	17.4(±3.36)	-0.011
ABQ permeate	0.05(±0.04)	NA	NA	NA	NA
ABQ feed	5.99(±0.67)	0.11(±0.02)	1.86(±0.21)	4.9(±0.99)	-0.016(±0.002)
ABQ concentrate	15.81(±1.46)	0.29(±0.03)	1.89(±)	13.2(±1.67)	-0.015(±0.001)
MDC permeate	0.17(±0.09)	0.0036	NA	NA	NA
MDC feed	17.26(±2.41)	0.34(±0.02)	2.10(±0.14)	18.3(±2.51)	-0.0097 (±0.0002)
MDC concentrate	46.63(±17.04)	0.82(±0.29)	2.14(±0.10)	44.9(±14.6)	-0.0013 (±0.0002)

[a] S is the slopes of linerized plots for UV absorbance from 300 nm to 400 nm (In Abs~λ).
[b] Parenthesis are the standard deviation.
[c] NA=not available

EEM maps were obtained for one sample per week during experiments for each site. Three main peaks were distinguished in most of the maps: tryptophan-like (peak T_1 and T_2), UV humic-like (peak A) and visible humic-like fluorescences (peak C).

4.3.1 RDO Site

Figure 4.6 shows UV-vis absorbance spectra of samples from RDO. Absorbance of all permeate samples were no more than 0.02 A.U. at wavelength of 230 nm and above and less than 0.3 A.U. below 230 nm. Feed and concentrate samples had very strong absorbance below 250 nm before dilution, but had absorbance of less than 0.1 A.U. at 230 nm and above after 10-fold dilution. Above 300 nm, absorbance of all of the samples was no more than 0.03 A.U. Therefore, based on the absorbance spectra and the fluorescence maxima at excitation wavelengths 220 nm, 230 nm, 270 nm, 280 nm and 340 nm, EEMs of diluted feed, recycle and concentrate samples did not require inner-filter correction at excitation wavelength 270 nm and above. Otherwise, at excitation wavelength below 270 nm, fluorescence intensities of feed, recycle and concentrate samples were corrected for inner-filter effects. SUVA values were relatively constant during experiment and varied between 2.4 and 2.9 m^{-1} L/mg.

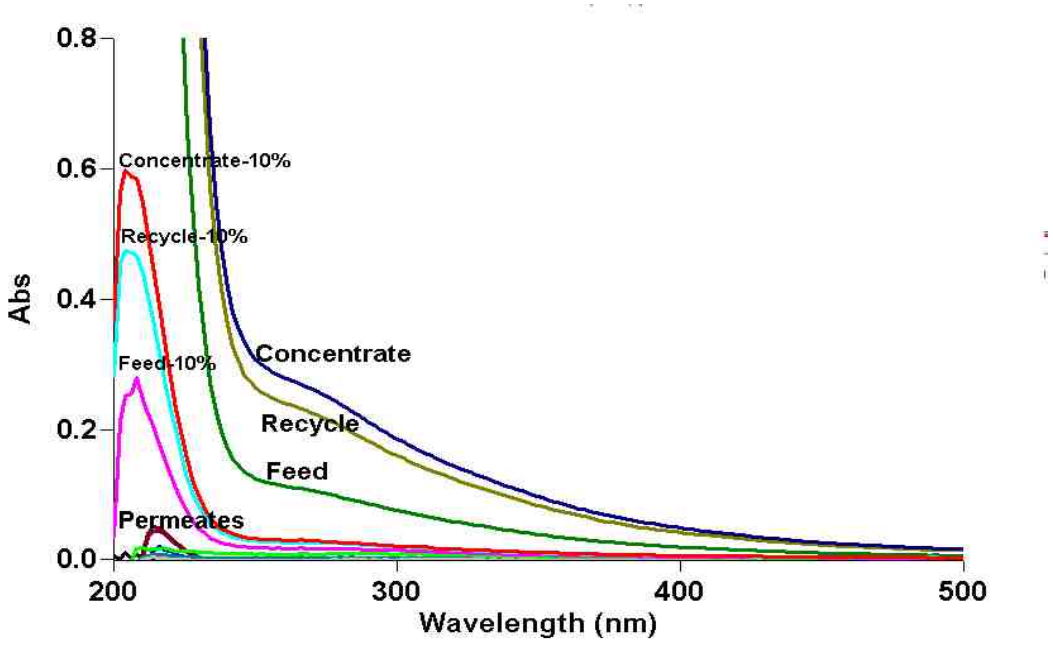

Figure 4.6 UV-vis absorbance spectra of feed, recycle, concentrate and permeate samples on May. 21 of 2007 at RDO (10% denotes 10-fold dilution of sample).

Three main peaks and a weak peak were identified in fluorescence contour maps for all of feed, recycle and concentrate samples (Figure 4.7). A main peak was located at excitation/emission wavelengths (λ_{ex}/ λ_{em}) 230/420-428 nm and it was described as UV humic-like fluorescence (peak A) [Coble, 1996]. Due to its broad peak, maximum emission wavelength ranges from 420-428 nm. Another main peak was located at longer excitation wavelength λ_{ex}/ λ_{em} of 340/425 nm as visible humic-like fluorescence (peak C) [Coble, 1996]. The most intense peak was identified at λ_{ex}/ λ_{em} of 230/356 nm (peak T_1), and a weak peak was also found with fluorescence maximum of λ_{ex}/ λ_{em} around 290/350-360 nm (peak T_2). Peak T_1 and T_2 have been ascribed to protein-like fluorescence, in which the fluorescence arises from the aromatic amino acid tryptophan with λ_{ex}/ λ_{em} of 220-290/340-360 nm [Wolfeis, 1985]. Practically, it was difficult to locate the emission maximum center of peak T_2 because the fluorescence of this weak peak overlapped seriously with the more intense peak C. Although fluorescence of peak T_1 also overlapped with peak A, the fluorescence signals were strong and both peaks could be distinguished and located. However, fluorescence overlapping resulted in alteration of the contour shapes for all of the four peaks (Figure 4.7). Peak A appeared as a more narrow ellipse in all of the feed, recycle and concentrate samples instead of the circular shape of standard sample from IHSS. Peak C also changed to more elliptical shape along the first order of Raman scattering line. At this site, the emission intensities of peak T_1 were close to peak A and more intense than peak C. Peak B was obscured by the peak A and C and could not be separated from those two peaks clearly. No fluorescence residual was found for permeate samples at this site except on Jun.11 of 2007 when fluorescence residual

could be identified with emission intensity less than 20 A.U. at emission wavelength of 360 nm and under which was attributed mostly by peak T_1.

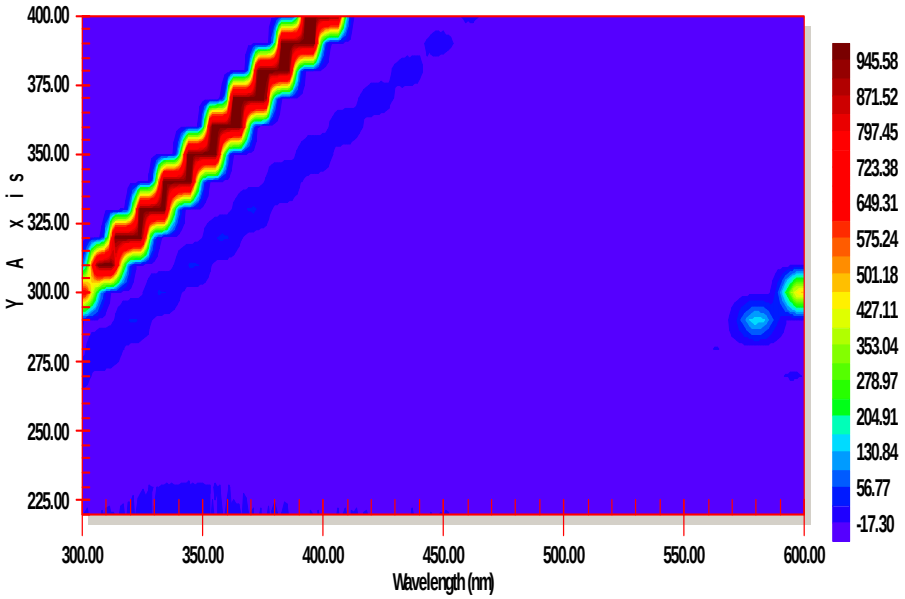

a. RDO permeate

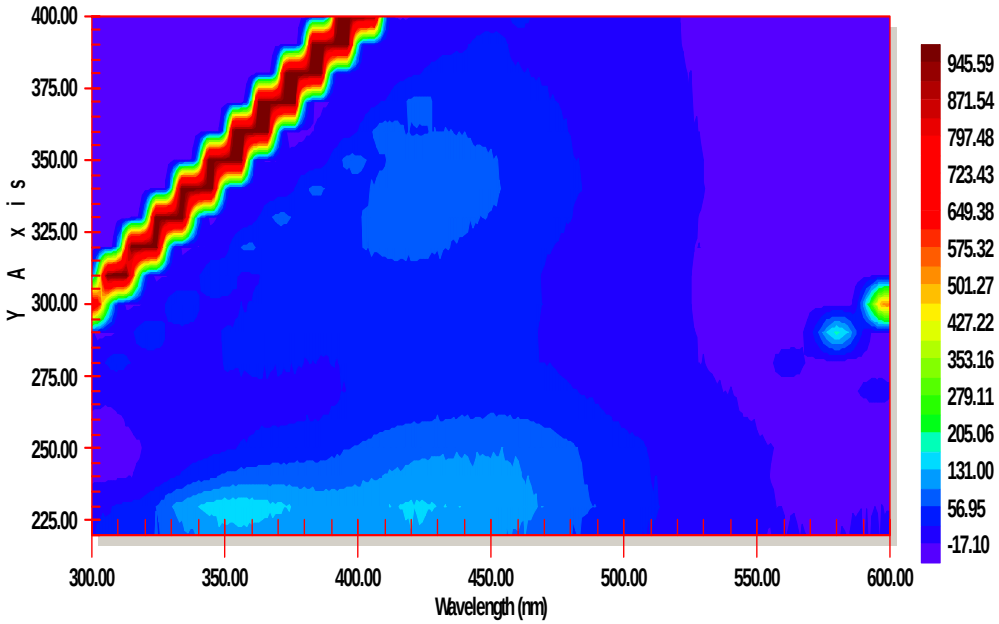

b. RDO feed

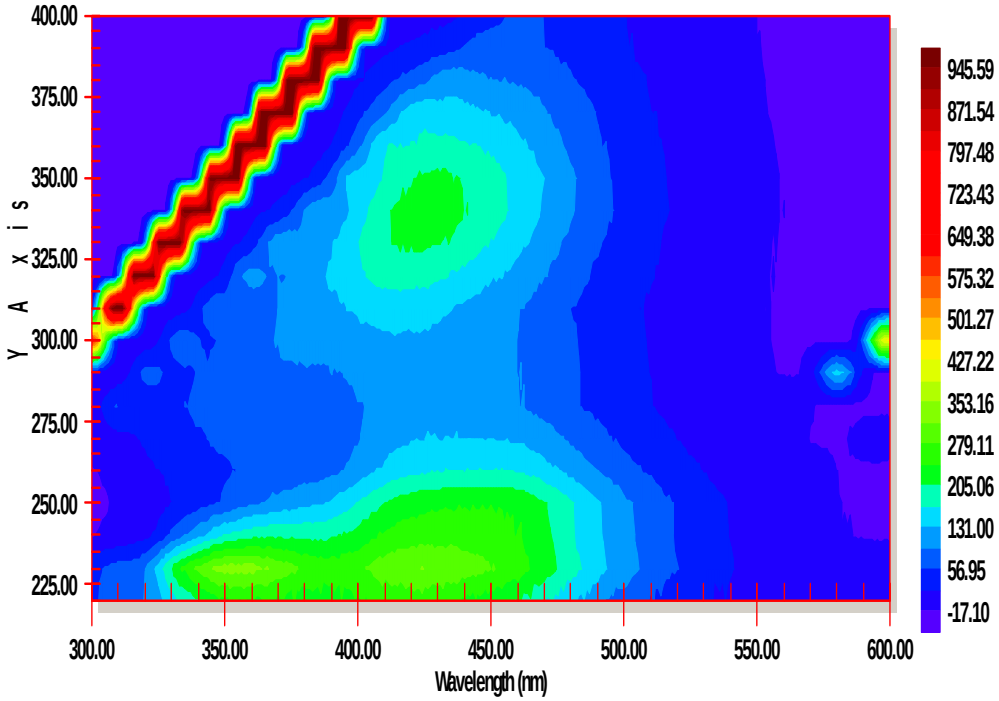

c. RDO concentrate

Figure 4.7 Contour plots of permeate (a), feed (b) and concentrate (c) samples on May. 21 of 2007 at RDO. Feed and concentrate samples were diluted to 10-fold from their original concentration.

4.3.2 ABQWWTP Site

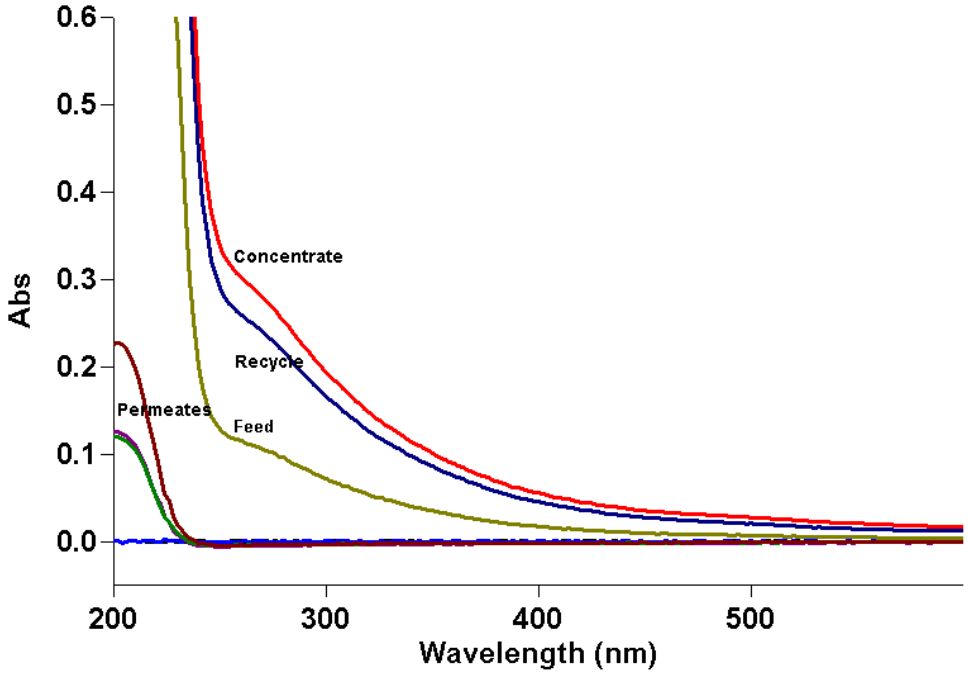

Figure 4.8 UV-vis absorbance spectra of feed, recycle, concentrate and permeate samples on January. 28 of 2008 at ABQWWTP.

UV absorbance spectra at ABQWWTP site are presented in Figure 4.8, which are similar to those from RDO.

Fluorescence of feed, recycle and concentrate samples from ABQWWTP site are very similar to those from the RDO site and they are presented in Figure 4.9. Peak A, B, C have their major fluorescence maxima at $\lambda_{ex}/\lambda_{em}$ of 230/429, 250/460 and 340/425 respectively, and fluorescence center of peak T_2 at $\lambda_{ex}/\lambda_{em}$ of 290/356 nm although this peak overlapped with humic-like fluorescence peaks, peak A and C. The overlap of peak T_2 with peak A and C had more effect on peak C which was elongated along the first order of Raman scattering line. Peak T_1 ($\lambda_{ex}/\lambda_{em}$ = 230/350 nm) was blue shifted from the fluorescence center of sample from RDO site where peak T_1 occurring at 230/356 nm.

Overlapping between peak A and peak T_1 didn't affect the location of these two peaks. Peak T_1 was more intense than humic-like peaks.

All of the permeate samples (Figure 4.9, a) had very small protein-like fluorescence residuals (<30 AU) and no humic-like residual except on Dec. 23, 2007.

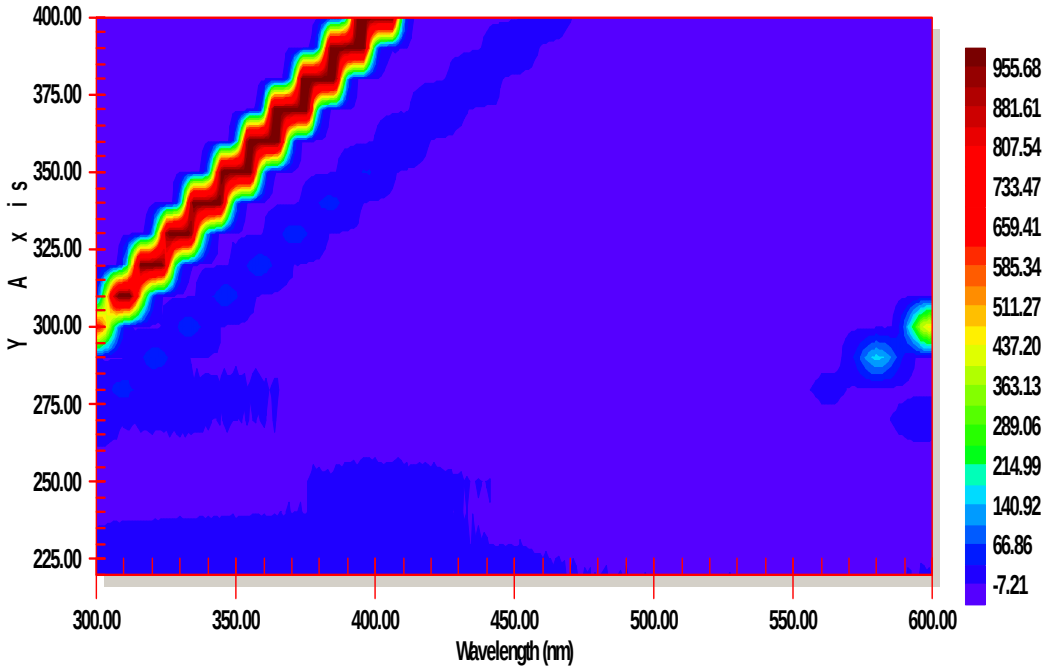

a ABQWWTP permeate

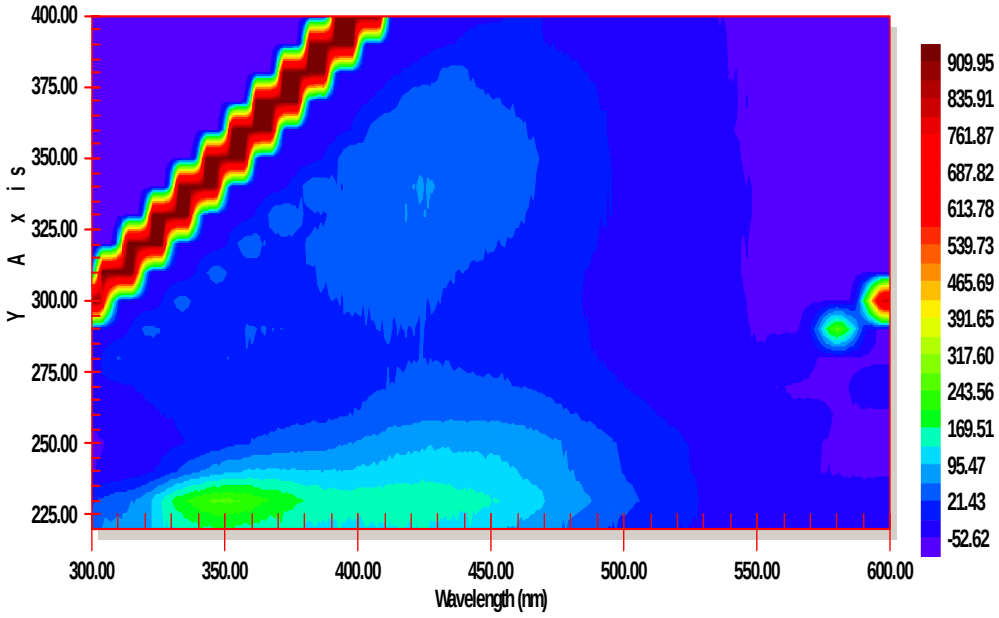

b. ABQWWTP feed

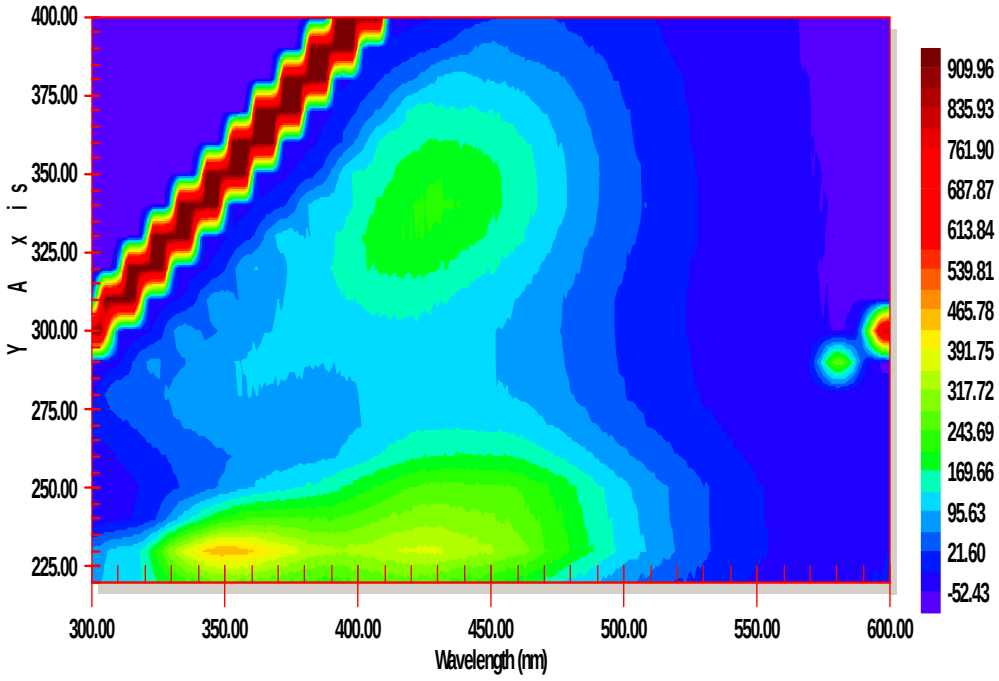

c. ABQWWTP concentrate

Figure 4.9 Contour plots of permeate (a), feed (b) and concentrate (c) samples on February 2nd of 2008 at ABQWWTP.

4.3.3 MDC Site

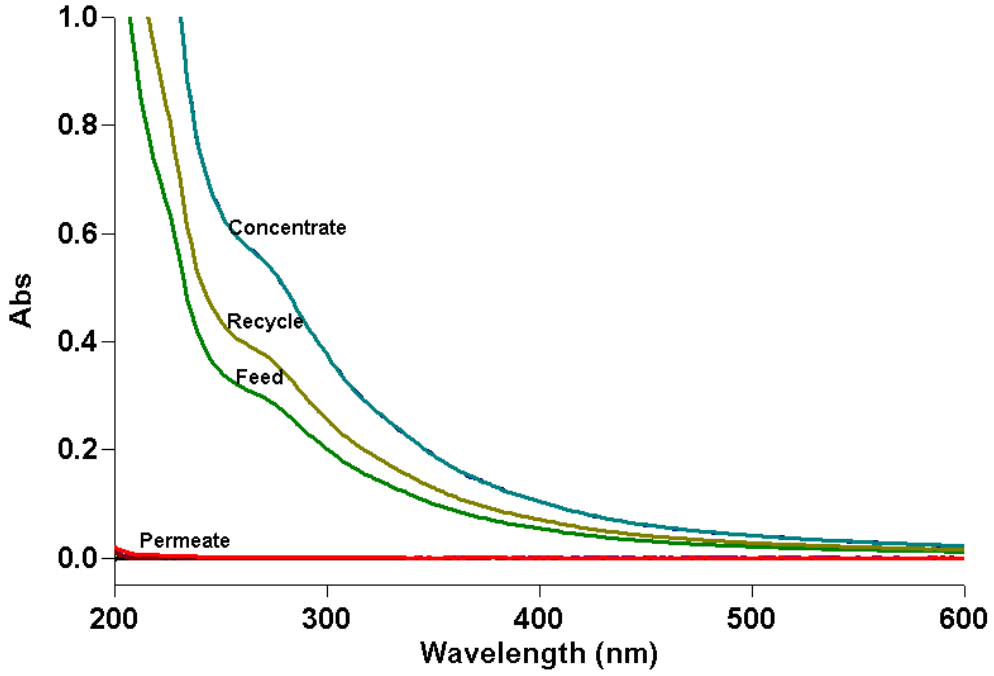

Figure 4.10 UV-vis absorbance spectra of feed, recycle, concentrate and permeate samples on Aug. 3 of 2007 at MDC site.

UV-vis spectra of feed, recycle and concentrate from MDC had strong absorbance under 300 nm (Figure 4.10). Shoulders were identified around 260-290 nm and 230 nm respectively at absorbance spectra for all these three samples. Appearance of shoulders was consistent with absorbance of high concentrated tryptophan-like molecules.

EEMs generated for permeate, feed and concentrate samples are presented in Figure 4.11. Six fluorescence peaks were observed clearly for both feed and concentrate samples. Peak A has excitation and emission maximum wavelength at 230/420 nm (UV humic-like fluorophores). With almost the same emission wavelength, peak C, occurring at $\lambda_{ex}/\lambda_{em}$=340/425 nm, was referred to visible humic-like fluorophores. At shorter emission wavelength, more pronounced peaks were identified at $\lambda_{ex}/\lambda_{em}$=230/356 (350) nm and 270/356 nm. They were assigned to tryptophan-like fluorophores of peak T_1 and

peak T_2 respectively. In addition, another type of protein-like fluorescence — tyrosine-like fluorescence was observed clearly. The major tyrosine-like fluorescence maximum occurred at $\lambda_{ex}/\lambda_{em}$ = 220/309 nm as peak S_1, and a minor tyrosine-like fluorescence located at $\lambda_{ex}/\lambda_{em}$= 280/309 nm were assigned to peak S_2 [Yamashita and Tanoue, 2003] (Figure 4.11 and Figure 4.12), which overlapped with first order Raman scattering line. Although humic-like fluorescence still overlapped with tryptophan-like fluorescence, six peaks could be distinguished from each other from the EEM contour plots and their fluorescence maximum could be identified easily. Unlike the fluorescence spectra from RDO and ABQ samples, peak C appears circular shape as in the standard from IHSS. The overlapping of peak S_2 with the Raman scattering does not interfere with determining its location because its emission intensity is greater than the Raman scattering intensity, and corrected emission intensities were obtained by subtracting scatter background.

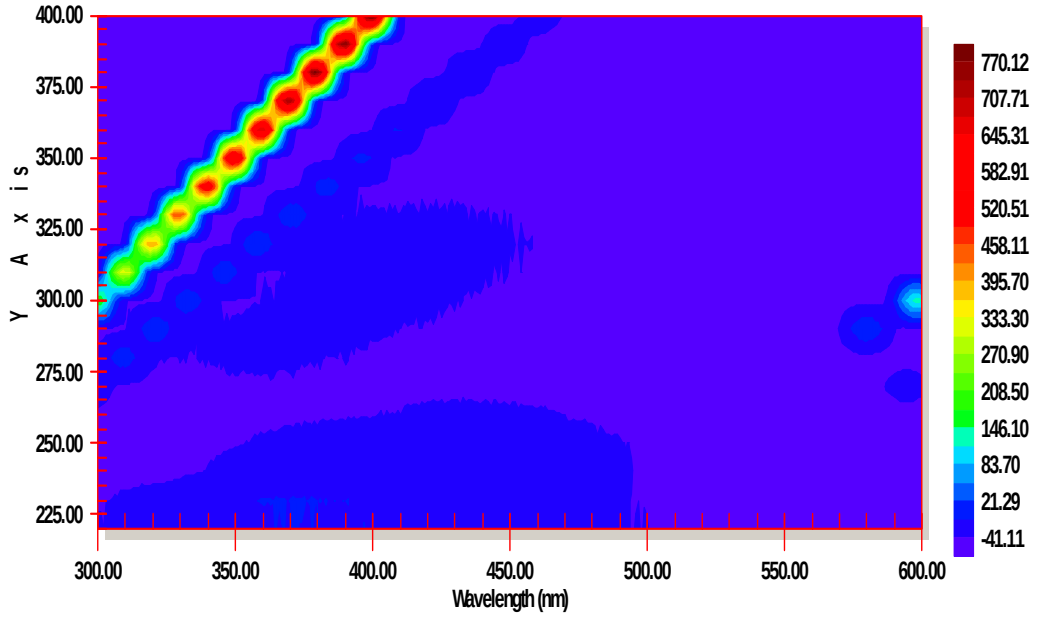

a. MDC permeate

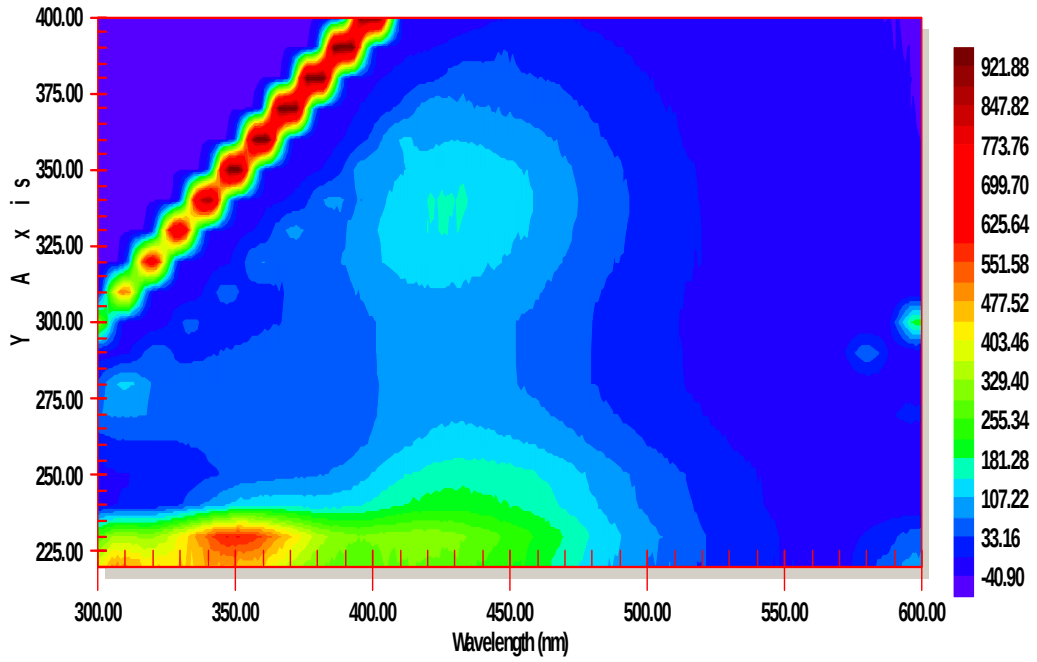

b. MDC feed

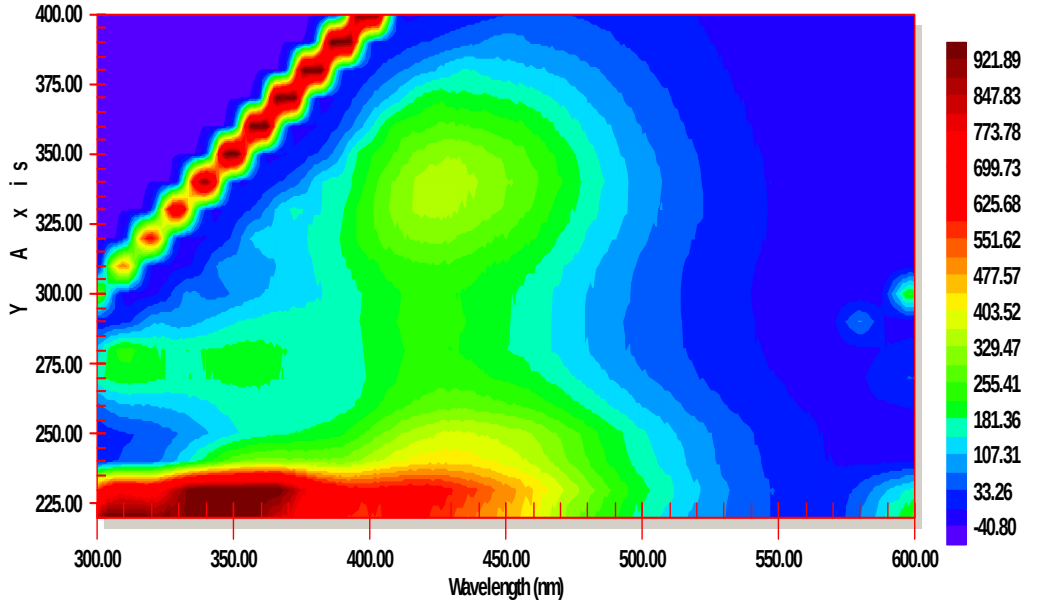

c. MDC concentrate

Figure 4.11 Contour plots of permeate (a), feed (b) and concentrate (c) samples on July. 12 of 2007 at MDC.

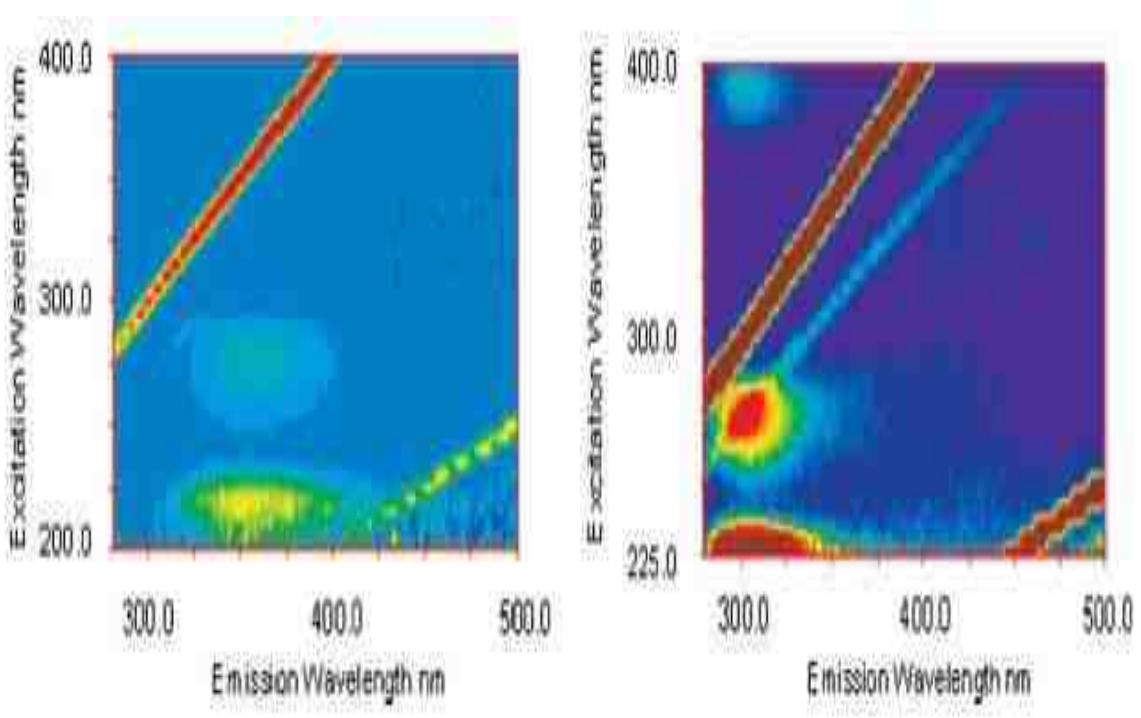

Figure 4.12 Typical contour plots of authentic tyrosine and tryptophan standards [Hudson, 2007].

At this site, peak T_1 is always more intense than humic-like fluorescence in all of the feed and concentrate samples for all dates, and peak S_1 is more intense than peak T_1 on some days (7/18, 8/1, 8/3, 8/17) in recycle and concentrate samples. But it seemed there was no any date that peak S_1 is more intense than peak T_1 in the feed water at this site. When peak S_1 are more intense than peak T_1 in recycle and concentrate samples, the maximum emission intensity of peak S_1 in feed samples is very close to peak T_1 intensity. On the other hand, if peak T_1 is more intense than peak S_1 in recycle and concentrate samples, peak T_1 shows much higher abundance of intensity than peak S_1 in feed samples.

All of the permeate samples from MDC had protein-like and humic-like fluorescence residuals. Generally, the traces of protein-like fluorescence (peak T_1 and T_2)

were stronger than humic-like (peak A and C), except for 7/25 and 8/17 when the permeate samples of these two days had very little protein-like fluorescence residual.

The RO units were cleaned by chemicals instead of backwash with permeate after the system was run for three weeks. The samples on Aug. 22 and Sept. 10 of 2007 were obtained after the membranes were cleaned and they show different fluorescence features from other samples. Peak T_1 was much more pronounced than peak A, C and S_1 in the recycle and concentrated samples, even when recycle and concentrate samples were diluted to 1.25%, the fluorescence intensity of peak T_1 was still over the range of detection. Recycle and concentrate samples were not diluted to lower factor than 1.25%, because at very high dilutions, the fluorescence signature of any dilution water has to be carefully considered as a possible interferent [Henderson, 2009]. The permeate samples had obvious residuals of both tryptophan-like and UV humic-like fluorophores with fluorescence intensity of 130 au and 60 au respectively. The permeate samples from 8/22 and 9/10 still had relative intensive protein-like fluorescence residual and observed humic-like residual, suggested that even after membrane was chemically cleaned, there might be foulants left on the surface or in the pore of membranes. These foulant residuals helped protein- and humic-like fluorescent molecules transport through membrane and spoiled the performance of membrane filtration.

When EEMs were collected one or two weeks after sampling from the plant, the intensities of protein-like peaks were enhanced in all of the feed, recycle and concentrate samples, especially the concentrate samples could increase about one to twenty factor comparing to the normal ones, the longer of the samples were stores in the refrigerator, the greater of the enhancement were made. In order to investigate if it was the result of

microorganisms' activities, saturated heavy metal $HgCl_2$ solution was added to feed and concentrate samples to prevent local microbial from production. 3DEEM fluorescence of samples with $HgCl_2$ had no difference from the ones without $HgCl_2$: same types of peaks, same position of each peak and the maximum intensities were fairly close.

4.4 DISCUSSION

4.4.1 Fluorescence features of DOM

It is noteworthy that the fluorescence maximum emission and excitation wavelengths were identified at the same locations and they don't shift at all for feed, recycle and concentrate samples from three sites. In addition, fluorescence features for RDO and ABQWWTP are fairly similar. Fluorescence emission center of peak A, B, C and T_2 occurred at exactly the same position for RDO and ABQWWTP sites (Table 4.2). Peak T_1 center at ABQWWTP located at $\lambda_{ex}/\lambda_{em}$ = 230/350 nm while $\lambda_{ex}/\lambda_{em}$= 230/356 nm at RDO site. Comparatively, centers of peaks A and T_2 at the MDC site are different from those peaks from RDO and ABQWWTP. For instance, peak A located at $\lambda_{ex}/\lambda_{em}$= 230/420 nm and peak T_2 at $\lambda_{ex}/\lambda_{em}$= 270/356 nm, λ_{em} of peak A and λ_{ex} of peak T_2 blue shift relative to RDO and ABQWWTP. However, peak C and peak T_1 occur at the same positions as those peaks in the RDO and ABQWWTP sites.

Table 4.2 Fluorescence features at RDO, ABQWWTP and MDC sites.

Peaks	RDO site		ABQ site		MDC site	
	$\lambda_{ex}/\lambda_{em}$ (nm)	FI/TOC[a] (au L/mg)	$\lambda_{ex}/\lambda_{em}$ (nm)	FI/TOC (au L/mg)	$\lambda_{ex}/\lambda_{em}$ (nm)	FI/TOC (au L/mg)
A	230/429	f[b]:302	230/429	f:148	230/420	f:378
		c[c]:285		c:139		c:355
B	250/460	NA	250/460	NA	hard to locate	NA
C	340/425	f:185	340/425	f:71	340/427	f:126
		c:203		c:89		c:159
T_1	230/356	f:310	230/350	f:210	230/350(356)	f:798
		c:287		c:182		c:550
T_2	290/356	f: 84	290/356	f: 32	270/356	f: 113
		c: 95		c: 49		c: 263
S_1	N/A[d]		N/A		220/309	f:338
						c:387
S_2	N/A		N/A		280/309	f:118
						c:102

[a] FI/TOC were average values during experiment
[b] f: feed water sample; [c] c: concentrate sample
[d] N/A: Not available

A. Tyrosine-like and Tryptophan-like fluorescence

In studies of protein chemistry, tyrosine residues in proteins and polypeptides often do not emit fluorescence in the presence of tryptophan residues because the emission energy of tyrosine residue was transferred to the excitation energy of tryptophan residue or quenched by neighboring groups [Yamashita and Tanoue, 2003]. In general, the denaturation of proteins leads to an increase in the observed fluorescence of tyrosine [Lakowicz, 1983].

Tyrosine-like fluorescence was observed together with trypotophan-like fluorescence only at MDC site indicated that these two types of protein-like fluorescence were not directly derived from intact proteins or bacteria. Addition of $HgCl_2$ in the wastewater samples didn't alter fluorescence signals features, neither λ_{ex} or λ_{em} shift or fluorescence intensity change, provides proof for this assumption. They may be derived from denatured proteins or debris left by microorganisms. But due to fluorescence center close to that of the tryptophan-like and much weak emission intensity compared to trytophan-like fluorescence, tyrosine-like fluorescence is often obscured by tryptophan-like fluorescence when the concentration of the tyrosine-like fluorophores was not high.

Tyrosine-like fluorescence is present, sometimes with greater intensity than tryptophan-like fluorescence in the sewage-derived organic matter such as MDC samples indicated that significant amount of tyrosine-like flurophores were in the wastewater samples. Yamashita [Yamashita and Tanoue, 2003] found that tyrosine-like fluorescence has greater intensity than tryptophan-like fluorescence in almost all their seawater samples, while other researchers [Coble, 1996; Commack et al., 2004] stated that tryptophan-like fluorescence were more intense and tyrosine-like fluorescence is not

observed in estuarine and fresh water samples. The reason why tyrosine-like fluorescence intensity is much lower than that of tryptophan-like at RDO and ABQWWTP sites if they existed in the samples may be the lower concentration of tyrosine-like fluorophores in the samples from wastewater sources or its lower quantum yield. Intensive tyrosine-like fluorescence at MDC suggested that biodegradation of tyrosine-like fluorophores in the lagoon was much less efficient than by MBR or activated sludge system.

In several samples stored over one week, unusually high fluorescence intensities were observed. Although samples were stored at 4 ˚C in the refrigerator in the dark, the microorganisms in the wastewater may have remained active and produced more fluorophores, resulting in enhanced protein-like fluorescence. Humic-like fluorescence doesn't change suggesting that this activity didn't produce new humic-like fluorophores or quench humic-like fluorescence. The fact that no change occurred for samples before and after $HgCl_2$ addition implied two things: first, it was not protein that responsible for all of the fluorophores, even for the protein-like fluorophores--tyrosine-like and tryptophan-like fluorophores, they did not likely directly come from protein molecules because saturated $HgCl_2$ solution would denature them if these molecules were in the solution. These findings suggested that protein-like fluorescence observed in this study was not derived directly from living microorganisms but rather from amino acids in the non-living molecular mass DOM pool. Therefore, the sooner to analyze of the wastewater samples, the closer to investigate the real nature of wastewater.

B. Protein-like versus humic-like fluorescence

Different pretreatments of RO led to different fluorescence properties for both humic-like and protein-like fluorophores. At RDO and ABQWWTP sites, the pretreatments were either MBR or activated sludge system, so peak T_2 and/or other peaks such as peak B might have intramolecular interaction with peak C, and energy transition became easier between these fluorophores, thus resulted in contour plots of peaks T_2 and C distorting their shapes along Raman scattering band. Another possibility was some of tryptophan-like and humic-like fluorophores were degraded by bacteria into smaller fluorescence functional structures which emitted fluorescence at the same regions with tryptophan-like and humic-like fluorescence. As a consequence, the distorted contour plots derived from superposed tryptophan-like, humic-like fluorophores and their degraded functional structures. At MDC, protein-like fluorophores might not have intramolecular interaction with humic-like fluorophores, therefore no electron or energy transition occurred between the fluorophores; moreover, maybe there was no effective degradation occurred like RDO or ABQWWTP sites for tryptophan-like and humic-like fluorophores. Consequently all of fluorophores kept their own characteristics, and their emission centers were clear enough for visual identification. It may be concluded that biological treatment degraded protein-like and humic-like fluorophores, but also produced new fluorophores which include both of protein-like and humic-like fluorescent functional structures. The new fluorophores have the identical or similar fluorescent functional groups, therefore fluorescence maxima located at the same region and contour shape changed.

At all three of the sites, tryptophan-like fluorescence was always stronger than

humic-like fluorescence in feed, recycling and concentrate samples. In general, the order of maximum fluorescence intensities was: tryptophan-like (T_1) > UV humic-like (Peak A) > visible humic-like (Peak C) > tyrosine-like (S_1) at RDO and ABQ sites while tryptophan-like (T_1) > tyrosine-like (S_1) > UV humic-like (Peak A) > visible humic-like (Peak C) at MDC site. This differs from fresh water where humic-like fluorescence dominates over protein-like fluorescence (refer to Chapter 3).

Table 4.3 Fluorescence maxima intensity ratio at three sampling sites.

	T_1/A[a]		T_2/C		T_1/T_2		S_1/S_2		A/C	
Sites	feed	Conc[b].	feed	conc.	feed	conc.	feed	conc.	feed	conc.
RDO	1.11	1.07	0.38	0.44	4.30	3.61	N/A	N/A	1.72	1.61
ABQ	1.43	1.29	0.41	0.55	9.27	5.08	N/A	N/A	2.47	2.15
MDC	1.72	1.38	0.59	0.77	15.38	13.56	7.83	19.44	4.60	8.00

[a] all ratios were the average during experiment.
[b] conc. was concentrate sample

Due to high fluorescence intensity and clear fluorescence center, generally, the tryptophan-like peak (peak T_1) was chosen as an example to establish the potential relationships at three sites. In addition, peak T_2 was a reference to peak T_1. The ratio T_1/A was more stable than T_2/C and was less affected by the measurement uncertainty (Figure 4.13).

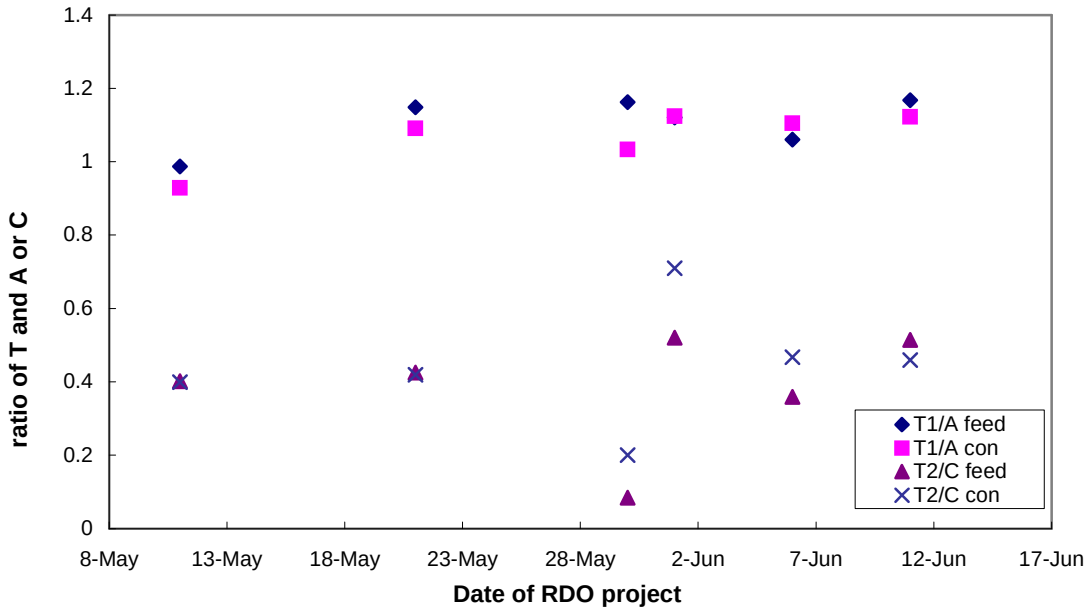

Figure 4.13 Dynamics of ratio between protein-like and humic-like fluorescence intensity during 30 days of RDO project.

The ratios of T_1/A varied between 1 in the RDO and 2 in the MDC and the different ratios indicated that the composition of organic matter from these two site were different. Generally, the ratios of T_1/A in the feed water were slightly larger than in concentrates at all three project sites. At RDO site, the average ratios were very close (as 1.11 in the feed sample and 1.07 in the concentrate sample), while at MDC with high TOC, the average ratios changed from 1.94 in the feed samples to 1.56 in the concentrate samples. Even with similar TOC values (average TOC=6 mg/L in the feed and 16 mg/L in the concentrate at ABQWWTP) as RDO (average TOC were 5 mg/L and 12 mg/L respectively), the average ratios at ABQ were 1.43 and 1.29 respectively. The average T_1/A ratio of feed water at MDC is almost 2 times higher than RDO revealed that MDC samples constituted with more fresh organic materials. Higher T_1/A ratio in feed than concentrate water demonstrated that feed water contained more labile organic matter and

concentrate sample had more recalcitrant matter—either refractory humic-like fluorophores or biologically-resistant humic-bound proteinaceous constituents or both [Stevenson, 1983]. Samples at RDO inhabited more aromatic and less microbial in nature due to their lowest T_1/A ratio. In contrast, the samples at MDC had a lower aromacity with the highest biological activity because of the highest T_1/A ratio. The protein-like fluorescence residual and very little or no humic-like fluorescence trace in permeate samples provided the evidence that the more recalcitrant matter in concentrate water might be humic-like material other than microbial derived matter. These results indicated that RO membranes more efficiently remove humic-like material relative to protein-like material. This conclusion was supported by the evidences that lower T_1/A ratio at RDO compared to ABQ and permeate samples at RDO had no any fluorescence residual while they still had different extent residual at ABQ, even the samples from the these two sites had the similar TOC. Since RO process is based on size, retained peaks A and C and permeable of peaks S and T suggested that molecular weight of humic-like fluorophores are larger that those of protein-like fluorophores.

4.4.2 Optical methods and their relations to TOC and protein concentration

A. SUVA and FI/TOC

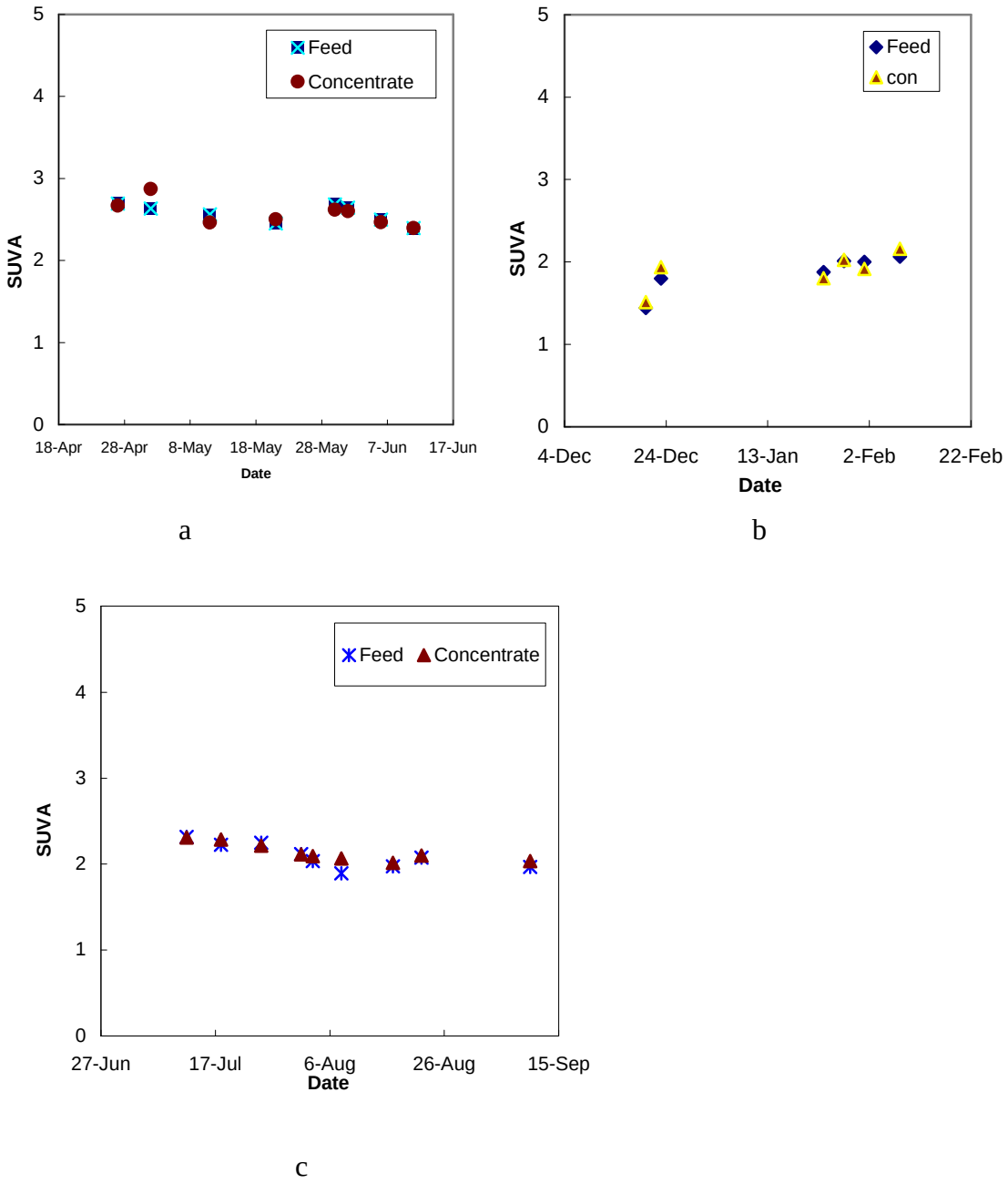

Figure 4.14 SUVA of three sites at (a) RDO site, (b) ABQ site and (C) MDC site during experiment.

The SUVA is an indicator of the degree of aromaticity of DOC. Higher SUVA values may indicate higher concentration of carbon-carbon double bonds and a larger degree of humification [Chin et al., 1994]. SUVA values of RDO were higher than those

of ABQ and MDC, therefore DOC from RDO samples may be have the most condensed structures such as more resistant aromatic humic-like matter and ABQ have the least humic-like concentration. Although the water samples from RDO and ABQ came from the residential wastewater system, the large difference in SUVA values may be due to the different pretreatment processes before RO membrane. The pretreatment was MBR at RDO site and activated sludge system at ABQ site. Even though MBR is a compact model of activated sludge system with filter, MBR was not good enough for the removal of refractory humic-like organic matter because of its short process time and/or its limited species of microorganisms and/or limited contact space. On the other hand, activated sludge system at ABQ site allowed organic matter to contact longer time with different types of microorganisms, thus more aromatic portion of DOM was biodegraded. This conclusion was supported by the evidence that carbon normalized fluorescence intensity (FI/TOC) at RDO site were almost two times larger than ABQ site.

SUVA values of feed water samples at all three sites were very close to those of concentrate values for each day indicating that nearly all of organic matters chromophores in feed water were concentrated in concentrate samples. The evolution of SUVA over time is shown in Fig 4.14. In general, SUVA values were relatively consistent, varying between 2.4~2.9 m^{-1} L/mg at RDO site, 1.4~2.1 m^{-1} L/mg at ABQ and 1.9~2.3 m^{-1} L/mg at MDC.

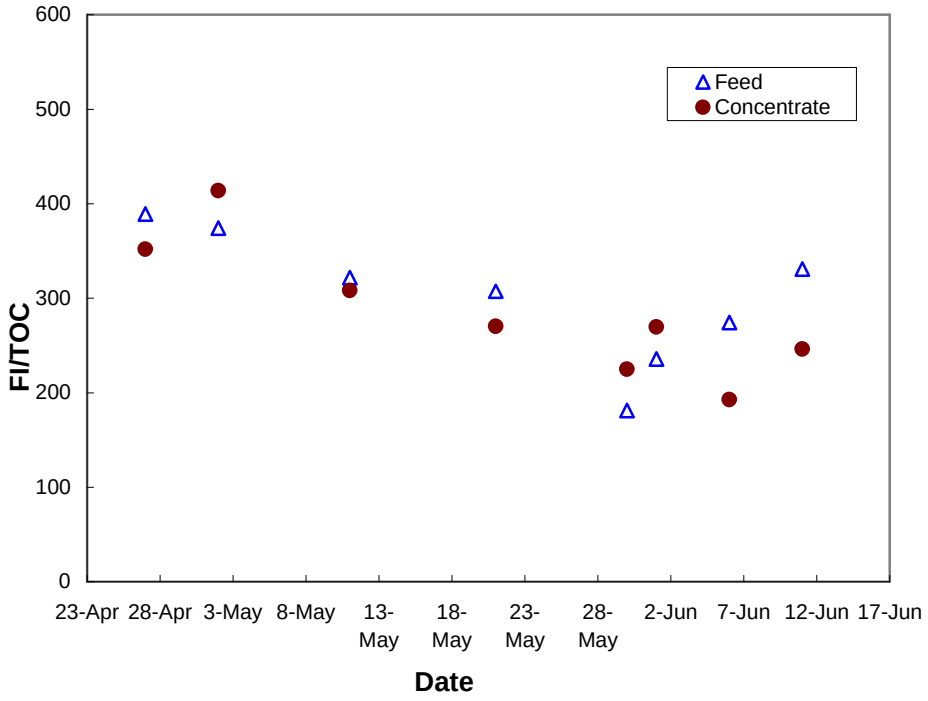

a.RDO

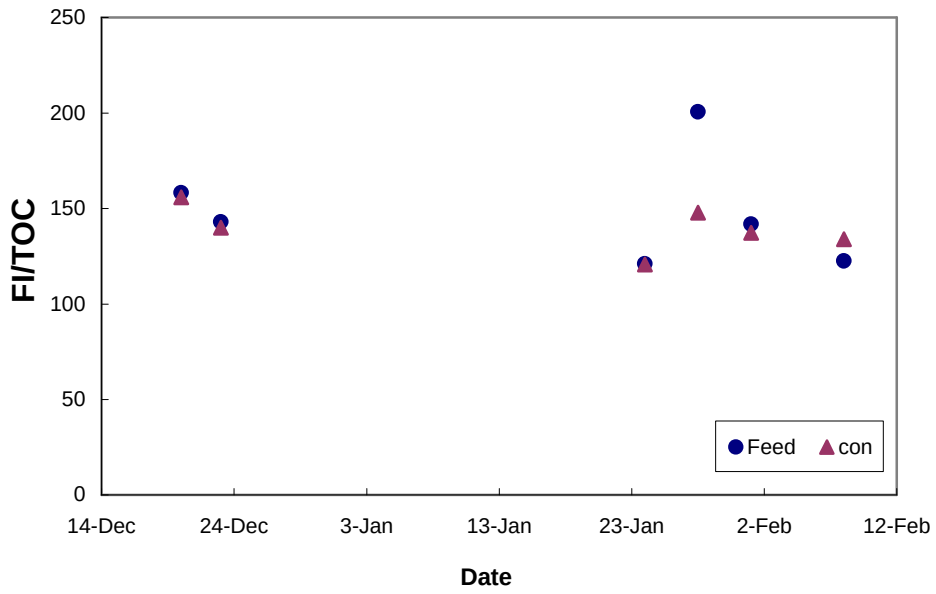

b.ABQWWTP

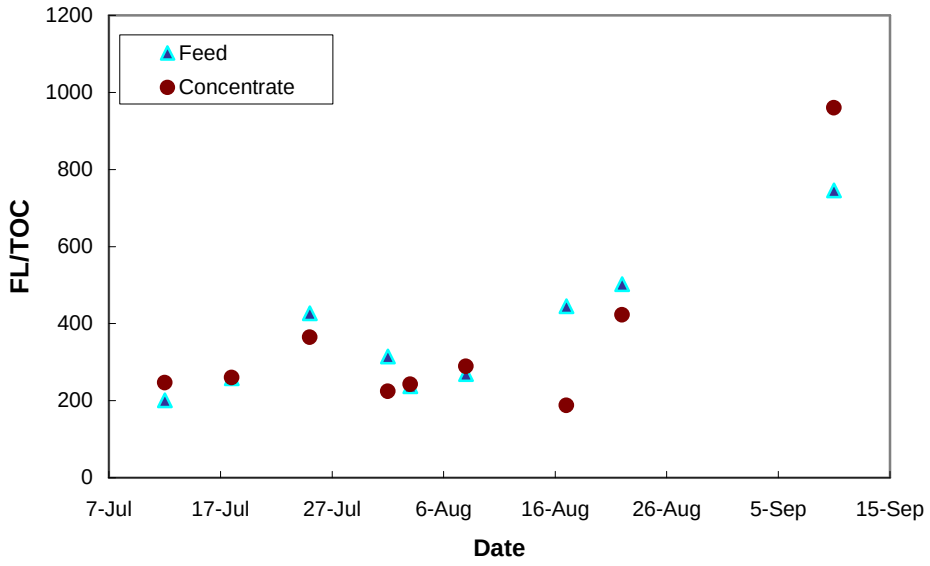

c.MDC

Figure 4.15 Evolution of TOC-normalized fluorescence intensities (FI/TOC) of peak A from feed and concentrate samples at (a) RDO, (b) ABQWWTP and (c) MDC sites.

The trends of TOC normalized florescence intensities (FI/TOC) (Figure 4.15) are different than SUVA trends. The normalized intensities of peak A change with time and vary sample to sample. In addition, normalized intensities of feed samples were not always close to those of the concentrates. Similar trends were observed for peak C and T (not shown). Considering the TOC normalized florescence intensities are inconsistent with time and it seemed they were more likely affected by some unclear factors, for instances, changes in quantum yield due to possible quenchers or change in conformation. FI/TOC may be not the intrinsic property of organic matter and could not be treated as surrogate parameter as SUVA.

B. Optical prediction of protein concentration

Understanding dissolved organic nitrogen can be useful in designing new water treatment processes to remove these components from potable water sources. Nitrogen-rich constituents in DOM such as proteins represent an important class of the problematic hydrophilic NOM fraction related to undesirable DBPs formation.

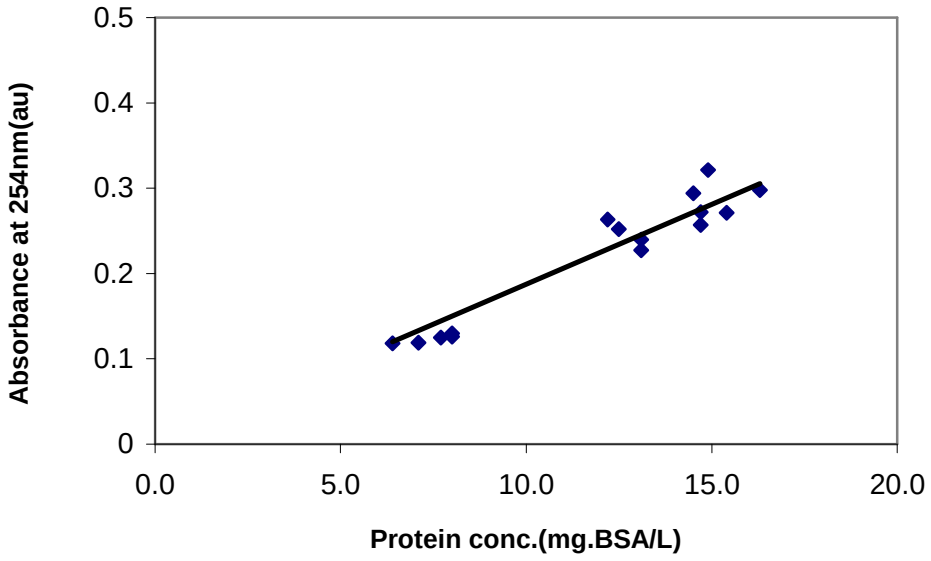

a.RDO

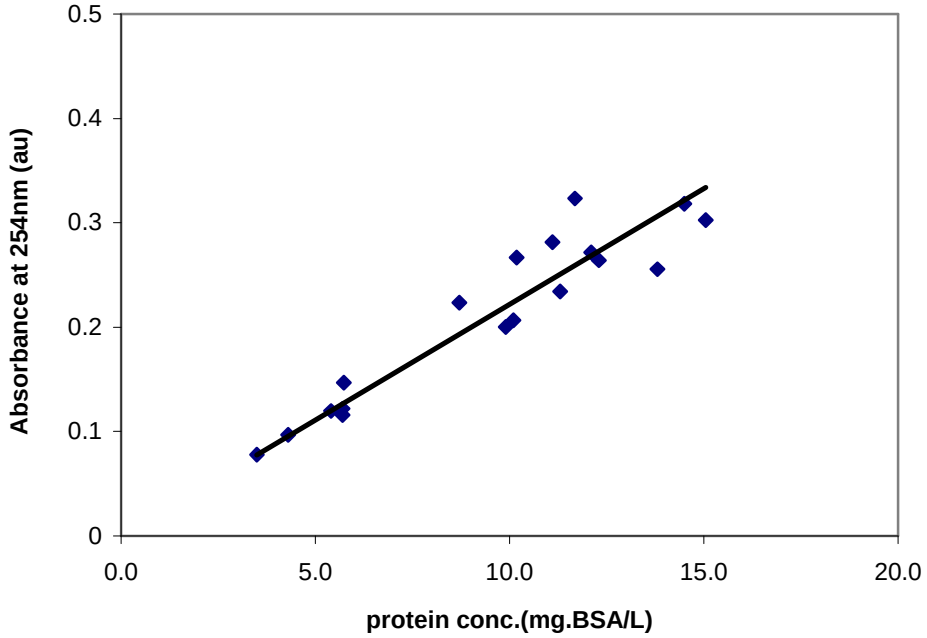

b.ABQWWTP

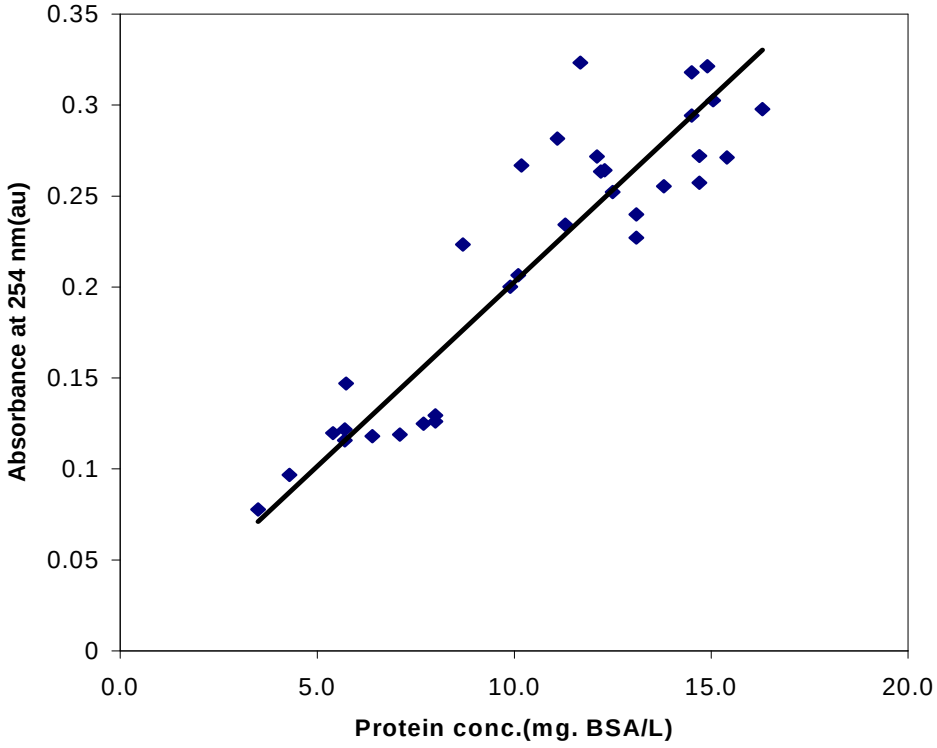

c. RDO+ ABQWWTP

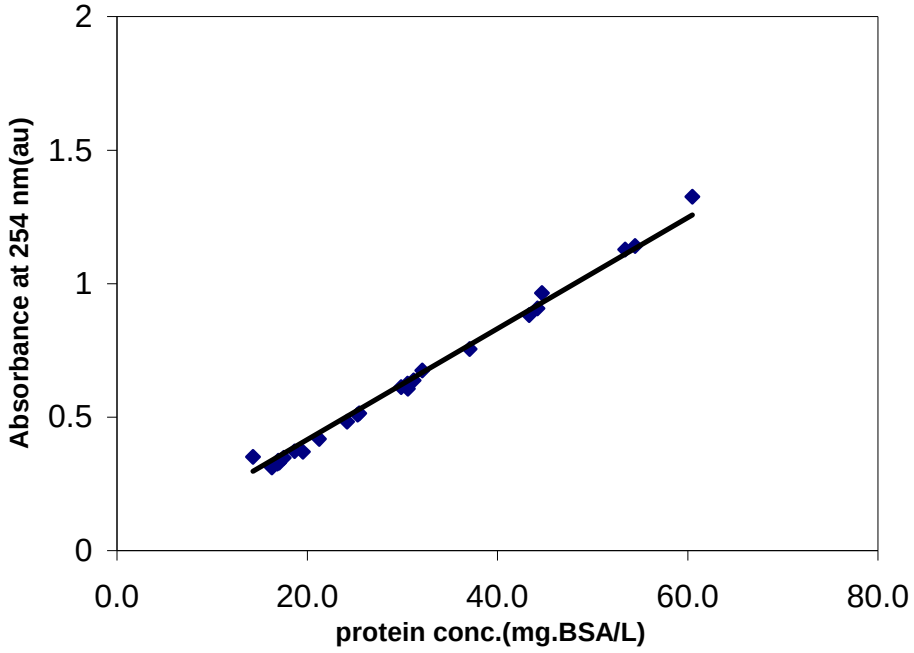

d.MDC

Figure 4.16 Correlations between protein concentration and absorbance at 254 nm at RDO site (a), ABQ site (b), RDO+ABQ (c) and MDC site (d).

From Figure 4.16, linear relationships were observed between protein content and UV absorbance at 254 nm for each of a single day at all of three sites, and they have significant correlations. In addition, linear regression of the total data pool (The data pool for a given site is all the samples taken over the duration of the study at that site) during experiment at MDC site gave a linear regression R^2= 0.99. Although this linear relationship did not fit as well for the data pools during experiments at RDO and ABQ sites comparing to MDC, they still have R^2 as 0.93 and 0.88 respectively. Slopes from three different sites are also closely identical demonstrated the linear relationship fit both high and low protein concentration. Therefore, absorbance at 254 nm can be used to measure protein concentration rapidly and conveniently.

Very similar linear correlations were also applied to protein content data and TOC data (Figure 4.17). Quite close fluorescence intensity of peak A and T_1 explain the lower regression value (R^2 = 0.5 for RDO+ABQWWTP) for TOC was contributed considerably by both of humic-like and protein-like fluorophores. However, significant regression value (R^2 = 0.97) suggested protein-like fluorophores constituted most TOC for MDC water samples. The different slopes among RDO (0.74), ABQWWTP (1.2) and MDC (1) indicated various TOC distribution and the contributions by different types of fluorophores, especially by protein-like fluorophores.

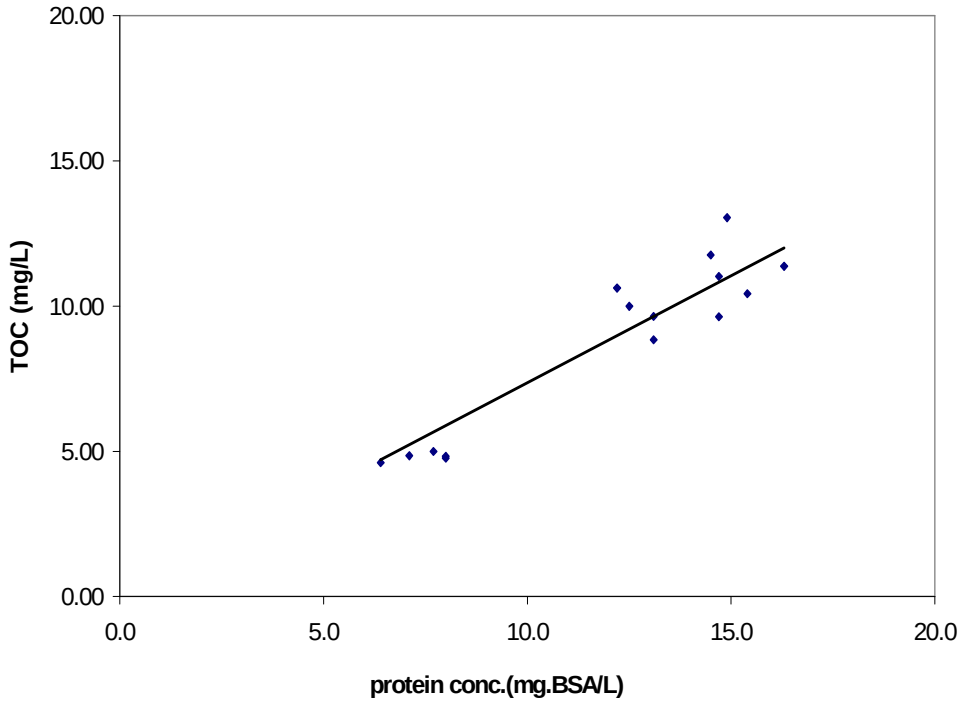

a.RDO

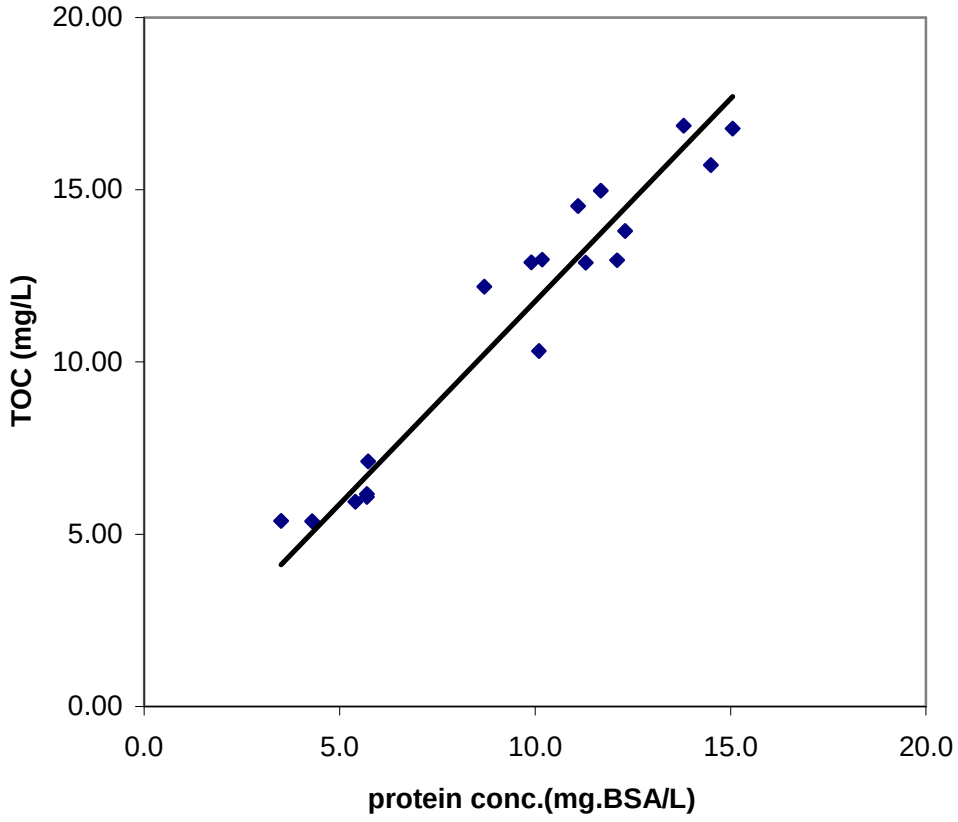

b.ABQWWTP

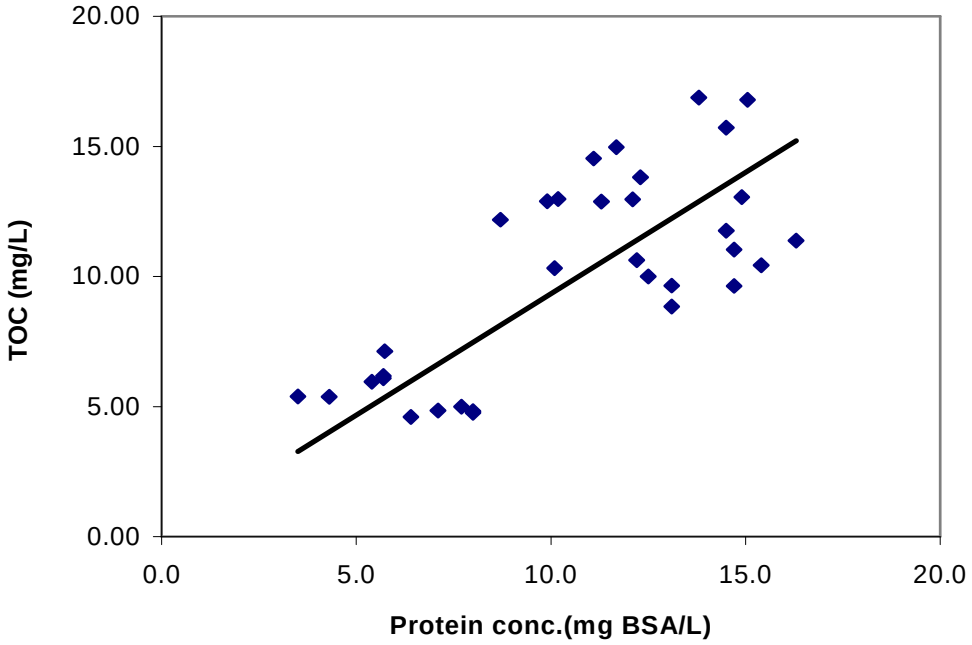

c. RDO+ ABQWWTP

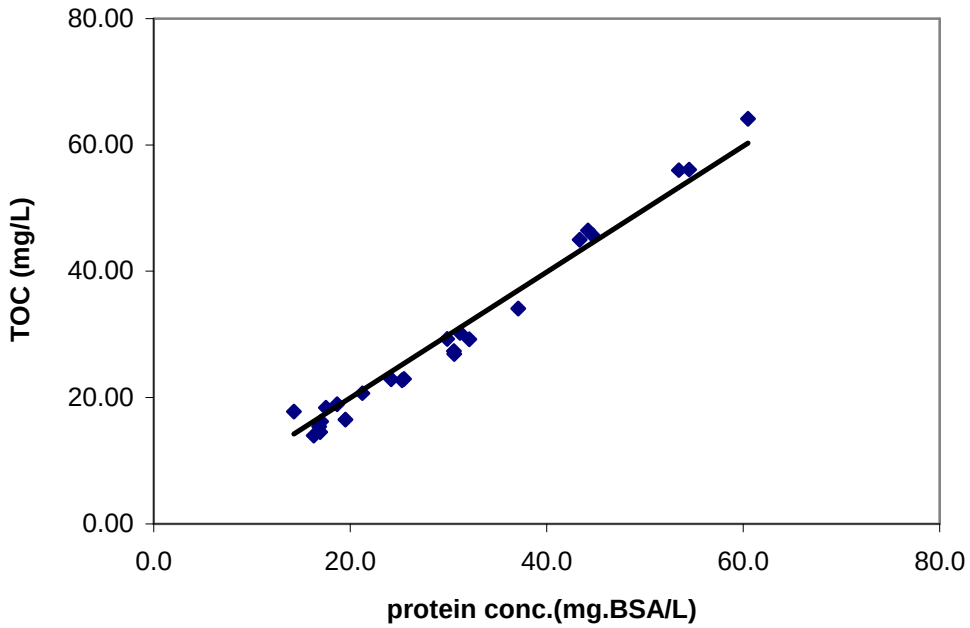

d.MDC

Figure 4.17 Correlations between protein concentration and TOC at RDO site (a), ABQ site (b), RDO+ABQWWTP (c) and MDC site (d).

Since protein degradation products are believed to be the sources of tryptophan-like and tyrosine-like fluorophores [Coble, 1996], it is reasonable to hypothesize a relationship between peaks T and S and protein concentration. Many recent works stated that tyrosine-like peaks excited at around 220-280 nm [Yamashita and Tanoue, 2003; Baker and Inverarity, 2004; Mayer et al., 1999], while it could not tell if the maximum excitation wavelength was 220 nm because it seemed that fluorescence center was below 220 nm from the contour plots. In this paper, the maximum excitation wavelength occurs at 220 nm and the higher noise/signal ratio at shorter excitation wavelengths than higher ones. Although fluorescence intensity deriving from longer excitation wavelengths at 265-280 nm and 275-285 nm were referred to tyrosine-like (peak S_2) and tryptophan-like (peak T_2) peaks by Yamashita [Yamashita and Tanoue, 2003], the shorter excitation

wavelengths at 220 nm (peak S_1) and 230 nm (peak T_1) were preferred to the two protein-like peaks in this study due to two reasons: first, peak S_2 was overlapped with Raman scattering band, thus, the accuracies of peak intensity became worse even after Raman scatter was subtracted because both intensities were weak; second, the overlapping of peak T_2 with humic-like fluorescence made it hard to identify the fluorescence center of peak T_2 when trypotaphan-like fluorescence abundance was small. The publications like to correlate T_2 to water quality parameters such as BOD, TOC etc because their instruments limited excitation wavelength shorter than 250 nm. But the identification is hard when this peak seriously overlapped with peak C, and peak intensity is very weak when DOM concentration is low (<10 mg/L) in river water or advanced treated wastewater. Therefore, this study chose both of peak T_1 and T_2 to correlate with forementioned parameters. The advantages of peak T_1 are the fluorescence center is very easy to located even it is overlap with peak A, furthermore, the fluorescence intensity is much more intensive than peak T_2. In comparison, peak T_2 was picked when its fluorescence center is clear and emission intensity is not too weak.

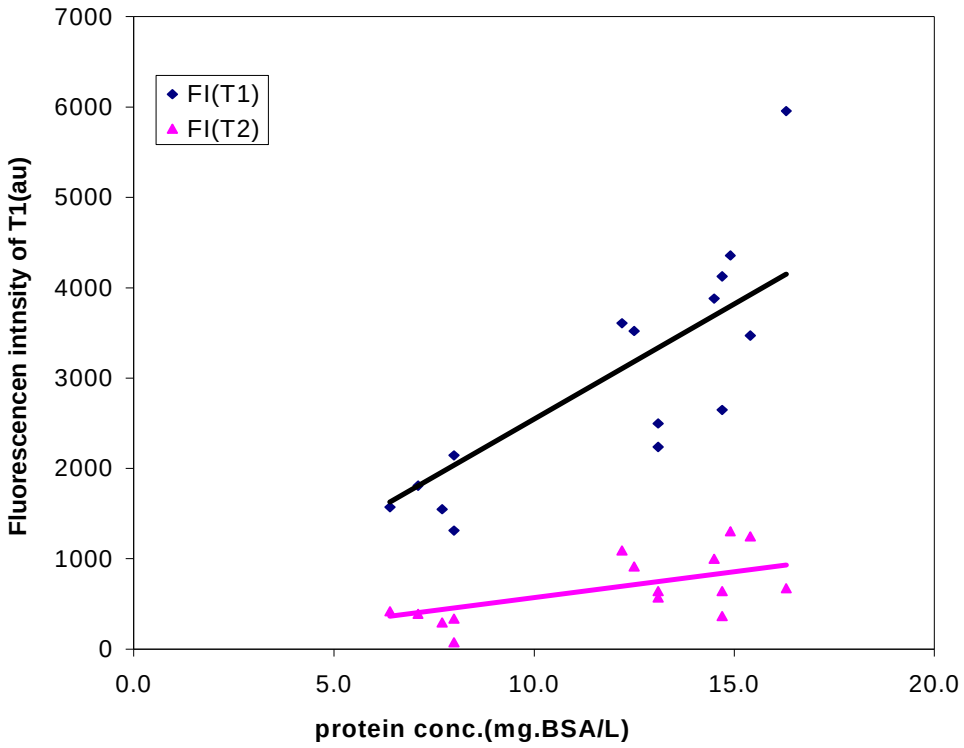

a.RDO

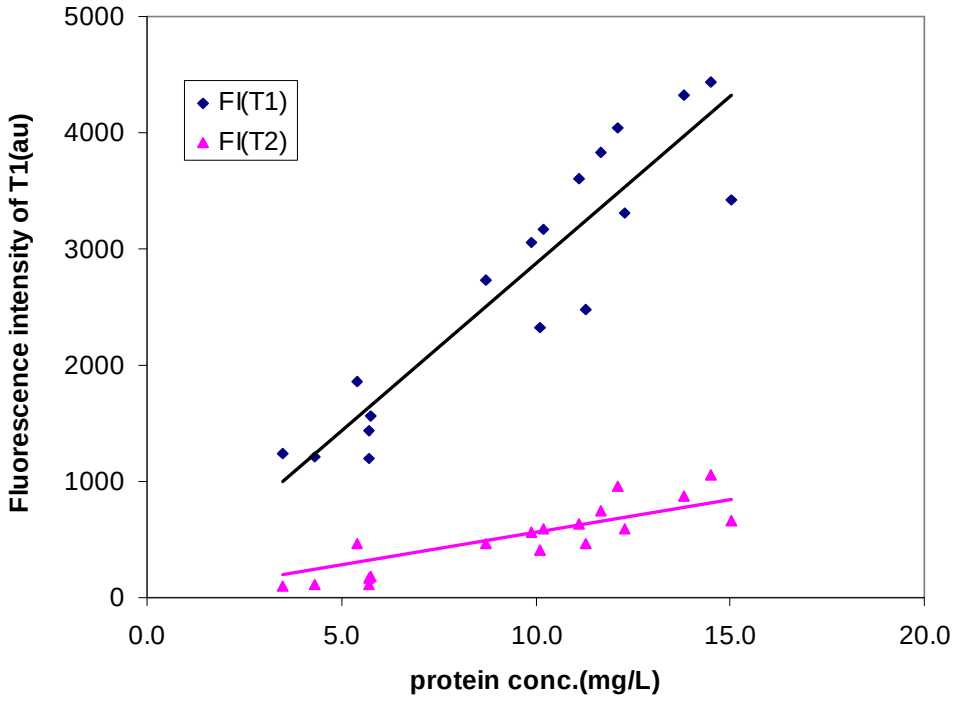

b.ABQWWTP

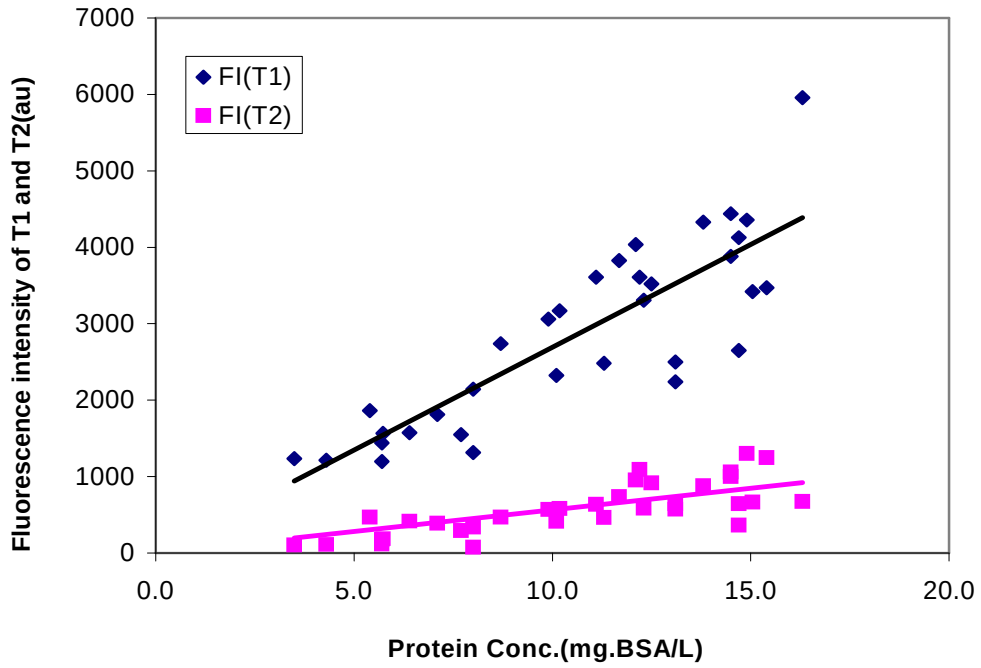

c. RDO+ABQWWTP

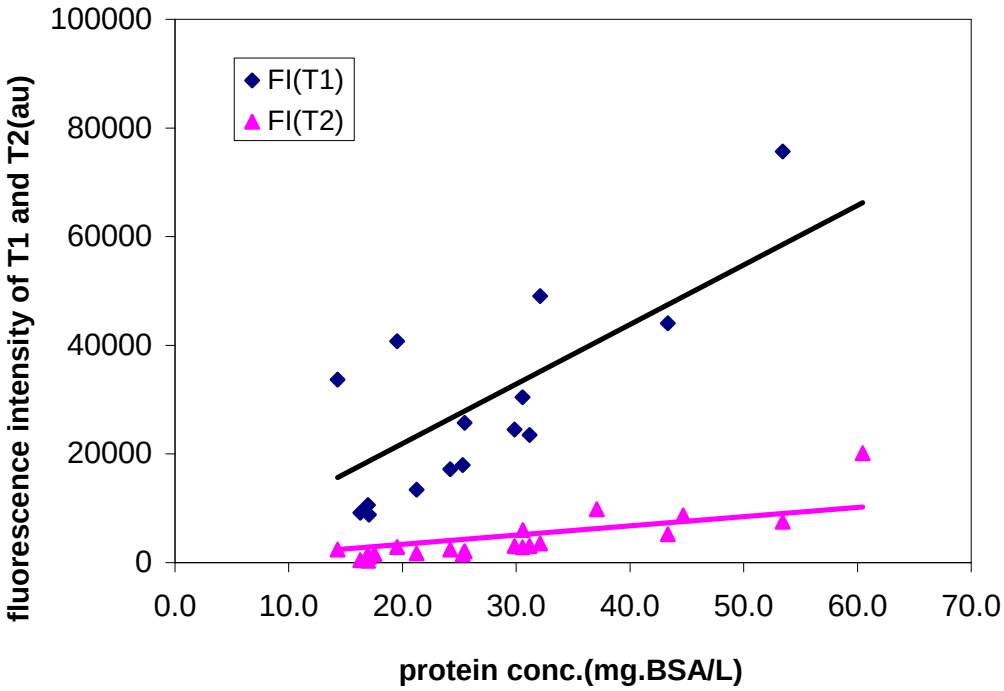

d.MDC

Figure 4.18 Correlations between protein content and fluorescence intensity of peak T_1 and T_2 at RDO site (a), ABQWWTP site (b), RDO+ABQWWTP (c) and MDC site (d).

Figure 4.18 shows that fluorescence intensity of peak T_1 is positively correlated with protein concentration, and can fit a linear trend line with regressions R^2 around 0.7 (RDO, T_1), 0.8 (ABQWWTP, T_1), 0.6 (MDC, T_1) and 0.4 (RDO, T_2), 0.8 (ABQWWTP, T_2), 0.8 (MDC, T_2) respectively (Table 4.4). The linear relationship which fits Peak T_1 is worse than Peak T_2 at MDC site. This may be a consequence of uncertainty in fluorescence intensity due to very strong protein-like fluorescence and high background fluorescence intensities from peak T_1. This phenomenon explains why some researchers would like to refer peak T_2 to protein-like fluorophores: the reproducibility and precision of measurements of protein-like peak were lowered in the shorter wavelength region in natural waters [Yamashita and Tanoue, 2003]. In this regard, therefore, choosing which peak to construct relationship with DOM properties depends on the factors such as protein-like fluorophores concentration, fluorescence maxima identification of each peak and fluorescence spectrometer set-up parameters etc. Based on Yamashita's conclusions [Yamashita and Tanoue, 2003] and my results, fluorescence intensities deriving from longer excitation wavelengths were referred to as protein-like peaks when Peak T_2 or S_2 is discernible and Peak T_2 could be distinguished from humic-like fluorescence; conversely, fluorescence intensities from shorter excitation wavelengths as protein-like peaks would be better if fluorophore concentration is not high and instrument could scan excitation wavelengths down to 220 nm.

Table 4.4 Correlations between protein concentration and surrogate parameters

	TOC			Absorbance at 254 nm			FI *(T_1)			FI (T_2)		
	Slope	R^2	St. Dev	Slope	R^2	St. Dev	Slope	R^2	St. Dev	Slope	R^2	St. ev
RDO	0.82	0.89	1	0.02	0.93	0.02	309	0.68	765	71	0.44	288
ABQ	1.1	0.93	1.1	0.02	0.88	0.03	283	0.85	451	71	0.78	142
RDO+ ABQ	0.76	0.54	2.7	0.02	0.84	0.03	273	0.72	635	70	0.61	213
MDC	1	0.98	2	0.02	0.99	0.02	1335	0.61	11771	303	0.74	2360

* FI are the maxima emission intensities

Although protein concentration correlated more strongly with absorbance at 254 nm and TOC than with fluorescence intensity of tryptophan-like fluorophores, this may not be the case when humic-like fluorescence dominate the EEM spectra. Thus, these good correlations highlight the importance of application of fluorescence for water quality monitoring, therefore knowing the approximate value of protein concentration with calibration curve by measuring protein-like fluorescence maximum emission intensity. This method is fast and easy-to-use. Recent publications highlight that future research should focus on utilizing and analyzing fluorescence measurements as an independent test of water quality, rather than as a surrogate for well-known, traditional parameters that may be less meaningful. The question of development of this application is associated with calibration in a complex sample matrix, since wastewater samples exhibit great variation which affects fluorescence more than absorbance and introduces errors to fluorescence as well as chemical and biochemical measurements. However, these drawbacks can not hinder 3DEEM technique become a simple, sensitive and selective tool to monitor water quality and contamination in contrast to other conventional tedious technologies.

4.4.3 Performance of RO membranes

By investigating both of excitation and emission maximum wavelengths, no any shift occurred for feed, recycle or concentrate samples, only intensities were different. This result demonstrated that there was no any structure or configuration change for both of protein-like and humic-like fluorophores before and after RO filtration and RO procedures just rejected organic matters without any transformation, addition or less these macmolecules.

Compared with results from RDO and ABQWWTP projects where all of the fluorophores were removed by the membrane treatment, the visible fluorescence traces left in the permeate samples at MDC indicated RO membrane performance have problems for the DOM removal before direct potable usage although over 90% DOM were rejected. In most cases, these fluorescence traces in permeates were contributed mainly by protein-like fluorescence when TOC concentration was very high. The humic-like fluorescence residuals were still observed in permeates. Obvious fluorescence residuals left at MDC project demonstrated that either performance of RO was despoiled due to RO fouling with high TOC concentration after a long running time or some fluorescent molecules could permeate through this RO membrane. The penetrated fluorophores have the similar generic fluorescing materials presented in protein-like and humic-like fluorophores. Furthermore, the set-up was shut down frequently after running for two weeks and membrane performance became worse late after. In this regard, pretreatment is very crucial to RO membrane performance. Since MF itself could not degrade big structures such as protein-like and humic-like fluorophores, it just removes most of them based on molecular size separation. The non-degraded high concentrated

protein-like and humic-like fluorophores, especially the former, could not be removed completed by RO membrane and maybe resulted in membrane fouling. Therefore, pretreatment of RO with lagoon and MF combination may be not a good option for high protein concentration removal.

Nearly, all of the permeate samples from RDO, MDC and ABQWWTP sites had more or less of protein-like trace levels indicated that RO is not good enough for complete protein-like fluorophores removal. On the other hand, opposed to protein-like fluorophores, RO membrane had much better performance on humic-like fluorophores removal. Since hydrophobicity of DOM and membrane material are the significant factors to determine treatability by RO membrane. The difference in these two types of fluorophores rejection might imply hydrophobicities of protein-like and humic-like fluorophores. Because hydrophobic RO membranes surface (polyamide) could favor the adsorption of hydrophobic portion of solutes by hydrophobic interactions and result in higher retention for hydrophobic fractions. The statements [Gray and Bolto, 2003; Fan, 2001; Jarusuthiak et al., 2002; Lin et al., 2000] that hydrophilic, neutral compounds are most likely to remain at trace levels in the membrane permeate while hydrophobic, charged DOC is rejected, and the experiments results that RO preferentially rejected humic-like fluorophores than protein-like fluorophores as well as the speculation that protein-like fluorophores may be derived from protein and humic-like fluorophores derived from humic substances suggested that the protein-like fluorophores are hydrophilic while humic-like fluorophores are hydrophobic.

4.5 CONCLUSIONS

At all of three sites, tryptophan-like fluorescence dominated over humic-like fluorescence because sewage-derived DOM is dominated by organic matter originating from microbial activity. It was different from natural water which is dominated by natural organic matter derived from plant material, where humic-like fluorescence is predominant. Such differences in spectral signatures could facilitate the tracking of sewage contamination in river water and seawater. Therefore, it is predicted that fluorescence can be used as a rapid and sensible tool to distinguish the sample origin or track contamination by comparing peak types and relative peak abundance as well as correlate fluorescence features with water quality parameters.

The result of protein-like fluorophores having very little residual and almost no any humic-like fluorescence in the permeate samples suggested that RO membrane is very efficient to eliminate humic-like fluorophores but not protein-like fluorophores even the concentration of protein were not high. However, RO filtration is a promising technology with its powerful removal of organic substances in advanced wastewater treatment for portable water purpose. Membrane fouling problem can be solved by setting up an efficient pretreatment process.

4.6 REFERENCES

Baker, A., and Inverarity, R. (2004) Protein-like fluorescence intensity as a possible tool for determining river water quality. *Hydrol. Process.* 18, 2927-2945.

Baker, A., Ward, D., Lieten S.H., Perieta R., Simpson E.C., and Slater M. (2004) Measurement of protein-like fluorescence in river and wastewater using a handheld spectrophotometer. *Water Research* 38, 2934-2938.

Baker, D.J., Salvi, S.M.l., Langenhoff, A.A.M., and Stuckey, D.C. (2000) Soluble microbial products in ABR treating glow-strength wastewater. J. Environ. Eng. 126, 239-249

Bersillon, J.L. (1988) Fouling analysis and control. *Future industrial prospects of membrane processes* (Eds: Cecille, L., Toussaint, J.C.)Elsevier, Oxford, pp,234-247.

Chen, W., Westerhoff, P., Leenheer, J.A., and Booksh, K. (2003) Fluorescence excitation-emission matrix regional integration to quantify spectra for dissolved organic matter. *Environ. Sci. Technol.* 37, 5701-5710.

Chin, Y.P., Aiken,G., and O'Loughlin, E. (1994) Molecular weight, polydispersity and spectroscopic properties of aquatic humic substances. *Environ. Sci. Technol.* 28, 1853-1858.

Coble, P.G., Del Castillo, C.E., and Avril, B. (1998) Distribution and optical properties of CDOM in the Arabian Sea during the 1995 Southwest Monsoon. *Deep-Sea Res. II* 45, 2195-2223.

Coble, P.G. (1996) Characterization of marine and terrestrial DOM in seawater using excitation-emission matrix spectroscopy. *Marine Chemistry* 51(4) 325-346.

Coble, P.G., Green, S.A., Blough, N.V., and Gagosian, R.B. (1990) Characterization of dissolved organic matter in Black Sea by fluorescence spectroscopy. *Nature* 348,432.

Commack, W.K.L., Kalf, J., Pairie, Y.T., and Smith, E.M. (2004) Fuorescent dissolved organic matter in lakes: relationship with heterotrophic metabolism. *Limnology and Oceanograph* 49(6), 2034-2045.

Creighton, T.E. (1993) Proteins, structure and molecular properties, 2nd ed. Freeman, NY.

Dialynas, E., Mantzavinos, D., and Diamadopoulos, E. (2008) Advanced treatment of the reverse osmosis concentrate produced during reclamation of municipal wastewater. *Water Res.*2, 4603-4608.

Dunn, M. J. (1992) Protein determination of total protein concentration. *Protein Purification Methods* (Eds: Harris, E. L. V., Angal, S.) Oxford: IRL Press.

Fan, L., Harris, J., Roddick, F., and Booker, N. (2001) Influence of the characteristics of natural organic matter on the fouling of microfiltration membranes. *Water Res.* 35, 4455.

Fan, L.H., Nguyen T., and Harris, J.L. (2008) Low-pressure membrane filtration of secondary effluent in water reuse: pre-treatment for fouling reduction. *Journal of Membrane Science.* 320, 135-142.

Field, E., Howe, K., Thomson, B., Jim, R., and Kottenstette, R. (2008) Fouling of RO membranes treating Effluent from wastewater treatment processes. *AWRA report* .

Gray, S.R., and Bolto, B.A. (2003) Predicting NOM fouling rates of low pressure membranes. *Proceeding of the International Membrane Science and Technology (IMSTEC)*, Sydney, Australia.

Henderson, R.K., Baker, A., Murphy,K.R., Hambly, A., Stuetz, R.M., and Khan, S.J. (2009) Fluorescence as a potential monitoring tool for recycled water systems: A review. *Water Res.* 43, 863-881.

Howe, K.J., and Clark, M.M. (2002) Fouling of microfiltration and ultrafiltration membranes by natural waters. *Environ. Sci. Technol.* 36, 3571-3576

Hudson, N., baker, A., Ward, D., Reynolds, D.M., Brunsdon, C., Carliell-Marquet, C., and Browning, S. (2008) Can fluorescence spectrometry be used as a surrogate for the biochemical oxygen demand (BOD) test in water quality assessment? An example from South West England. *Science of the Total Environment* 391(1), 149-158.

Jarusuthiak, C., Amy, G., and Croue, J.P. (2002) Fouling characteristics of wastewater effluent organic matter (EFOM) isolates on NF and UF membranes. *Desalination* 145, 247.

Kilduff, J.E., Mattaraj, S., Wigton, A. (2004) Effects of reverse osmosis isolation on reactivity of naturally occurring dissolved organic matter in physicochemical processes. *Water Res.* 38, 1026-1036.

Lakowicz, J.R. (2006) *Principle of fluorescence spectroscopy.* 3rd ed. Springer, New York.

Langergraber, G., Fleischmann, N., and Hofstaedter, F. (2003) A multivariate calibration procedure for UV-vis spectrometric quantification of organic matter and nitrate in wastewater. *Water Science and Technology* 47(2), 63-71.

Lee, N., Amy, G., Croue, J.P., and Busson, H. (2004) Identification and understanding of fouling in low-pressure membrane (MF/UF) filtration by natural organic matter (NOM), *Water Res.* 38,4511-4523.

Lee, S., Ang, W.S., Elimelech, M. (2006) Fouling of reverse osmosis membranes by hydrophilic organic matter: implications for water reuse. *Desalination* 187, 313.

Lin, C.F., Lin, T.Y., and Oiver ,J.H. (2000) Effects of humic substance characteristics on UF performance. *Water Res.* 34(4), 1097-1106.

Lowry, O. H., Rosebrough, N. J., Farr, A.L., and Randall, R. J. (1951) Protein measurement with the Folin-Phenol reagents. *J. Biol. Chem.* 193, 265-275.

Mallevialle, J., Anselme, C., and Marsigny, O. (1989) Effects of humic substances on membrane processes. in: I.H.Suffet, P. MacCarthy(Eds.), *Aquatic humic substances: influence on fate and treatment of pollutants* (Eds: Suffet, I.H., MacCarthy, P.) ACS, Washington, DC, 749-767.

Mayer, L.M., Schick L.L., and Loder III, T.G. (1999) Dissolved protein fluorescence in two Mar. Estuaries. *Marine Chemistry* 64, 171-179.

Mcllvaine, R. (2008) Reverse Osmosis. *Chemical Engineering* 8, 20-24.

Reynolds, D.M. (2002) The differentiation of biodegradable and non-biodegradable dissolved organic matter in wastewaters using fluorescence spectroscopy. *J.Chem.Technol.Biotechnol* 77, 965-972.

Shon, H.K. Vigneswaran, S., Kim, I.S. (2006) Fouling of ultrafiltration membrane by effluent organic matter: A detailed characterization using different organic fractions in wastewater. *Journal of Membrane Science* 278, 232-238.

Marhaba, T.F (2000) Fluorescence technique for rapid identification of DOM fractions. *J. Environmental Engineering* 145-152.

Ujang, Z., Ng, K.S., Hazmin, T.,Hamzah, T., Roger P., Ismail, M.R., Shahabudin, S.M., and Abdul Hamid, M.H. (2007) Application of immersed MF (IMF) followed by reverse osmosis (RO) membrane for wastewater reclamation: A case study in Malaysia. *Water Science & Technology* 56, 103-108.

Wolfeis, O.S. (1985) The fluorescence of organic natural products. *Molecular Luminescence Spectroscopy. Part I: Methods and Applications* (Ed: Shulman S.G.) Wiley, New York, 167-370.

Wu F.C., Evans R.D., and Dillon P.J. (2003) Separation and characterization of NOM by high-performance liquid chromatography and on-line three-dimensional excitation emission matrix fluorescence detection. *Environ. Sci. Technol.* 37, 3687-3693

Yamashita,Y., and Tanoue, E. (2003) Chemical characterization of protein-like fluorophores in DOM in relation to aromatic amino acids. *Marine Chemistry* 82, 255-271.